

Featured Article

# A systematic integrated analysis of brain expression profiles reveals *YAP1* and other prioritized hub genes as important upstream regulators in Alzheimer's disease

Min Xu<sup>a,b,1</sup>, Deng-Feng Zhang<sup>a,\*,\*,1</sup>, Rongcan Luo<sup>a,b</sup>, Yong Wu<sup>a,b</sup>, Hejiang Zhou<sup>a</sup>, Li-Li Kong<sup>a,c</sup>,  
Rui Bi<sup>a</sup>, Yong-Gang Yao<sup>a,b,d,\*</sup>

<sup>a</sup>Key Laboratory of Animal Models and Human Disease Mechanisms of the Chinese Academy of Sciences & Yunnan Province, Kunming Institute of Zoology, Kunming, Yunnan, China

<sup>b</sup>Kunming College of Life Science, University of Chinese Academy of Sciences, Kunming, Yunnan, China

<sup>c</sup>Institute of Health Science, Anhui University, Hefei, Anhui, China

<sup>d</sup>CAS Center for Excellence in Brain Science and Intelligence Technology, Chinese Academy of Sciences, Shanghai, China

## Abstract

**Introduction:** Profiling the spatial-temporal expression pattern and characterizing the regulatory networks of brain tissues are vital for understanding the pathophysiology of Alzheimer's disease (AD).

**Methods:** We performed a systematic integrated analysis of expression profiles of AD-affected brain tissues (684 AD and 562 controls). A network-based convergent functional genomic approach was used to prioritize possible regulator genes during AD development, followed by functional characterization.

**Results:** We generated a complete list of differentially expressed genes and hub genes of the transcriptomic network in AD brain and constructed a Web server ([www.alzdata.org](http://www.alzdata.org)) for public access. Seventeen hub genes active at the early stages, especially *YAP1*, were recognized as upstream regulators of the AD network. Cellular assays proved that early alteration of *YAP1* could promote AD by influencing the whole transcriptional network.

**Discussion:** Early expression disturbance of hub genes is an important feature of AD development, and interfering with this process may reverse the disease progression.

© 2017 the Alzheimer's Association. Published by Elsevier Inc. All rights reserved.

## Keywords:

Alzheimer's disease; Differential expression; Convergent functional genomic; Upstream regulator; Database

## 1. Introduction

Alzheimer's disease (AD) is the most prevalent neurodegenerative disease in the elderly and is characterized by progressive memory loss and cognitive impairment. Patho-

logical hallmarks of AD include the presence of extracellular amyloid  $\beta$  (A $\beta$ ) plaques and intracellular neurofibrillary tangles, synaptic dysfunction, neuronal loss, and brain atrophy [1]. The occurrence and development of AD is affected by age, genetic, and environmental factors [2]. Previous linkage analyses have identified the A $\beta$  production-related genes *APP*, *PSEN1*, and *PSEN2* as the causal genes for familial AD, whereas genome-wide association studies (GWASs) have identified two dozen of the susceptibility loci responsible for sporadic AD [3,4]. Despite the fact that remarkable advances have been made in the understanding of the genetic basis of AD, the pathophysiology of AD is not well understood. A complete characterization of the

The authors declare no conflict of interest.

<sup>1</sup>These authors contributed equally to this work.

\*Corresponding author. Tel./Fax: +86-871-68125440.

\*\*Corresponding author. Tel.: +86-871-68125441; Fax: +86-871-68125440.

E-mail address: [zhangdengfeng@mail.kiz.ac.cn](mailto:zhangdengfeng@mail.kiz.ac.cn) (D.-F.Z.), [yaoyg@mail.kiz.ac.cn](mailto:yaoyg@mail.kiz.ac.cn) (Y.-G.Y.)

transcriptomic alterations and the regulatory mechanisms that underpin AD may provide essential evidence to fill the gap.

Gene expression profiling of postmortem brain tissues from AD patients and normal controls has identified numerous dysregulated genes and contributed to the understanding of the biological processes disrupted during AD pathogenesis [5–31]. Among the list of differentially expressed genes (DEGs), dysfunction of mitochondrial pathways, calcium signaling, and neuroinflammation were consistently observed in AD, to name a few [32]. Nevertheless, the statistical power and consistency of previous individual studies were limited, mainly due to relatively small sample sizes [5–31]. A comprehensive, robust, cross-validated list of DEGs based on a large sample size is urgently needed in AD research. It is also important to understand the spatial-temporal expression pattern and regulatory network of these DEGs. Identifying the genes which play central regulatory roles during AD pathogenesis, and finding how these genes regulate the downstream DEGs, is vital for understanding both the pathophysiology of AD and looking for potential targets for drug therapy (Fig. 1A).

In this study, we performed an integrative analysis of available high-throughput brain expression profiling data sets from AD patients and controls using a convergent functional genomic (CFG) method [33,34], in an attempt to answer the aforementioned questions (Fig. 1B). We merged all the available expression data for four brain regions affected by AD (entorhinal cortex [EC], hippocampus [HP], temporal cortex [TC], and frontal cortex [FC]) [5–30] through cross-platform normalization to achieve the largest AD brain expression data set for these brain regions (1246 samples, including 139 HP, 78 EC, 697 FC, and 332 TC). We investigated the regulation pattern of DEGs in AD brain and prioritized hub genes and potential upstream regulator genes by the CFG method [33,34], which integrated various levels of AD-related data including GWAS, protein-protein interaction (PPI), brain expressional quantitative trait loci (eQTL), and expression data of mouse AD models. We have been able to provide a complete and robust list of DEGs and hub regulators and identified several candidate upstream regulators in DEG networks, such as *YAP1* in the glial cell differentiation module. Our functional experiments with *YAP1* have suggested that expression perturbations of upstream regulator genes at the early stage of

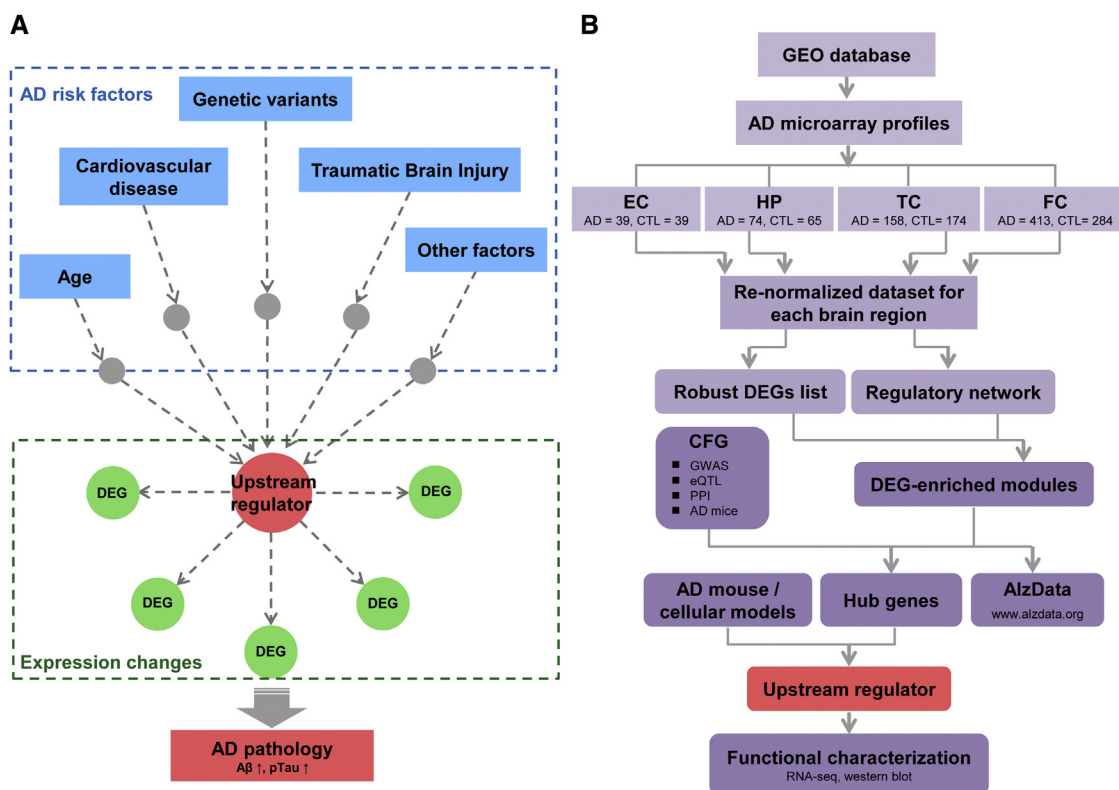


Fig. 1. Rationale and workflow of the present study. (A) Upstream regulator genes would respond to AD risk factors, influence expression of downstream genes, and thus promote AD pathology. Aβ ↑: increase of amyloid β level; pTau ↑: increase of phosphorylated tau. (B) We retrieved and renormalized all relevant expression data sets of samples with and without AD in entorhinal cortex (EC), hippocampus (HP), temporal cortex (TC), and frontal cortex (FC) and then analyzed for DEGs in the compiled data sets. We explored the gene prioritization and regulatory pattern in AD using coexpression network analysis and spatial-temporal expression data of AD mouse and cellular models and identified hub genes in the DEG-enriched coexpression networks. A convergent genomic approach (CFG) integrating multiple lines of evidence (including population genetic association, genetic regulation of expression, protein-protein interaction, early expression alteration, and pathology correlation in AD mice) was used to prioritize potential upstream genes. Abbreviations: eQTL, expressional quantitative trait loci; AD, Alzheimer's disease; CTL, control; DEG, differentially expressed gene; GEO, Gene Expression Omnibus; GWAS, genome-wide association study; PPI, protein-protein interaction.

AD development might be damaging, by affecting expression of downstream genes and so further promoting AD progression. Candidate upstream regulators found in this study might act as potential therapeutic targets for the treatment of AD. The list of all AD-related DEGs and their biological prioritization are available online through our Web server at <http://www.AlzData.org>.

## 2. Materials and methods

### 2.1. Study design and rationale

We initially retrieved and renormalized all relevant expression data of four brain regions (EC, HP, TC, and FC) with and without AD and then pinpointed the DEGs in the compiled data sets. We then explored the regulatory pattern of these DEGs through coexpression network analysis of the renormalized expression data. We hypothesized that the DEGs might be regulated by several hub genes in the DEG-enriched coexpression modules/networks. A CFG approach integrating multiple lines of evidence [33,34], for example, population genetic association, genetic regulation of expression, PPI, gene expression alteration, and pathology correlation in AD mice, was used to prioritize hub genes. In addition, hub genes that met the following criteria were considered likely to be early causal/driver upstream genes: (1) had a response to inducing factors (e.g., A $\beta$  deposits or genetic risk alleles), (2) had expression alterations earlier than the emergence of AD pathology, and (3) were highly correlated with expression of downstream DEGs. Potential upstream regulators were functionally characterized *in vitro*. The flowchart and rationale of this study are shown in Fig. 1A and 1B.

### 2.2. AD expression data collection and filtration

All the original microarray data regarding AD were retrieved from Gene Expression Omnibus (<https://www.ncbi.nlm.nih.gov/geo>) by searching with the keyword "Alzheimer." An exhaustive, nonredundant data retrieval was achieved for EC, HP, TC, and FC following a series of criteria (see [Supplementary Methods](#)). By January 2016, 20 GSE series of expression data sets had been obtained. After manual inspection and filtration, there were four data sets retained for EC (GSE26927 [18,29], GSE48350 [8], GSE26972 [16], GSE5281 [7,9]); five data sets for HP (GSE28146 [14], GSE48350 [8], GSE5281 [7,9], GSE29378 [23], GSE36980 [25]); five data sets for TC (GSE37263 [13], GSE29652 [15], GSE36980 [25], GSE15222 [10], GSE5281 [7,9]); and eight data sets for FC (GSE12685 [11], GSE48350 [8], GSE66333 [30], GSE53890 [27], GSE36980 [25], GSE15222 [10], GSE5281 [7,9], GSE33000 [28]) ([Supplementary Table 1](#)). A total of 1246 human postmortem brain samples (684 AD and 562 controls) were compiled for the detailed analysis. Note that among the 20 data sets, GSE15222 for TC and GSE33000 for FC have far more samples than any other studies of the same brain regions, combining these two data sets with others may blur effects of studies with a relatively small sample

size. Therefore, we used these two studies as independent validation data sets for the compiled data set of different studies. Thus, we have 269 AD and 271 controls from four brain regions in stage 1 (for EC: 39 vs. 39; for HP: 74 vs. 65; for TC: 52 vs. 39; and for FC: 104 vs. 128) for subsequent analyses (DEG detection and coexpression network construction). Detailed information about data collection, filtration, and sample compositions of each brain region was shown in [Supplementary Methods and Supplementary Table 1](#). The original metadata of each data set including all sample information were accessible at the [Alzdata.org](http://www.alzdata.org) Web server (<http://www.alzdata.org/download.html>).

### 2.3. Raw data preprocessing, renormalization, and detection of DEGs

Individual expression data set for each brain region was subjected to data normalization, log<sub>2</sub> transformation, probe filtration, and probe mapping to entrez gene IDs (see [Supplementary Methods](#)). All processed expression data from the same brain region were merged by algorithm ComBat in R package *inSilicoMerging* [35,36]. The ComBat is an empirical Bayes method that is recommended for removal of batch effects [37,38]. As revealed by our principal variance component analysis [39], ComBat used in this study eliminated the batch effects almost completely in all four combined brain regions ([Supplementary Methods and Supplementary Fig. 1](#)).

Cross-platform normalized expression data for each brain region was used to detect DEGs between AD patients and normal controls. The expression profiling was adjusted for age and gender by using a linear regression model during the identification of DEGs. Differential expression analysis was conducted by R package *limma* and the Benjamini-Hochberg's method was used to correct for multiple comparisons [40].

### 2.4. Coexpression network construction and identification of hub genes

Coexpression networks for individual brain region (region-specific network) and combined expression profiles of all four brain regions (multitissue network) were constructed by using package *weighted gene coexpression network analysis* in R (<https://www.r-project.org>) [41–46] for cases and controls, respectively. Expression residuals after adjustment for age and sex using a linear model were used as input for network construction ([Supplementary Methods](#)). Coexpression modules were detected in cases and controls from stage-1 samples, and each module was assigned to a unique color. Pairwise preservation tests (indicated by Z-score and module membership (kME) correlations computed by *weighted gene coexpression network analysis*) were applied to assess module conservation across brain regions (in cases and controls, respectively), and between cases and controls in multitissue networks. Intramodule connectivity (k) value for each gene in cases ( $k_{AD}$ ) or controls ( $k_{CTL}$ ) was calculated independently based on the AD-only or control-only multitissue networks, respectively, and was scaled relative to the

maximally connected gene in each module. As most of the coexpression modules were strongly preserved across brain regions (Supplementary Figs. 2–4), multitissue networks constructed with the combined expression profiles of all four brain regions in AD and controls were used for subsequent analyses. Hub genes were defined as genes with  $k > 0.8$  in the AD or control network and were subjected to subsequent analyses [41–46]. Of note, there were some hub genes with a significantly lower (loss-of-connectivity) or higher (gain-of-connectivity) connectivity in the AD network compared with the control network, albeit the overall pattern of the connectivity distribution was preserved in the AD and control networks ( $r = 0.7$ ,  $P < 2.2 \times 10^{-16}$ ). We presented the summary statistics of the connectivity for all genes at our [AlzData.org](http://AlzData.org) Web server. Anyone who is interested in loss-of-connectivity or gain-of-connectivity hub genes can access this Web resource for reference.

### 2.5. Convergent functional genomics

The CFG approach integrated multiple lines of AD-related evidence [33,34] and scored each gene based on this evidence (CFG score). A gene was defined as AD-related if it (1) had at least one locus being significantly associated with AD ( $P < .001$ , from the International Genomics of Alzheimer's Project [4]); (2) was associated with eQTLs that showing an AD risk in International Genomics of Alzheimer's Project ( $P_{\text{GWAS}} < .001$  and  $P_{\text{eQTL}} < .001$ ) [4,47]; (3) physically interacted with any AD core genes (*APP*, *PSEN1*, *PSEN2*, *APOE*, or *MAPT*) ( $P < .05$ ) according to the Human Gene Connectome. [48,49]; (4) were correlated with AD pathology in AD mice ( $P < .05$ ) at the expression level [50]; or (5) showed an early differential expression in AD mice ( $P < .05$ ) [50]. One point was assigned if any of the aforementioned evidence was observed; otherwise zero point, leading to a CFG score ranging from 0 to 5 points (Supplementary Methods).

### 2.6. Cellular characterization of an upstream hub gene

A U251 glia cell line (U251-APP cell) with a stable expression of mutant APP (APP-K670N/M671L), constructed in our previous studies [51,52], was used in the cellular assay. We harvested cells with knockdown or overexpression of the hub gene at 72 hours after transfection for RNA sequencing (RNA-seq) and western blotting (WB). RNA-seq of each treatment was performed in triplicate (data are accessible at [AlzData.org](http://AlzData.org), <http://www.alzdata.org/download.html>; or GSE100891, <https://www.ncbi.nlm.nih.gov/geo/query/acc.cgi?acc=GSE100891>). WB was repeated three times (Supplementary Methods). DEGs were detected in cells with *YAP1* knockdown or overexpression versus scramble cells by using RNA-seq data. WB for GAPDH was used as a loading control to measure the densitometry of *YAP1*, *BACE1*, *PSEN1*, *PSEN2*, nicastrin, amyloid  $\beta_{42}$  ( $A\beta_{1-42}$ ), *CDK5*, and *GSK3 $\alpha/\beta$* . The densitometric signal of phosphorylated tau at threonine 181 (pTau181) or serine 396 (pTau396) was determined by the ratio

of the phosphorylated protein to total tau. ImageJ 1.50i (National Institutes of Health, Bethesda, Maryland, USA) was used to evaluate the densitometry.

### 2.7. Statistical analysis

Genes with  $\log_2$  fold change greater than 0.1 ( $|\log\text{FC}| > 0.1$ ) and FDR smaller than 0.05 ( $\text{FDR} < 0.05$ ) were defined as DEGs in AD patients in the combined data set. For data sets of AD mouse or cellular models, and data set of cells with *YAP1* knockdown or overexpression, genes with  $|\log\text{FC}| > 0.1$  and  $P < .05$  were regarded as DEGs. Enrichment of biological process in Gene Ontology of target gene sets was analyzed by DAVID 6.8 (<https://david.ncifcrf.gov>) [53]. Fisher's exact test was used to test whether DEGs or cell type-specific genes (Supplementary Methods) were significantly enriched in a target gene set, and the Benjamini-Hochberg's method in R package was used to adjust for multiple comparisons. Comparisons of relative protein levels between two groups from the WB experiment were conducted by the Student's *t* test using the PRISM software (GraphPad Software, Inc., La Jolla, CA, USA). Network was visualized by using GeneMANIA plugin in the Cytoscape software [54,55].

## 3. Results

### 3.1. DEGs list and [AlzData.org](http://AlzData.org) Web server of compiled AD brain expression profiling

In total, 1246 postmortem brain samples containing highly curated and focused expression data from four brain regions were obtained (Supplementary Table 1). As the fold change was affected by the sample size that was used for identifying DEGs and the analyzed sample sizes of the four brain regions were different in this study, an increase of the cutoff of fold change might cause a bias for scoring DEGs in these brain regions (Supplementary Table 2). Therefore, we defined the DEGs using a relatively low threshold ( $|\log\text{FC}| > 0.1$ ,  $\text{FDR} < 0.05$ ) for differential expression. Around 9% to 20% of the total genes in the merged data set could be identified as DEGs in the four brain regions (Supplementary Table 3). Our final DEG list of the merged data sets captured a high proportion of the DEGs in the original studies, ranging from 30% to 70% (except for GSE12685 [13%]; Supplementary Table 4), indicating a reasonably high confidence of the DEGs identified by the merged data sets. With the enlarged sample size, we were able to identify DEGs that were missed in previous individual studies (from 15% to 70%, Supplementary Table 3), especially when the sample size of individual studies was relatively small (e.g., in EC and HP). This quite variable range might be partially caused by limited coverage or power of the originally individual data sets and a relatively low threshold in our DEG definition. Among the list, 139 genes had a consistently differential expression in all four brain regions, with 35 genes being upregulated and 104 genes being downregulated (Fig. 2A

and Supplementary Table 5). Consistent with previous studies [7,9,10,28], the expression pattern of well-known AD-risk genes, such as *APP*, *PSEN1*, and *PSEN2*, across EC, HP, TC, and FC was only slightly altered or unchanged in AD patients. Only one GWAS risk gene *MEF2C* [4] showed consistent downregulation in all four brain regions (Supplementary Table 6).

For easy access to the complete list of DEGs for each brain region (top DEGs for each region were listed in Supplementary Table 7), we established a Web server at [www.AlzData.org](http://www.AlzData.org). At this Web server, it is possible to search, browse, or download the differential expression pattern of genes of interest in either an individual GSE series or the normalized data sets along with graphic views and statistical results (Supplementary Figs. 5–8).

### 3.2. Dysregulated pathways in four regions of AD brain

We investigated the biological pathways dysregulated in different brain regions based on the identified DEGs. As shown in Fig. 2B, DEGs related to the metabolic

processes were significantly enriched in all four brain regions, which indicated a global dysregulation of energy metabolism across all brain regions during AD development. Processes involved in the synaptic functions were enriched in EC, HP, and TC, but not FC (which is the last brain region affected by AD [1]). The cortex had an enrichment of DEGs involved in the neurotrophin tropomyosin-related kinase receptor signaling pathway and mitogen-activated protein kinase (MAPK) pathway. In contrast to early affected brain regions (EC, HP, and TC), DEGs in FC were mainly involved in toll-like receptors signaling pathways, which have been reported to mediate microglia activation and promote clearance of A $\beta$  [56]. The overall pattern of the DEG-enriched pathways (Supplementary Table 8) based on our normalized data sets was consistent with previous reports [5,7–9,11,13–15,20,23,24,57,58]. Intriguingly, DEGs related to the Hippo signaling pathway were enriched in EC (the first brain region affected by AD [1]), which has not been reported in individual expression studies.

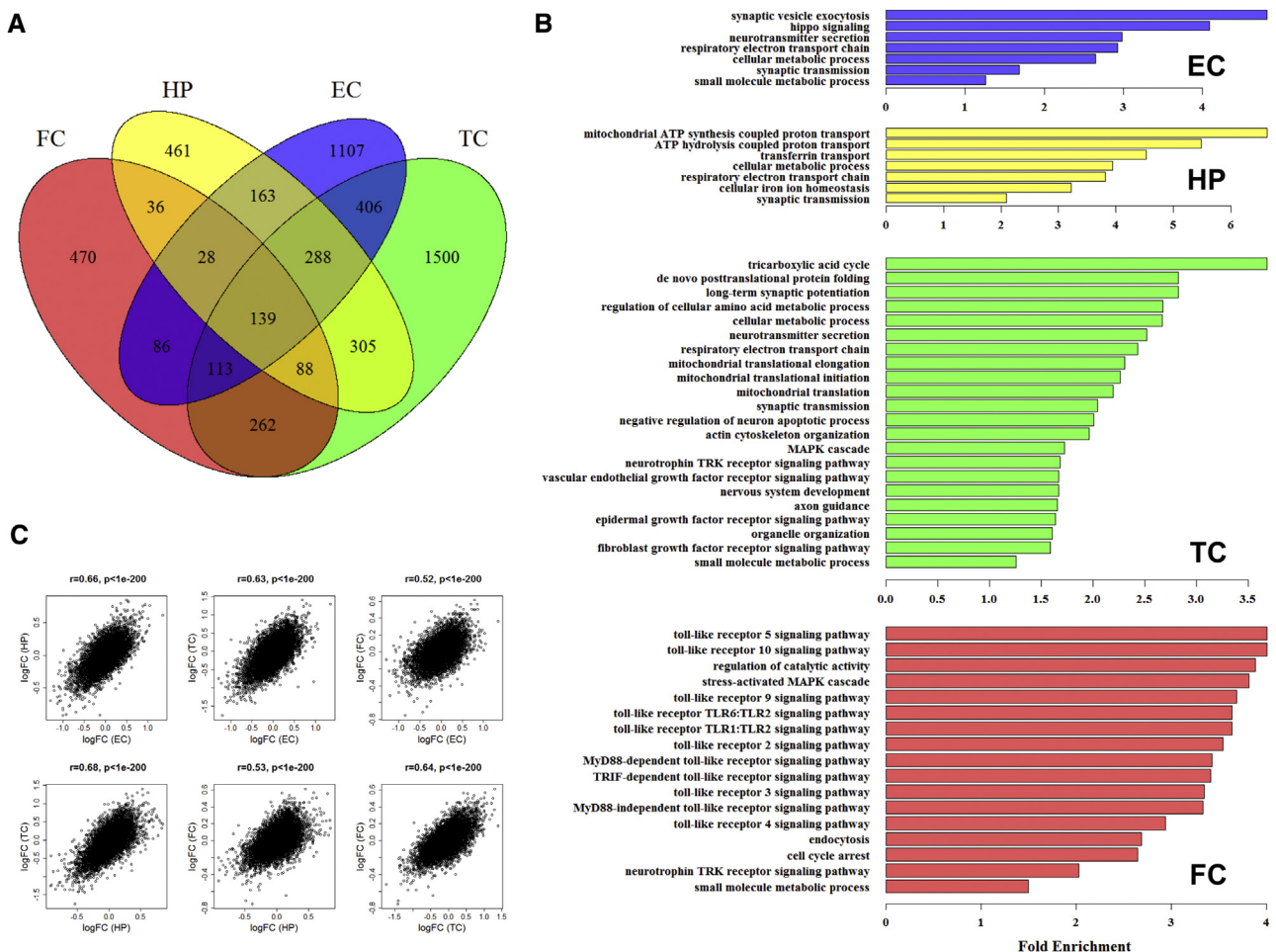


Fig. 2. Summary of differential expression. Distribution of (A) differentially expressed genes and (B) disrupted pathways in entorhinal cortex (EC), hippocampus (HP), temporal cortex (TC), and frontal cortex (FC). Enrichment of biological processes in Gene Ontology (GO) of the target gene sets was analyzed by DAVID 6.8 (<https://david.ncifcrf.gov>) [53]. Shown are enriched terms with FDR <0.05; x-axis, fold enrichment; y-axis, names of the enriched GO terms. (C) Correlation of gene expression changes between each pair of brain regions. Abbreviations: logFC, log<sub>2</sub> fold change of expression of a gene in AD patients compared with controls; p, P-value calculated by Pearson's correlation; r, Pearson's correlation; AD, Alzheimer's disease.

### 3.3. Coexpression network and DEG-enriched modules

In addition to the identification of dysregulated genes and pathways, we attempted to explore the disturbed networks and their regulatory pattern in AD brain. A coexpression network, which served as a high-order functional module, was constructed and subjected to subsequent analysis. Expression alterations and coexpression network structures were highly correlated (Fig. 2C,  $P < 1 \times 10^{-200}$ ) and preserved among EC, HP, TC, and FC (Supplementary Figs. 2–3), indicating a similar expression network organization in brain regions. Therefore, to increase the statistical power and achieve a more refined network structure, we combined the expression data of all four brain regions and built a multitissue coexpression network for AD patients (AD network) and controls (control network) using the stage 1 samples (269 AD patients and 271 controls), respectively. We noted that different brain tissues might have distinct expression and network patterns during AD progression. Our current strategy of using a multitissue coexpression network does not rule out a region-specific network or regulation pattern.

In the AD network, 13 transcriptional modules were found, with a modular size ranged from 155 to 3626 genes. The observed variable size of the modules might reflect different levels of organization and complexity of gene regulation in AD brain. Among these modules, five modules were significantly enriched with DEGs (Fig. 3A and Supplementary Table 9), and the genes in these five modules were mainly involved in synaptic transmission, myelination, transcription regulation, glial cell differentiation, and regulation of inflammation response, respectively (Fig. 3B). Single-cell RNA-Seq data (GSE67835 [59]) showed that genes in each module had a cell-type specificity and were consistent with their predicted modular biological functions (Fig. 3B). AD core genes, such as *APP*, *PSEN1*, *PSEN2*, *MAPT*, and *APOE*, all appeared in the DEG-enriched modules, supporting the biological relevance of these modules with AD. These five DEG-enriched modules were defined as disturbed networks in AD and were used for identifying hub regulators.

### 3.4. Identification and prioritization of hub genes

A hub gene holds nodes together and is important for the integrity and proper functioning of the whole network [60]. In the five modules, we identified 156 hub genes with  $k > 0.8$  (AD network,  $k_{AD} > 0.8$ ; control network,  $k_{CT} > 0.8$ ). To prioritize these hub genes, we introduced a CFG approach integrating data from GWAS, brain eQTL, PPI, and AD mouse models as supporting evidence [4,47–50]. Genes in DEG-enriched modules had an overall higher CFG score than genes in non-DEG-enriched modules ( $t$  test,  $P = 5.53 \times 10^{-11}$ ; Fig. 3C), and the score showed significantly positive correlation with connectivity (Pearson's correlation  $r = 0.766$ ,  $P = 2.39 \times 10^{-12}$ ) in DEG-enriched modules, whereas no such tendency was

observed in non-DEG-enriched modules (Pearson's correlation  $r = -0.145$ ,  $P = .348$ ) (Fig. 3C). Therefore, hub genes in DEG-enriched modules were more likely to be AD relevant compared with nonhubs or hubs of non-DEG-enriched modules and thus deserved further investigation. Indeed, the well-known AD genes *APP*, *MAPT*, *APOE*, and *BINI* showed top CFG signals ( $CFG \geq 4$ ), indicating that the CFG system could assign proper weight to genes that were involved in AD. Of note, most of these well-recognized AD-risk genes presented low connectivity ( $k < 0.8$ ) (Supplementary Table 6), whereas two GWAS reported top genes *FERMT2* and *MS4A6A* that were implicated in tau metabolism and inflammatory response, respectively [61], were also hub genes (Supplementary Table 6). For these 156 hub genes observed in the five DEG-enriched modules, 89 received at least two lines of AD-related evidence ( $CFG$  score  $> 1$ ; Supplementary Table 10) and were prioritized as highly AD-relevant hub genes. The full genome-wide CFG prioritization results can be retrieved at the [AlzData.org](http://AlzData.org) Web server.

### 3.5. Identification of 17 potential upstream regulators and highlighting the transcriptional coactivator *YAPI*

To investigate the potentially causal role of the hub genes, we examined the early expression patterns of the 89 hub genes by using AD mouse or cellular models (A $\beta$  treatment). Fifty-eight genes showed early expression alterations in the hippocampus of 2-month-old AD mice (a model of preclinical stage, Mouseac [50]) (Supplementary Table 10). Among these genes, 17 genes had a consistent trend of differential expression in AD mouse or cellular model data sets (Mouseac [50], GSE29317 [62], and GSE31372 [63]). These genes had central positions (hub) in the network and were differentially expressed at the early stage and therefore might act as potential upstream regulators in AD. We then considered whether there were transcriptional factors, which might be more likely to be upstream driver regulators, in those early-altered hub genes. Among the upstream regulators, we found that *YAPI* (the main effector of the Hippo signaling pathway [64]) in module “red” (Fig. 3D; Supplementary Table 10) was the only gene with transcriptional activity and therefore was of particular interest.

### 3.6. Functional validation of regulatory and upstream roles of *YAPI*

The aforementioned prioritization had indicated that the transcriptional cofactor *YAPI* was a hub node ( $k_{AD} = 0.84$ , module “red”) in the AD network and showed a high level of AD relevance ( $CFG$  score = 3). Notably, the connectivity of *YAPI* increased from 0.50 in the control network to 0.84 (in the corresponding module) in the AD network, supporting a gain-of-connectivity position of *YAPI* in AD pathology. Moreover, we observed that *YAPI* was downregulated in hippocampus of AD mice at the early stage (2 months old, before the onset of A $\beta$  deposits or tau tangle, Fig. 4A) [50]. Importantly, the early declined

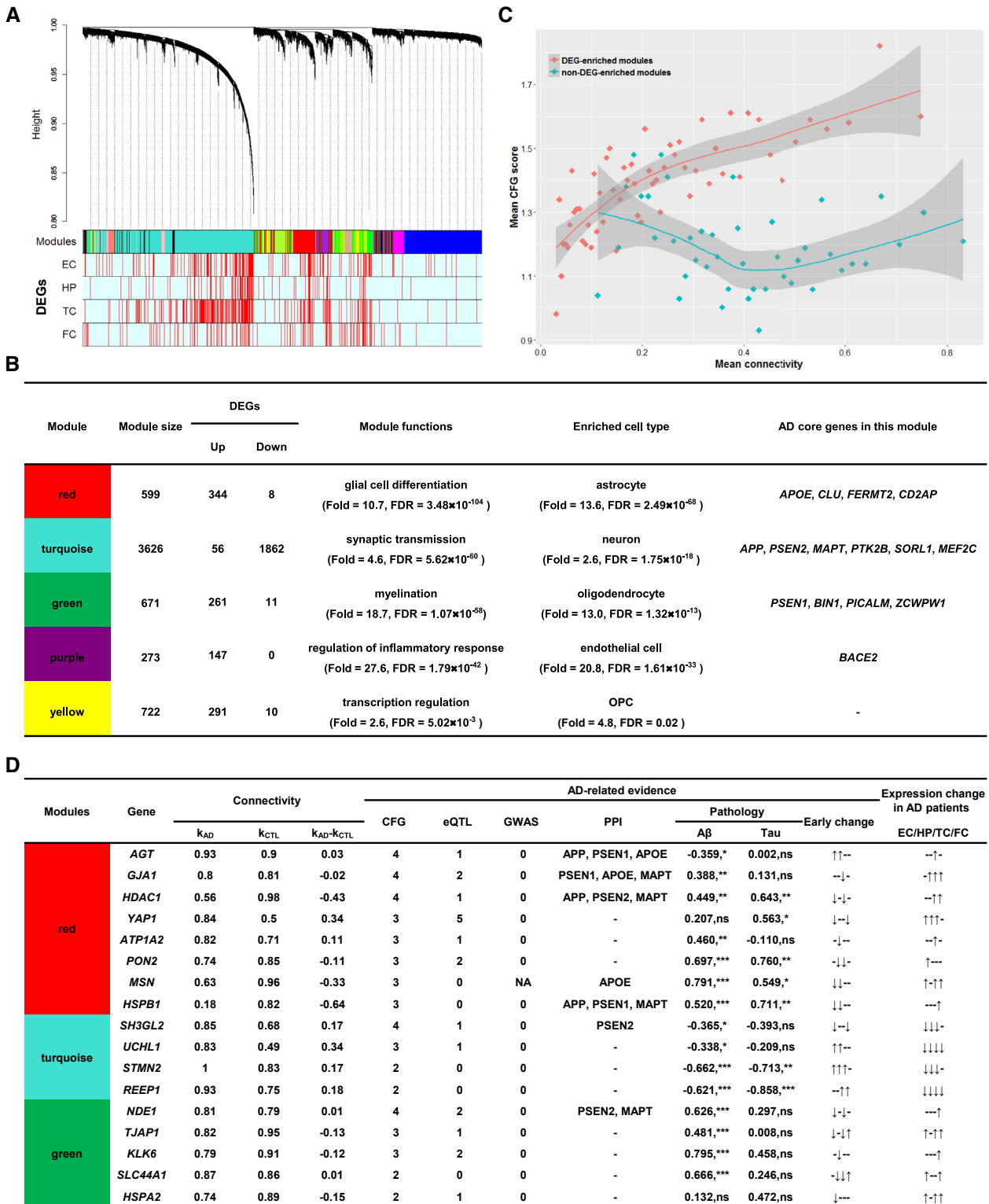


Fig. 3. Coexpression modules, DEG-enriched modules, hub genes, and upstream regulator genes. Hub genes in DEG-enriched modules were important candidate genes in AD. (A) DEG-enriched modules in AD coexpression network. Tree branches were colored by module membership (row 1) and expression changes in entorhinal cortex (EC, row 2), hippocampus (HP, row 3), temporal cortex (TC, row 4), and frontal cortex (FC, row 5). DEGs and non-DEGs were marked by red and light cyan, respectively. (B) Putative functions and related AD core genes in each DEG-enriched module. (C) Hub genes in DEG-enriched modules had a higher level of AD-related evidence than those in non-DEG-enriched modules ( $P = 5.53 \times 10^{-11}$ ). The connectivity was divided into 100 intervals, ranging from 0 to 1. Genes with a connectivity falling in the same interval were combined as one set (dot) and were featured by mean connectivity (x-axis) and mean CFG score (y-axis). Correlation between mean connectivity and mean CFG score was measured by Pearson's correlation. Difference of mean CFG score

expression of *YAPI* could be verified in incipient AD patients [14] and in A $\beta$ -treated neonatal astrocyte (from APP/PSEN1 double mutant transgenic mice [62]) (Fig. 4B and 4C). The opposite expression tendency was observed in old AD mice [50] (Fig. 4A) and AD patients of severe stage [14] (Fig. 4B and 4D). Expression alterations of hub genes at the early stage might be a response to upstream trigger factors, for example, A $\beta$  deposit or risk SNPs, and further influence downstream genes and disease development (Fig. 1A). Indeed, our analysis revealed that the mRNA expression level of *YAPI* can respond to several GWAS reported AD-risk SNPs (Supplementary Table 11) [4,47] and A $\beta$  treatment (GSE29317 [62], Fig. 4C), thus supporting the upstream role of *YAPI* in AD.

Downregulation of *YAPI* at the early stage of AD development was hypothesized to be a damaging event, and therefore, any direct interference with *YAPI* could increase AD pathology, and vice versa. We detected the changes of key proteins involved in A $\beta$  production and tau phosphorylation in response to *YAPI* deficiency and redundancy. As expected, knockdown of *YAPI* significantly increased the A $\beta$ <sub>1-42</sub> level and tau phosphorylation (pTau181 and pTau396), and the opposite tendency was observed in cells overexpressing *YAPI* (Fig. 4E). Moreover, proteins responsible for A $\beta$  generation (i.e.,  $\beta$ -cleavage enzyme BACE1 and  $\gamma$ -cleavage enzyme components, including PSEN1, PSEN2, and Nicastrin), and proteins phosphorylate tau (i.e., CDK5 and GSK3 $\alpha/\beta$ ) all showed a consistent tendency to alter with changing levels of A $\beta$  production and tau phosphorylation (Fig. 4E), supporting a damaging role of down-regulated *YAPI*.

To test our hypothesis that expression perturbation of *YAPI* as an upstream hub regulator could promote AD pathogenesis by disrupting expression of downstream genes (Fig. 1A), we performed RNA sequencing of U251-APP cells with *YAPI* knockdown or overexpression (Supplementary Fig. 9). In total, 3154 and 1467 DEGs were found for *YAPI* overexpression and knockdown, respectively. Among these DEGs, 1008 genes were affected by both *YAPI* reduction and overexpression with opposite direction of differential expression and were considered to be real downstream genes regulated by *YAPI*. Notably, these

*YAPI*-regulated genes ( $N = 455$ , Supplementary Table 12) were significantly enriched in DEG-enriched modules (Fisher's exact test,  $P = 2.33 \times 10^{-9}$ ) but not in non-DEG-enriched modules (Fisher's exact test,  $P = 1.00$ ), adding a robust support to the hub role and global impact of *YAPI* on the whole AD transcriptomic network (Fig. 5). Of note, the experimentally confirmed target genes (e.g., *YES1* and *TEAD1*) of *YAPI* were captured in both coexpression modules and our RNA-seq data, albeit we observed no enrichment of *YAPI*-regulated genes in the *YAPI*-centered module. All these results suggested that the reduction of *YAPI*, and the downstream effects consequent on this, might play a key role at the early stages of AD development.

According to the single-cell RNA-seq data of mouse ([http://web.stanford.edu/group/barres\\_lab/brainseqMariko/brainseq2.html](http://web.stanford.edu/group/barres_lab/brainseqMariko/brainseq2.html)) and human brain ([http://www.alzdata.org/single\\_RNAseq.php](http://www.alzdata.org/single_RNAseq.php)), *YAPI* was primarily expressed in astrocytes. Given that genes in the *YAPI*-centered module were also enriched in astrocytes (FDR =  $2.49 \times 10^{-68}$ , Fig. 3B), dysregulation of astrocyte-expressed genes such as *YAPI* and *APOE* in AD subjects may be important factors in the onset of AD.

#### 4. Discussion

AD is characterized by the presence in the brain of A $\beta$  plaque, tau tangles, and neuron loss [1], but the molecular changes underpinning these pathological features have not been fully elucidated. The characterization of transcriptional alterations of the brain during disease development might offer some insights into the pathogenesis of AD. Dozens of studies looking at the expression profiling of brain tissues with and without AD have been reported [5-31], and a large number of AD-related DEGs were identified [5-31], albeit the conclusions were often affected by small sample size and poor levels of statistical robustness. A comprehensive list of DEGs and a systematic analysis of the priority of genes and regulatory networks, based on a considerable large sample size, are vital for understanding the pathophysiology of AD and for identifying potential targets for drug therapy.

Access to brain tissues has long been and will continue to be a challenge in Alzheimer's research. Previous studies

between DEG-enriched modules and non-DEG-enriched modules was measured by unpaired Student's *t* test. A strong positive correlation between mean connectivity and mean CFG score was observed for DEG-enriched modules ( $r = 0.766$ ,  $P = 2.39 \times 10^{-12}$ ), whereas no correlation was observed in non-DEG-enriched modules ( $r = -0.145$ ,  $P = .348$ ). (D) Candidate upstream regulator genes. Connectivity of a gene in AD network ( $k_{AD}$ ) or in control network ( $k_{CTL}$ ) was estimated for each module;  $k_{AD} - k_{CTL}$ , an index to show the gain-of-connectivity (positive value) or loss-of-connectivity (negative value) in the AD network compared to the control network. Expression correlation ( $r$ ) of the target gene and AD pathology in AD mice (Pearson's correlation,  $P < .05$ ) was performed for the A $\beta$  line AD mice in Mouseac (marked as A $\beta$ ) [50] and the tau line AD mice in Mouseac (marked as tau) [50]; Early change: expression alterations in hippocampus of 2-month-old AD mice (in an order of HO-TASTPM: homozygous APP/PSEN1 double mutant mice, HET-TASTPM: heterozygous APP/PSEN1 double mutant mice, TAS10: human mutant APP mice, TAU: mutant human MAPT mice) [50]; Expression change in AD patients: expression changes of the target gene in AD patients in the merged data sets of entorhinal cortex (EC), hippocampus (HP), temporal cortex (TC), and frontal cortex (FC); "↑", upregulated; "↓", downregulated; "-", no reported AD core genes, or no significant cell-type enrichment, no significant PPI interaction, expression correlation or expression change; "NA", not applicable due to missing related data for the target gene. Abbreviations: AD, Alzheimer's disease; CFG, convergent functional genomics score based on the total number of lines of AD-related evidence; DEG, differentially expressed gene; eQTL, the total number of risk SNPs based on the IGAP data set [4] ( $P < .001$ ) that were able to regulate expression of the target gene (Braincloud [47],  $P < .001$ ); GWAS, the total number of risk SNPs within the target gene based on the IGAP data set [4] ( $P < .001$ ); PPI, AD core genes (*APP*, *PSEN1*, *PSEN2*, *MAPT*, and *APOE*) that had a significant protein-protein interaction ( $P < .05$ ) with the target genes [48,49]. ns,  $P > .05$ ; \* $P < .05$ ; \*\* $P < .01$ ; \*\*\* $P < .001$ .



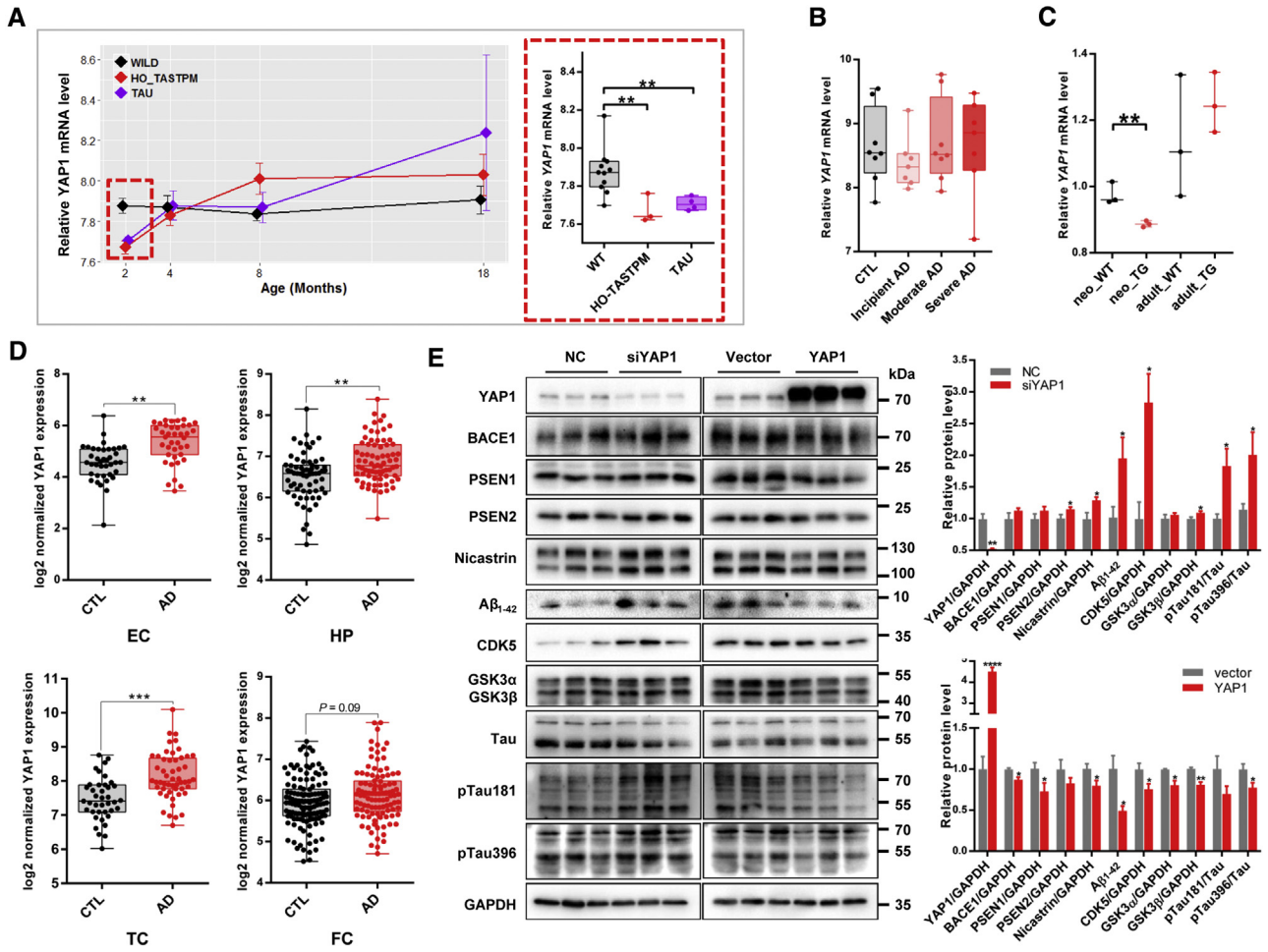


Fig. 4. *YAP1* was an upstream regulator in Alzheimer's disease (AD) network. (A) mRNA expression of *YAP1* was downregulated at the early stage and upregulated at the late stage in AD mice (Mouseac [50], WILD: wild-type mice; HO\_TASTPM: homozygous APP/PSEN1 double mutant mice; TAU: mutant human MAPT mice). (B) The same tendency was observed in incipient to severe AD patients (GSE28146 [14], AD: AD patients, CTL: controls). (C) mRNA expression of *YAP1* was downregulated in A $\beta$ -treated neonatal astrocyte (GSE29317 [62], neo\_WT/adult\_WT: astrocytes cultured on brain sections from neonatal/adult wild-type mice; neo\_TG/adult\_TG: cultured astrocytes from brain sections of neonatal/adult APdE9 mice [APP/PSEN1 double mutant]). (D) mRNA expression level of *YAP1* was upregulated in AD patients in merged data sets (EC: entorhinal cortex, HP: hippocampus; TC: temporal cortex, FC: frontal cortex). (E) Knockdown of *YAP1* expression led to increased A $\beta$  production and tau phosphorylation in U251-APP cells, whereas overexpression of *YAP1* had opposite effects. Western blotting was performed for cell lysate (cytosolic proteins) and culture supernatant (A $\beta$ <sub>42</sub>). GAPDH was used as the loading control to measure the densitometries of *YAP1*, BACE1, PSEN1, PSEN2, nicastrin, amyloid  $\beta$ 42 (A $\beta$ <sub>42</sub>), CDK5, and GSK3 $\alpha/\beta$ . The densitometric signal of phosphorylated tau at threonine 181 (pTau181) or serine 396 (pTau396) was determined by the ratio of the phosphorylated protein to total tau. Quantitative data were represented as mean  $\pm$  SEM of three independent experiments. Statistical differences were calculated by the Student's *t* test. \**P* < .05, \*\**P* < .01, \*\*\**P* < .001, \*\*\*\**P* < .0001.

have taken the advantage of accumulated sample collection in reported microarray data sets through meta-analysis [7,9,65]. However, the meta-analysis had some limitations as it mixed samples at the statistical level rather than starting with the original expression data. In this study, we have used the cross-platform normalization method, which has better performance in the detection of robust DEGs than meta-analysis, and provides a complete expression profiling at the individual level for downstream analyses [33,34,66]. Based on the enlarged, highly curated sample collection (1246 brain tissues), we were able to get a complete list of DEGs in AD brain. The finalized DEG list covered not only a high proportion of the DEGs reported in individual studies but also DEGs that were missed in individual studies. To make our results a

usable resource, we constructed a publicly available, user-friendly Web server (AlzData: [www.alzdata.org](http://www.alzdata.org)). This list of DEGs and the open-access Web server might benefit future hypothesis-driven researches. It should be mentioned that the neuronal expressed genes might appear to be lower in AD samples, as AD-affected brain regions had fewer neurons and greater numbers of microglia and astrocyte among AD subjects compared with controls [67]. It is difficult to differentiate, therefore, the true expression changes at the cellular level from those that reflect cell population changes.

In addition to producing the DEG lists, we performed the gene coexpression network analysis, to identify functionally related gene modules and hub genes in the regulatory network. The coexpression module could serve as a

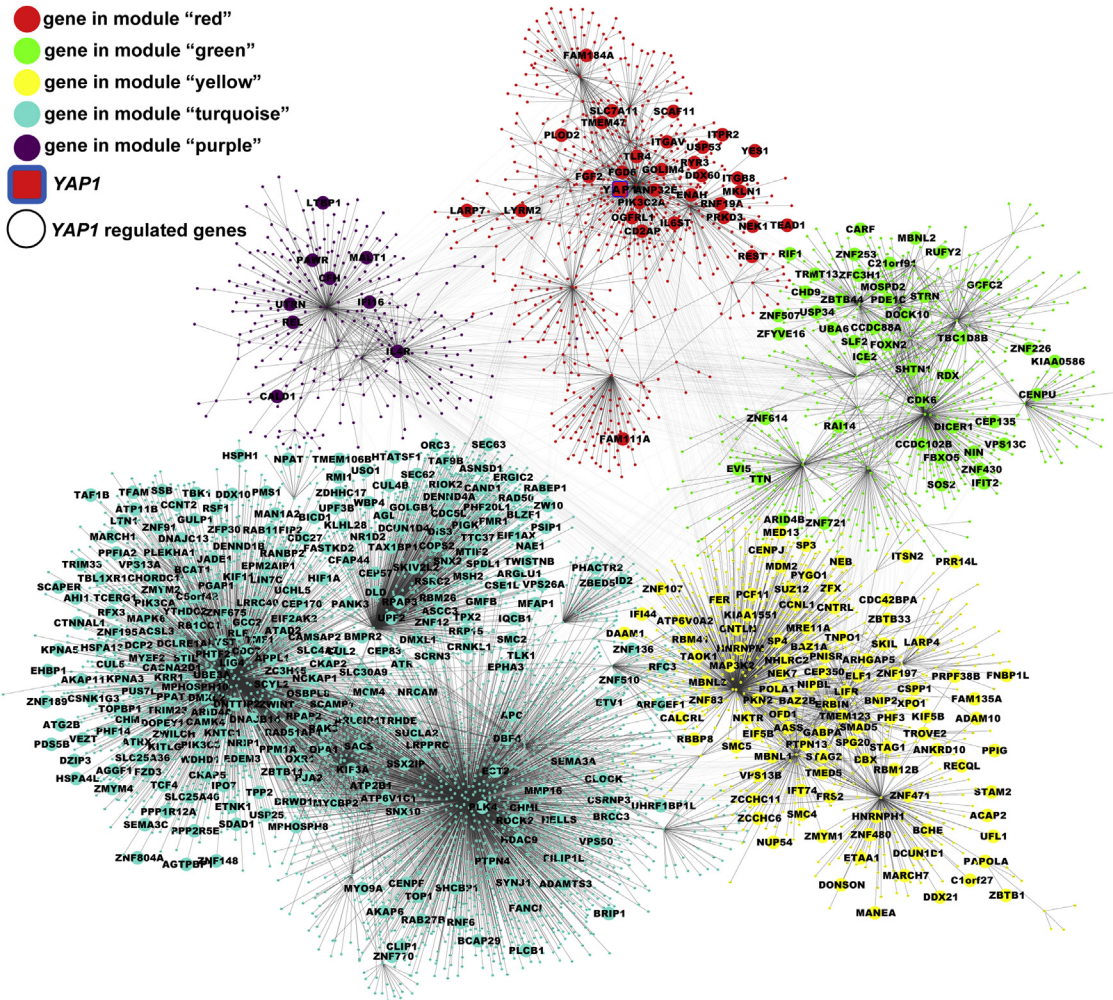


Fig. 5. Global impact of *YAP1* alteration in the DEG-enriched coexpression network. Coexpression network of the DEG-enriched modules (module “red,” “turquoise,” “green,” “yellow,” and “purple”) was constructed for normalized expression data sets of all brain regions. *YAP1*-regulated genes (marked in circle with gene name) were identified by RNA-seq of the U251-APP cells with *YAP1* overexpression or knockdown. Abbreviation: DEG, differentially expressed gene.

robust, high-order, functional unit. Identification of the hub genes, which are essential for the integrity of the functional module [60], offers a possibility to explore the disrupted regulatory pattern in AD brain. The coexpression network method had been widely recognized and was used to identify central genes in gene expression networks [24,68]. For instance, Zhang et al. combined massive microarray (376 AD patients and 173 controls) and eQTL data and identified a hub gene *TYROBP* as the key causal regulator of the microglia module in AD brain [24]. The hub gene, *TYROBP*, was featured as a central node in our analysis for AD cases ( $n = 269$ ,  $k_{AD} = 1$  in module “green-yellow”) and controls ( $n = 271$ ,  $k_{CTL} = 0.83$  in module “greenyellow”). Moreover, we found that *TYROBP* was an early-altered gene and was positively correlated with pathology of AD mouse, supporting its robust role in AD. *YWHAZ*, which was identified to be a hub gene in AD and aging [68,69], together with its family members *YWHAH/YWHAJ/YWHAH*, were also featured in our results. The *SYT1* gene in the synaptic transmission module,

reported as an important molecule for neurotransmitter release at the synapse [70], showed the highest connectivity ( $k_{AD} = 1$  in module “turquoise”) in our results. The consistency of these identified hub genes between our study and previous reports [24,68–70] indicates the repeatability and importance of the focus on hub genes. Nevertheless, there might be hundreds of hub genes and it is necessary to reduce this list of genes. In addition, a systems biology approach using other high-throughput data is warranted to fully characterize the genetic architecture of AD. Recently, Mukherjee et al. integrated massive PPI with genetic association data and indicated novel AD-risk genes [71], and this acts as a good example of this method.

Different from those previous network analyses that were mainly based on eQTL [24], or PPI data [71], in this study, we used a CFG approach integrating multiple lines of biological evidence (GWAS, eQTL, PPI, AD pathology correlation, and early alteration) to identify the hub genes which are highly relevant in AD. We found that the CFG score was positively correlated with connectivity (Fig. 3C) with

remarkable significance, and hub genes in the DEG-enriched modules showed a higher level of AD relevance. This observation suggested that it is desirable to focus on several prioritized genes selected from the numerous AD-related hub genes. The prioritized hub genes might act as key targets for the characterization of the regulatory pattern in AD brain.

As it is important to distinguish whether these hub genes are upstream drivers of AD or just downstream effectors, we analyzed the temporal expression of the hub genes with the help of AD mouse and cellular models, based on the hypothesis that gene expression changes before the emergence of AD pathology are more likely to be causal [50]. A dozen hub genes with early expression change were identified, such as *AGT*, *HDAC1*, *SH3GL2*, *STMN2*, *NDE1*, and *TJAPI* (Fig. 3D). *YAPI* is the only gene with transcription factor activity among these genes. The recognition of *YAPI* to be active in AD was not unexpected, as this gene had an active role in regulating neural precursor proliferation [72], neuronal specification [73], and neocortical astrocytic differentiation [74]. In addition, *YAPI* deletion could hyperactivate the inflammatory pathway and reactive astrogliosis [75]. The YAP/TAZ has also been proposed to be a downstream mediator of the APP signaling through a transcriptionally active protein complex containing APP and amyloid  $\beta$  precursor protein-binding family A member 3, also known as Mint3 and thus might mediate gene transcription induced by APP [76–78]. In our study, *YAPI* was downregulated in brain of preclinical AD mice and incipient patients and was decreased in response to A $\beta$  deposit and genetic risk alleles (Fig. 4 and Supplementary Table 11), showing a promising potential as a link of downstream dysregulated events with upstream inducing factors. Indeed, our RNA-seq data of cellular assay showed that *YAPI* alterations affected the expression profiles of downstream genes involved in the DEG-enriched modules. *YAPI* depletion promoted the pathological change of AD, whereas overexpression of *YAPI* had opposite effects on AD-related process (Figs. 4 and 5). All these results suggested that the reduction of *YAPI*, and the downstream effects consequent on this, might play a key role in the early stage of AD development. Moreover, we observed a gain-of-connectivity of *YAPI* in the AD network compared with control network in this study. This implicates that the gain of hub role of *YAPI* might be disease specific. The differential correlations between *YAPI* and downstream genes might indicate AD-specific changes in functional interactions and coordinated activities under specific conditions or perturbations, rather than a normal physiology function.

Intriguingly, we observed a positive correlation of the gene expression levels between *YAPI* and *REST* (the only functionally recognized upstream regulator in AD and aging [27]) in our compiled data sets (Supplementary Fig. 10). The damaging role of *YAPI* depletion was consistent with the observation with reduced *REST* [27]. *REST* was in the *YAPI*-centered module (module “red”), with a

moderate connectivity in the AD network ( $k_{AD} = 0.29$ ) and control network ( $k_{CT} = 0.42$ ). In contrast to the original report [27], we observed an increase of *REST* mRNA expression level in AD brains compared with controls. *YAPI* was also increased in AD brain compared with controls in all four brain regions in our combined data sets, which was different from its expression pattern at the early stage. We speculated that this was caused by a potentially compensatory effect. In our RNA-seq data, we observed an increase of *REST* expression in response to *YAPI* knockdown ( $\log_{2}FC = 0.292$ ,  $P = .0039$ ) and a decrease of *REST* expression in response to *YAPI* overexpression ( $\log_{2}FC = -0.305$ ,  $P = .0102$ ) (Supplementary Fig. 10). To determine if *YAPI* regulates *REST*, or if there is a compensatory feedback loop linking the expression of these two genes, we reanalyzed publically available expression data of neuronal cells with *REST* perturbation. We found no significant expression change of *YAPI* in response to knockdown (GSE28289 [79],  $P = .59$ ,  $\log_{2}FC = -0.09$ ) or knockout (GSE27341 [80],  $P = .7$ ,  $\log_{2}FC = -0.05$ ) of *REST*. Taken together, these results indicate that *YAPI* might be an upstream regulator of *REST*. These observations further supported the reliability of the upstream role of *YAPI* in AD development.

The identification of *YAPI*, as an upstream regulator, raised an important question whether modulation of the *YAPI* pathway, for example, use of *YAPI* activator at the early stage of cognitive impairment, would be a good approach for AD intervention. Note that *YAPI* and *TAZ* are major downstream effectors of the Hippo pathway that regulates key processes related to cell growth, tissue homeostasis, organ size, and regeneration [81–83], especially in ocular development [84,85] and liver regeneration [86]. *YAPI* acts as a central signal-responsive regulator of multipotent pancreatic progenitor in the embryonic development of pancreas [87]. Systemic effects should be taken into account when modulating the *YAPI* pathway. Although our finding indicates a protective role of increased *YAPI* level in AD, elevated *YAPI* activity has been found in several types of human cancers [81,83,88]. Therefore, overactivation of *YAPI* in the elderly with cognitive impairment might increase the risk of cancer and this would hinder future efforts using *YAPI* as a valid therapeutic target of AD.

Although we have provided a comprehensive and highly curated analysis of AD expression data sets, this study had several limitations. First, the cross-platform normalization only retained the common genes from different studies, thereby decreasing the total number of genes under consideration. Second, we did not include the most recently released expression data sets during our analysis, and we will include these data sets later for the [AlzData.org](http://AlzData.org) Web server. Third, the sample size in respect of hippocampus and entorhinal cortex available for study was still limited, and the larger sample size of the frontal cortex might contribute more weight to

the results. In addition, because of the lack of detailed information regarding RNA quality and potentially inconsistent diagnosis criteria for AD in some data sets, the results should be interpreted with caution.

In summary, we obtained a robust DEG list for four AD brain regions based on a large sample size. We identified several hub genes with multiple lines of AD-related supporting evidence and established a publicly accessible Web server for these results.

In particular, we found a previous unknown *YAP1*-initiated regulatory network active during AD development. Our results offer a place of reference for gene expression alterations in AD brain available to future hypothesis-driven, gene-central studies, as well as providing information about potential therapeutic targets. Further functional experiments, such as Chip-seq and animal experiments, are required to validate our results and to uncover the functions of the genes identified in this study.

### Acknowledgments

The authors thank Ian Logan for language editing and helpful comments and the three anonymous reviewers for their constructive comments and suggestions. This study was supported by the Key Program of National Natural Science Foundation of China (NSFC, 31730037), the Bureau of Frontier Sciences and Education (QYZDJ-SSW-SMC005), the Strategic Priority Research Program (B) (XDB02020003), and the West Light Foundation of the Chinese Academy of Sciences. The sponsor had no role in the study design, in the collection, analysis, and interpretation of data; in the writing of the article; or in the decision to submit the article for publication. The authors appreciate the colleagues for their sharing of expression data: John Hardy and colleagues for AD mouse models; Webster J., Gibbs R., Myers A., and colleagues for GSE15222; Nakabeppu Y., Hokama M., and colleagues for GSE36980; Liang and colleagues for GSE5281. The authors thank the International Genomics of Alzheimer's Project (IGAP) for providing summary results data for these analyses. The investigators within IGAP contributed to the design and implementation of IGAP and/or provided data but did not participate in analysis or writing of this report. IGAP was made possible by the generous participation of the control subjects, the patients, and their families. The i-Select chips were funded by the French National Foundation on Alzheimer's disease and related disorders. EADI was supported by the LABEX (laboratory of excellence program investment for the future) DISTALZ grant, Inserm, Institut Pasteur de Lille, Université de Lille 2, and the Lille University Hospital. GERAD was supported by the Medical Research Council (grant no. 503480), Alzheimer's Research UK (grant no. 503176), the Wellcome Trust (grant no. 082604/2/07/Z), and German Federal Ministry of Education and Research (BMBF): Competence Network Dementia (CND) grant no. 01GI0102, 01GI0711, 01GI0420. CHARGE was partly sup-

ported by the NIH/NIA grant R01 AG033193 and the NIA AG081220 and AGES contract N01-AG-12100, the NHLBI grant R01 HL105756, the Icelandic Heart Association, the Erasmus Medical Center, and Erasmus University. ADGC was supported by the NIH/NIA grants: U01 AG032984, U24 AG021886, U01 AG016976, and the grant ADGC-10-196728.

### Supplementary data

Supplementary data related to this article can be found at <http://dx.doi.org/10.1016/j.jalz.2017.08.012>.

### RESEARCH IN CONTEXT

1. Systematic review: The authors reviewed the related literature studies using PubMed and retrieved relevant data from Gene Expression Omnibus. There were dozens of studies focusing on expression alterations of Alzheimer's disease (AD) brain, and a few of them investigated the transcriptomic regulatory network. These relevant citations were appropriately cited.
2. Interpretation: Our data indicated potentially causal upstream regulators in the transcriptional network of AD brain. The findings were validated by functional assay and were consistent with previous observations.
3. Future directions: The article generated a robust differentially expressed gene list and a comprehensive Web server based on a large number of AD brain tissues, leading to a framework for continued studies of AD brain transcriptomics. The prioritized hub genes and upstream regulators might benefit further gene-centered, hypothesis-driven research.

### References

- [1] Serrano-Pozo A, Frosch MP, Masliah E, Hyman BT. Neuropathological alterations in Alzheimer disease. *Cold Spring Harb Perspect Med* 2011;1:a006189.
- [2] Alzheimer's association. 2016 Alzheimer's disease facts and figures. *Alzheimers Dement* 2016;12:459–509.
- [3] Tanzi RE. The genetics of Alzheimer disease. *Cold Spring Harb Perspect Med* 2012;2:a006296.
- [4] Lambert JC, Ibrahim-Verbaas CA, Harold D, Naj AC, Sims R, Bellenguez C, et al. Meta-analysis of 74,046 individuals identifies 11 new susceptibility loci for Alzheimer's disease. *Nat Genet* 2013; 45:1452–8.
- [5] Blalock EM, Geddes JW, Chen KC, Porter NM, Markesbery WR, Landfield PW. Incipient Alzheimer's disease: microarray correlation

- analyses reveal major transcriptional and tumor suppressor responses. *Proc Natl Acad Sci U S A* 2004;101:2173–8.
- [6] Dunckley T, Beach TG, Ramsey KE, Grover A, Mastroeni D, Walker DG, et al. Gene expression correlates of neurofibrillary tangles in Alzheimer's disease. *Neurobiol Aging* 2006;27:1359–71.
- [7] Liang WS, Dunckley T, Beach TG, Grover A, Mastroeni D, Walker DG, et al. Gene expression profiles in anatomically and functionally distinct regions of the normal aged human brain. *Physiol Genomics* 2007;28:311–22.
- [8] Berchtold NC, Cribbs DH, Coleman PD, Rogers J, Head E, Kim R, et al. Gene expression changes in the course of normal brain aging are sexually dimorphic. *Proc Natl Acad Sci U S A* 2008;105:15605–10.
- [9] Liang WS, Reiman EM, Valla J, Dunckley T, Beach TG, Grover A, et al. Alzheimer's disease is associated with reduced expression of energy metabolism genes in posterior cingulate neurons. *Proc Natl Acad Sci U S A* 2008;105:4441–6.
- [10] Webster JA, Gibbs JR, Clarke J, Ray M, Zhang W, Holmans P, et al. Genetic control of human brain transcript expression in Alzheimer disease. *Am J Hum Genet* 2009;84:445–58.
- [11] Williams C, Mehrian Shai R, Wu Y, Hsu YH, Sitzler T, Spann B, et al. Transcriptome analysis of synaptoneuroosomes identifies neuroplasticity genes overexpressed in incipient Alzheimer's disease. *PLoS One* 2009;4:e4936.
- [12] Astarita G, Jung KM, Berchtold NC, Nguyen VQ, Gillen DL, Head E, et al. Deficient liver biosynthesis of docosahexaenoic acid correlates with cognitive impairment in Alzheimer's disease. *PLoS One* 2010;5:e12538.
- [13] Tan MG, Chua WT, Esiri MM, Smith AD, Vinters HV, Lai MK. Genome wide profiling of altered gene expression in the neocortex of Alzheimer's disease. *J Neurosci Res* 2010;88:1157–69.
- [14] Blalock EM, Buechel HM, Popovic J, Geddes JW, Landfield PW. Microarray analyses of laser-captured hippocampus reveal distinct gray and white matter signatures associated with incipient Alzheimer's disease. *J Chem Neuroanat* 2011;42:118–26.
- [15] Simpson JE, Ince PG, Shaw PJ, Heath PR, Raman R, Garwood CJ, et al. Microarray analysis of the astrocyte transcriptome in the aging brain: relationship to Alzheimer's pathology and APOE genotype. *Neurobiol Aging* 2011;32:1795–807.
- [16] Berson A, Barbash S, Shaltiel G, Goll Y, Hanin G, Greenberg DS, et al. Cholinergic-associated loss of hnRNP-A/B in Alzheimer's disease impairs cortical splicing and cognitive function in mice. *EMBO Mol Med* 2012;4:730–42.
- [17] Cribbs DH, Berchtold NC, Perreau V, Coleman PD, Rogers J, Tenner AJ, et al. Extensive innate immune gene activation accompanies brain aging, increasing vulnerability to cognitive decline and neurodegeneration: a microarray study. *J Neuroinflammation* 2012;9:179.
- [18] Durrenberger PF, Fernando FS, Magliozzi R, Kashefi SN, Bonnett TP, Ferrer I, et al. Selection of novel reference genes for use in the human central nervous system: a BrainNet Europe Study. *Acta Neuropathol* 2012;124:893–903.
- [19] Sarvari M, Hrabovszky E, Kallo I, Solymosi N, Liko I, Berchtold N, et al. Menopause leads to elevated expression of macrophage-associated genes in the aging frontal cortex: rat and human studies identify strikingly similar changes. *J Neuroinflammation* 2012;9:264.
- [20] Silva AR, Grinberg LT, Farfel JM, Diniz BS, Lima LA, Silva PJ, et al. Transcriptional alterations related to neuropathology and clinical manifestation of Alzheimer's disease. *PLoS One* 2012;7:e48751.
- [21] Berchtold NC, Coleman PD, Cribbs DH, Rogers J, Gillen DL, Cotman CW. Synaptic genes are extensively downregulated across multiple brain regions in normal human aging and Alzheimer's disease. *Neurobiol Aging* 2013;34:1653–61.
- [22] Blair LJ, Nordhues BA, Hill SE, Scaglione KM, O'Leary JC 3rd, Fontaine SN, et al. Accelerated neurodegeneration through chaperone-mediated oligomerization of tau. *J Clin Invest* 2013;123:4158–69.
- [23] Miller JA, Woltjer RL, Goodenbour JM, Horvath S, Geschwind DH. Genes and pathways underlying regional and cell type changes in Alzheimer's disease. *Genome Med* 2013;5:48.
- [24] Zhang B, Gaiteri C, Bodea LG, Wang Z, McElwee J, Podtelezchnikov AA, et al. Integrated systems approach identifies genetic nodes and networks in late-onset Alzheimer's disease. *Cell* 2013;153:707–20.
- [25] Hokama M, Oka S, Leon J, Ninomiya T, Honda H, Sasaki K, et al. Altered expression of diabetes-related genes in Alzheimer's disease brains: the Hisayama study. *Cereb Cortex* 2014;24:2476–88.
- [26] Lai MK, Esiri MM, Tan MG. Genome-wide profiling of alternative splicing in Alzheimer's disease. *Genom Data* 2014;2:290–2.
- [27] Lu T, Aron L, Zullo J, Pan Y, Kim H, Chen Y, et al. REST and stress resistance in ageing and Alzheimer's disease. *Nature* 2014;507:448–54.
- [28] Narayanan M, Huynh JL, Wang K, Yang X, Yoo S, McElwee J, et al. Common dysregulation network in the human prefrontal cortex underlies two neurodegenerative diseases. *Mol Syst Biol* 2014;10:743.
- [29] Durrenberger PF, Fernando FS, Kashefi SN, Bonnett TP, Seilhean D, Nait-Oumesmar B, et al. Common mechanisms in neurodegeneration and neuroinflammation: a BrainNet Europe gene expression microarray study. *J Neural Transm (Vienna)* 2015;122:1055–68.
- [30] Simpson JE, Ince PG, Minett T, Matthews FE, Heath PR, Shaw PJ, et al. Neuronal DNA damage response-associated dysregulation of signalling pathways and cholesterol metabolism at the earliest stages of Alzheimer-type pathology. *Neuropathol Appl Neurobiol* 2016;42:167–79.
- [31] Bossers K, Wirz KT, Meerhoff GF, Essing AH, van Dongen JW, Houba P, et al. Concerted changes in transcripts in the prefrontal cortex precede neuropathology in Alzheimer's disease. *Brain* 2010;133:3699–723.
- [32] Cooper-Knock J, Kirby J, Ferraiuolo L, Heath PR, Rattray M, Shaw PJ. Gene expression profiling in human neurodegenerative disease. *Nat Rev Neurol* 2012;8:518–30.
- [33] Niculescu AB, Le-Niculescu H. Convergent functional genomics: what we have learned and can learn about genes, pathways, and mechanisms. *Neuropsychopharmacology* 2010;35:355–6.
- [34] Niculescu AB 3rd, Segal DS, Kuczenski R, Barrett T, Hauger RL, Kelsoe JR. Identifying a series of candidate genes for mania and psychosis: a convergent functional genomics approach. *Physiol Genomics* 2000;4:83–91.
- [35] Taminou J, Meganck S, Lazar C, Steenhoff D, Coletta A, Molter C, et al. Unlocking the potential of publicly available microarray data using inSilicoDb and inSilicoMerging R/Bioconductor packages. *BMC Bioinformatics* 2012;13:335.
- [36] Johnson WE, Li C, Rabinovic A. Adjusting batch effects in microarray expression data using empirical Bayes methods. *Biostatistics* 2007;8:118–27.
- [37] Chen C, Grennan K, Badner J, Zhang D, Gershon E, Jin L, et al. Removing batch effects in analysis of expression microarray data: an evaluation of six batch adjustment methods. *PLoS One* 2011;6:e17238.
- [38] Luo J, Schumacher M, Scherer A, Sanoudou D, Megherbi D, Davison T, et al. A comparison of batch effect removal methods for enhancement of prediction performance using MAQC-II microarray gene expression data. *Pharmacogenomics J* 2010;10:278–91.
- [39] Bushel P. pvca: Principal Variance Component Analysis (PVCA). R package version 1.10.0 2013. Available at: <https://bioconductor.org/packages/release/bioc/html/pvca.html>. Accessed September 27, 2017.
- [40] Ritchie ME, Phipson B, Wu D, Hu Y, Law CW, Shi W, et al. limma powers differential expression analyses for RNA-sequencing and microarray studies. *Nucleic Acids Res* 2015;43:e47.
- [41] Zhang B, Horvath S. A general framework for weighted gene co-expression network analysis. *Stat Appl Genet Mol Biol* 2005;4:Article17.

- [42] Langfelder P, Horvath S. WGCNA: an R package for weighted correlation network analysis. *BMC Bioinformatics* 2008;9:559.
- [43] Langfelder P, Zhang B, Horvath S. Defining clusters from a hierarchical cluster tree: the Dynamic Tree Cut package for R. *Bioinformatics* 2008;24:719–20.
- [44] Langfelder P, Horvath S. Fast R functions for robust correlations and hierarchical clustering. *J Stat Softw* 2012;46:i11.
- [45] Langfelder P, Luo R, Oldham MC, Horvath S. Is my network module preserved and reproducible? *PLoS Comput Biol* 2011;7:e1001057.
- [46] Horvath S, Dong J. Geometric interpretation of gene co-expression network analysis. *PLoS Comput Biol* 2008;4:e1000117.
- [47] Colantuoni C, Lipska BK, Ye T, Hyde TM, Tao R, Leek JT, et al. Temporal dynamics and genetic control of transcription in the human prefrontal cortex. *Nature* 2011;478:519–23.
- [48] Itan Y, Mazel N, Mazel B, Abhyankar A, Nitschke P, Quintana-Murci L, et al. HGCS: an online tool for prioritizing disease-causing gene variants by biological distance. *BMC Genomics* 2014;15:256.
- [49] Itan Y, Zhang SY, Vogt G, Abhyankar A, Herman M, Nitschke P, et al. The human gene connectome as a map of short cuts for morbid allele discovery. *Proc Natl Acad Sci U S A* 2013;110:5558–63.
- [50] Matarin M, Salih DA, Yasvoina M, Cummings DM, Guelfi S, Liu W, et al. A genome-wide gene-expression analysis and database in transgenic mice during development of amyloid or tau pathology. *Cell Rep* 2015;10:633–44.
- [51] Zhang DF, Li J, Wu H, Cui Y, Bi R, Zhou HJ, et al. CFH variants affect structural and functional brain changes and genetic risk of Alzheimer's disease. *Neuropsychopharmacology* 2016;41:1034–45.
- [52] Xiang Q, Bi R, Xu M, Zhang DF, Tan L, Zhang C, et al. Rare genetic variants of the transthyretin gene are associated with Alzheimer's disease in Han Chinese. *Mol Neurobiol* 2017;54:5192–200.
- [53] Huang da W, Sherman BT, Lempicki RA. Systematic and integrative analysis of large gene lists using DAVID bioinformatics resources. *Nat Protoc* 2009;4:44–57.
- [54] Shannon P, Markiel A, Ozier O, Baliga NS, Wang JT, Ramage D, et al. Cytoscape: a software environment for integrated models of biomolecular interaction networks. *Genome Res* 2003;13:2498–504.
- [55] Montojo J, Zuberi K, Rodriguez H, Kazi F, Wright G, Donaldson SL, et al. GeneMANIA Cytoscape plugin: fast gene function predictions on the desktop. *Bioinformatics* 2010;26:2927–8.
- [56] Landreth GE, Reed-Geaghan EG. Toll-like receptors in Alzheimer's disease. *Curr Top Microbiol Immunol* 2009;336:137–53.
- [57] Liang WS, Dunckley T, Beach TG, Grover A, Mastroeni D, Ramsey K, et al. Neuronal gene expression in non-demented individuals with intermediate Alzheimer's Disease neuropathology. *Neurobiol Aging* 2010;31:549–66.
- [58] Antonell A, Llado A, Altiirriba J, Botta-Orfila T, Balasa M, Fernandez M, et al. A preliminary study of the whole-genome expression profile of sporadic and monogenic early-onset Alzheimer's disease. *Neurobiol Aging* 2013;34:1772–8.
- [59] Darmanis S, Sloan SA, Zhang Y, Enge M, Caneda C, Shuer LM, et al. A survey of human brain transcriptome diversity at the single cell level. *Proc Natl Acad Sci U S A* 2015;112:7285–90.
- [60] Barabasi AL, Oltvai ZN. Network biology: understanding the cell's functional organization. *Nat Rev Genet* 2004;5:101–13.
- [61] Karch CM, Goate AM. Alzheimer's disease risk genes and mechanisms of disease pathogenesis. *Biol Psychiatry* 2015;77:43–51.
- [62] Kurronen A, Pihlaja R, Pollari E, Kanninen K, Storvik M, Wong G, et al. Adult and neonatal astrocytes exhibit diverse gene expression profiles in response to beta amyloid *ex vivo*. *World J Neurosci* 2012;2:57–67.
- [63] Wakutani Y, Ghani M, Tokuhiro S, Bohm C, Chen F, Sato C, et al. Misprocessing of APP and accumulation of  $\beta$ -Amyloid causes early alteration of pathways implicated in late-onset Alzheimer disease. Available at: <https://www.ncbi.nlm.nih.gov/geo/query/acc.cgi?acc=GSE31372>. Accessed September 27, 2017.
- [64] Piccolo S, Dupont S, Cordenonsi M. The biology of YAP/TAZ: hippo signaling and beyond. *Physiol Rev* 2014;94:1287–312.
- [65] Puthiyedth N, Riveros C, Berretta R, Moscato P. Identification of differentially expressed genes through integrated study of Alzheimer's disease affected brain regions. *PLoS One* 2016;11:e0152342.
- [66] Taminau J, Lazar C, Meganck S, Nowe A. Comparison of merging and meta-analysis as alternative approaches for integrative gene expression analysis. *ISRN Bioinform* 2014;2014:345106.
- [67] De Strooper B, Karran E. The cellular phase of Alzheimer's disease. *Cell* 2016;164:603–15.
- [68] Miller JA, Oldham MC, Geschwind DH. A systems level analysis of transcriptional changes in Alzheimer's disease and normal aging. *J Neurosci* 2008;28:1410–20.
- [69] Liang D, Han G, Feng X, Sun J, Duan Y, Lei H. Concerted perturbation observed in a hub network in Alzheimer's disease. *PLoS One* 2012;7:e40498.
- [70] Kochubey O, Lou X, Schneggenburger R. Regulation of transmitter release by Ca(2+) and synaptotagmin: insights from a large CNS synapse. *Trends Neurosci* 2011;34:237–46.
- [71] Mukherjee S, Russell JC, Carr DT, Burgess JD, Allen M, Serie DJ, et al. Systems biology approach to late-onset Alzheimer's disease genome-wide association study identifies novel candidate genes validated using brain expression data and *Caenorhabditis elegans* experiments. *Alzheimers Dement* 2017. <http://dx.doi.org/10.1016/j.jalz.2017.01.016>.
- [72] Fernandez-L A, Northcott PA, Dalton J, Fraga C, Ellison D, Angers S, et al. YAP1 is amplified and up-regulated in hedgehog-associated medulloblastomas and mediates Sonic hedgehog-driven neural precursor proliferation. *Genes Dev* 2009;23:2729–41.
- [73] Musah S, Wrighton PJ, Zaltsman Y, Zhong X, Zorn S, Parlato MB, et al. Substratum-induced differentiation of human pluripotent stem cells reveals the coactivator YAP is a potent regulator of neuronal specification. *Proc Natl Acad Sci U S A* 2014;111:13805–10.
- [74] Huang Z, Hu J, Pan J, Wang Y, Hu G, Zhou J, et al. YAP stabilizes SMAD1 and promotes BMP2-induced neocortical astrocytic differentiation. *Development* 2016;143:2398–409.
- [75] Huang Z, Wang Y, Hu G, Zhou J, Mei L, Xiong WC. YAP is a critical inducer of SOCS3, preventing reactive astrogliosis. *Cereb Cortex* 2016;26:2299–310.
- [76] Swistowski A, Zhang Q, Orcholski ME, Crippen D, Vitelli C, Kurakin A, et al. Novel mediators of amyloid precursor protein signaling. *J Neurosci* 2009;29:15703–12.
- [77] Orcholski ME, Zhang Q, Bredesen DE. Signaling via amyloid precursor-like proteins APLP1 and APLP2. *J Alzheimers Dis* 2011;23:689–99.
- [78] Plouffe SW, Hong AW, Guan KL. Disease implications of the Hippo/YAP pathway. *Trends Mol Med* 2015;21:212–22.
- [79] Yu HB, Johnson R, Kunarso G, Stanton LW. Coassembly of REST and its cofactors at sites of gene repression in embryonic stem cells. *Genome Res* 2011;21:1284–93.
- [80] Arnold P, Scholer A, Pachkov M, Balwiercz PJ, Jorgensen H, Stadler MB, et al. Modeling of epigenome dynamics identifies transcription factors that mediate Polycomb targeting. *Genome Res* 2013;23:60–73.
- [81] Moroishi T, Hansen CG, Guan KL. The emerging roles of YAP and TAZ in cancer. *Nat Rev Cancer* 2015;15:73–9.
- [82] Yu C, Ji SY, Dang YJ, Sha QQ, Yuan YF, Zhou JJ, et al. Oocyte-expressed yes-associated protein is a key activator of the early zygotic genome in mouse. *Cell Res* 2016;26:275–87.
- [83] Mo JS, Meng Z, Kim YC, Park HW, Hansen CG, Kim S, et al. Cellular energy stress induces AMPK-mediated regulation of YAP and the Hippo pathway. *Nat Cell Biol* 2015;17:500–10.
- [84] Miesfeld JB, Gestri G, Clark BS, Flinn MA, Poole RJ, Bader JR, et al. Yap and Taz regulate retinal pigment epithelial cell fate. *Development* 2015;142:3021–32.

- [85] Kim JY, Park R, Lee JH, Shin J, Nickas J, Kim S, et al. Yap is essential for retinal progenitor cell cycle progression and RPE cell fate acquisition in the developing mouse eye. *Dev Biol* 2016;419:336-47.
- [86] Yimlamai D, Fowl BH, Camargo FD. Emerging evidence on the role of the Hippo/YAP pathway in liver physiology and cancer. *J Hepatol* 2015;63:1491-501.
- [87] Cebola I, Rodriguez-Segui SA, Cho CH, Bessa J, Rovira M, Luengo M, et al. TEAD and YAP regulate the enhancer network of human embryonic pancreatic progenitors. *Nat Cell Biol* 2015;17:615-26.
- [88] Stein C, Bardet AF, Roma G, Bergling S, Clay I, Ruchti A, et al. YAP1 exerts its transcriptional control via TEAD-mediated activation of enhancers. *PLoS Genet* 2015;11:e1005465.

# Did you know?

The screenshot displays the homepage of the journal *Alzheimer's & Dementia*. At the top, there is a search bar with a dropdown menu set to 'This Periodical' and a search button. Below the search bar, there are links for 'Advanced Search', 'MEDLINE', 'My Recent Searches', 'My Saved Searches', and 'Search Tips'. The main content area features the 'Current Issue' for November 2009, Vol. 5, No. 8, which is highlighted as 'Now Included on MEDLINE'. A 'Featured Articles' section lists several research papers, including one on cognitive performance in African Americans and another on telomere lengths in Alzheimer's disease. The left sidebar contains navigation links such as 'JOURNAL HOME', 'CURRENT ISSUE', 'ARTICLES IN PRESS', and 'SEARCH THIS JOURNAL'. The bottom of the page includes a 'JOURNAL ACCESS' section with a 'JOIN' button and a footer stating the journal is published by Elsevier for the Alzheimer's Association.

You can search **Alzheimer's & Dementia** and 400 top medical and health sciences journals online, including **MEDLINE**.

Visit [www.alzheimersanddementia.org](http://www.alzheimersanddementia.org) today!

## Supplementary Materials and Methods

### *1. Data collection and pre-processing*

We retrieved all the original microarray data regarding AD through searching the Gene Expression Omnibus (GEO, <https://www.ncbi.nlm.nih.gov/geo>) with keyword “Alzheimer”. To achieve reliable results, we performed an exhaustive, non-redundant data retrieval using the following series of criteria: 1) AD-related expression profiles in the ArrayExpress database (<https://www.ebi.ac.uk/arrayexpress/>) were checked to avoid potential omissions; 2) Studies with no genome-wide probes or few probes were filtered; 3) For those GSE series with possibly duplicated samples or identical sample resource, we retained the one with a larger sample size and excluded another; 4) Only expression profiles of human postmortem brain tissues from hippocampus (HP), entorhinal cortex (EC), frontal cortex (FC), and temporal cortex (TC), which were main regions affected by AD, were included; 5) Data retrieval and quality control were double-checked by two investigators. By January 2016, a total of 20 expression datasets were obtained: GSE12685 [1], GSE48350 [2], GSE66333 [3], GSE53890 [4], GSE36980 [5], GSE13214 [6], GSE15222 [7], GSE5281 [8, 9], GSE44770 [10], GSE33000 [11], GSE9770 [12], GSE37264 (exon level) [13], GSE37263 (gene level) [14], GSE29652 [15], GSE28146 [16], GSE1297 [17], GSE29378 [18], GSE26927 [19, 20], GSE26972 [21], and GSE4757 [22]. After manual inspection and filter, there were four datasets retained for EC (GSE26927, GSE48350, GSE26972, GSE5281), five datasets for HP (GSE28146, GSE48350, GSE5281, GSE29378, GSE36980), five datasets for TC (GSE37263, GSE29652, GSE36980, GSE15222, GSE5281), and eight datasets for FC (GSE12685, GSE48350, GSE66333, GSE53890, GSE36980, GSE15222, GSE5281, GSE33000) (Table S1). To ensure data quality, samples that were younger than 50 years old, or were outliers in our principal component analysis (PCA) of expression distribution, were excluded from this study. Finally, a total of 1246 brain samples for all four brain regions (684 AD and 562 control) were compiled for the detailed analysis. More information about sample compositions of each brain region was shown in Supplementary Table S1.

GEO soft-formatted expression datasets were downloaded and were checked for normalization and log<sub>2</sub> transformation; if not, mas5 method and log<sub>2</sub> transformation were applied by affy package in Bioconductor (<http://www.bioconductor.org/>) [23]. Probe IDs in each study were mapped to entrez IDs and probes mapping to multiple genome regions or without corresponding entrez IDs were filtered. A probe with more than 20% missing values in all samples was excluded; otherwise, missing value in this probe was replaced with the mean expression value of this probe. According to the data holder and the array manual, the missing values refer to signal not detected in the array. Furthermore, for a gene with multiple probes, median value of these probes was used. For microarray studies, there is a concern with respect to SNPs present in the genomic region targeted by the probes leading to spurious results. We mapped the probe sequences of the 17 highlighted upstream regulator genes to the human assembly GRCh37 (also known as hg19, <http://www.ensembl.org/info/website/tutorials/grch37.html>) and the dbSNP (<https://www.ncbi.nlm.nih.gov/projects/SNP/>). We identified no common (minor allele frequency > 0.05) variants within the probe region. Because GSE15222 for TC and GSE33000 for FC have far more samples than any other studies of the same brain regions, combining these two datasets with others may blur effects of studies with a relatively small sample size. Therefore, we used these two studies as independent validation datasets for the compiled dataset of different studies.



## **2. Cross-platform normalization**

Considering the fact that these microarray studies were processed in multiple batches, which would result in systematic error or “batch effects”, it is essential to adjust these microarray data for batch effects and standardize expression data at the probe level prior to analysis. Cross-platform normalization is a method that combines all expression data from different microarray studies into a unified dataset. This method could remove artifacts between different platforms (batch effects) and preserve “real” biological differences between experimental conditions, and was regarded to have a better performance in robust biomarker detection than the meta-analysis method [24]. A number of studies using this approach have established a good example in the field [25, 26]. As had been systematically evaluated by Chen et al. [27], ComBat, an empirical Bayes method, outperformed other programs by most of metrics (e.g. precision, accuracy, and overall performance). It was also recommended for adjusting data whose batch sizes are small [28]. We thus performed the cross-platform normalization to merge all expression data of each brain region by the algorithm ComBat in R package *inSilicoMerging* [29, 30]. The empirical Bayesian approach in ComBat assumes factors resulting in batch effects would affect the entire transcriptome in similar ways and adjusts for these common systematic batch biases across genes [29, 30].

Although ComBat was evaluated to be a good choice to remove batch effects [27], it is necessary to measure how much variation in the expression data was attributable to batch effects. To evaluate the efficiency and reliability of the batch effect removal by the ComBat method, we performed the principal variance component analysis (PVCA) using R package *pvca* [31], a recognized tool that could determine the sources of variability in a dataset and to quantify the magnitude of each source of variability. PVCA estimates source and proportion of variation through a integration of principal component analysis (PCA) and variance component analysis (VCA), and the resulting value represents the overall variation explained by that component. Our PVCA revealed that ComBat eliminated the batch effects (covariate = study) almost completely in all four combined brain regions (Supplementary Fig. S1). It is most likely that the detected difference in our combined datasets reflects true biological differences.

## **3. Differential gene expression analysis of merged datasets**

Cross-platform normalized expression data for each brain region was used to detect DEGs between AD patients and normal controls. Expression profiling was adjusted for age and gender by using a linear regression model during the identification of DEGs. Many other factors, such as APOE4 status, mini-mental state examination (MMSE) score, disease stage, postmortem interval (PMI), RNA integrity number (RIN), sample PH, sample preparation batch, and even diagnostic heterogeneity, would affect the detection of DEGs and should be taken into account for adjustment. Unfortunately, in most cases this kind of information was not available, thus hindering further adjustment in the overall analysis. For these samples with RNA quality and detailed sample information available, we found no difference regarding the RNA quality (RIN) in most cases, except for GSE66333 (Table S1). We also estimated the contribution of the confounding factors (age, sex, disease, study) to the variance of gene expression profiles by PVCA. We found that the contribution of study difference was marginal in our results.

In addition to the sample quality, we checked for each individual dataset for the related batch information regarding sample preparation and measurement. We found that some datasets were collected by using samples from different brain banks or were measured in batches (GSE29378, GSE37263, GSE48350, GSE15222, and GSE33000), whereas all the samples for most of the individual dataset were measured in a single platform. As described in the original studies, batch effects of GSE29378 [18], GSE37263 [14], and GSE48350 [2] were neglectable, while batch information was not available at the individual level for GSE15222 and GSE33000. Though the PVCA analysis showed that there were almost no batch effects of study difference and the biggest effect was the disease status (Supplementary Fig. S1), we cannot rule out the possibility of intra-dataset batch effects on final DEG detection. To make it clear and for potential cross-validation, we provided the original meta-data of each dataset including all sample information at the Alzdata.org webserver (<http://www.alzdata.org/download.html>). Anyone who has a special interest could retrieve the data and perform more stringent analysis with covariates adjustment in given datasets where RNA quality and detailed sample information was available. Information for the RNA quality of the respective dataset was provided in Table S1.

Differential expression analysis was conducted by R package *limma* and Benjamini-Hochberg's (BH) method was used to correct for multiple comparisons [32]. Enrichment of biological process in Gene Ontology of DEGs was analyzed by DAVID 6.8 (<https://david.ncifcrf.gov/>) [33].

#### **4. Co-expression network, hub genes, and DEG-enriched modules**

Weighted gene co-expression network analysis was used to construct gene co-expression networks by package WGCNA in R (<https://www.r-project.org/>) [34-38]. A co-expression network was constituted by a set of nodes and a set of edges connecting between pairs of nodes, with each node representing a single gene and each edge representing the Pearson correlation coefficient between expression levels of two genes. Co-expression network was constructed for four individual brain regions using the merged datasets, combined datasets of four brain regions (multi-tissue network), and each physiological state (AD or control). Expression residuals after adjusting for age and sex using a linear model were used as input for WGCNA. The correlation matrix was obtained by calculating the Pearson correlations between all gene pairs across all subjects in the dataset, and then were converted into an adjacency matrix using a power function (power  $\beta = 14$  for individual brain regions,  $\beta = 12$  for combined brain regions). For module detection in co-expression network, the adjacency matrix was further transformed into a topological overlap matrix (TOM), and hierarchical clustering was used to group genes based on the dissimilarity matrix (1-TOM), followed by a dynamic cut-tree algorithm to dynamically cut clustering dendrogram branches into gene modules. A height cutoff of 0.1 for combined brain regions and 0.3 for individual brain regions were used to merge modules whose expression profiles are highly similar. Each module was assigned to a unique color identifier to distinguish each other.

To assessing whether modules in co-expression networks were **preserved** across different brain regions, pairwise preservation tests were applied to the four brain regions. Module conservation (as evaluated by Z-score [38] and module membership (kME) correlations [39]) was computed by WGCNA.  $2 < Z\text{-score} < 5$  indicates weak preservation,  $5 < Z\text{-score} < 10$  indicates moderate preservation, and  $Z\text{-score} > 10$  indicates high preservation. Modules with kME showing a high correlation between two networks are highly preserved (Supplementary Fig. S2-S3). Connectivity (k) in a

co-expression network / module was defined as the sum of correlation strengths with other genes, a term reflecting the expression relationship between a gene and other genes in the same module. Intramodule connectivity ( $k$ ) of each gene in cases ( $k_{AD}$ ) and controls ( $k_{CTL}$ ) was calculated independently based on networks constructed with combined expression profiles of all four brain regions, and the connectivity was scaled relative to the maximally connected gene ( $k = 1$ ) in each module. Hub genes were defined as genes with  $k > 0.8$  in AD or control network.

Modules containing more DEGs than expected in any of the four brain regions were defined as DEG-enriched modules. DEGs enrichment analysis was performed by using Fisher's exact test, with adjustment for multiple comparisons by using the BH method. Single cell RNA-seq data from GSE67835 were used to define cell type specific genes for neurons, astrocytes, microglia, oligodendrocytes, oligodendrocyte precursor cells (OPCs) and endothelial cells [40]. Raw counts data were downloaded and normalized by R package DESeq2 [41]. Cell type specific genes were identified based on average expression level for one cell type versus the average expression level in the remaining cell types [42]. Enrichment of cell-type-specific genes for each module was calculated by Fisher's exact test and the BH method was used to adjust for multiple comparisons.

### 5. Convergent functional genomics (CFG)

The convergent functional genomic (CFG) approach integrated multiple lines of AD-related evidence [43, 44]. A CFG score was assigned to gene of interest based on the below five lines of evidence, with each line of evidence being assigned 1 point. The sum of the scores of the five lines of evidence resulted in a total CFG score ranging from 0 to 5:

1) Genetic association. If a gene had at least one locus being significantly associated with AD based on the summary statistics from the International Genomics of Alzheimer's Project [IGAP] [45], 1 point was assigned; otherwise zero point.

2) Genetic regulation of gene expression. If a gene was **associated with** Expression Quantitative Trait Loci (eQTLs) showing an AD-risk in IGAP data [45, 46], 1 point was assigned; otherwise zero point.

3) Protein-protein interaction. If a gene was physically interacted with any AD core genes (*APP*, *PSEN1*, *PSEN2*, *APOE*, or *MAPT*) [47, 48], 1 point was assigned; otherwise zero point.

4) Expression correlation with AD pathology. If the expression level of a gene was correlated with AD pathology in AD mice [49], 1 point was assigned; otherwise zero point.

5) Early alteration in AD mouse brain. If a gene showed differential expression in hippocampus of 2-month-old AD mice compared with age matched wild-type mice [49], 1 point was assigned; otherwise zero point.

Note that inclusion criteria for each piece of evidence should be consistent in principle. In the current study, to capture the cross-validated targets as possible as we can for an overall pattern analysis (Fig. 3C), the cutoff of significant *P-value* was thus arbitrarily set based on the manner of *P-value* distribution for each lines of evidence. We admitted that some targets with marginal significance at the single-dimension are most likely to be false positive, and genes with a higher level of significance at the single-dimension should be assigned more weight than genes with a lower level of significance at that dimension. However, it is reasonable to speculate that the gene of interest would be truly disease-related if it could be cross-validated by multiple lines of evidence, regardless of the level of significance at the single-dimension. As shown

in Table S6, the CFG approach could assign proper weight to those known AD genes such as *APP* and *APOE*. Details for each lines of evidence were described below.

### **5.1. Genetic association and expressional quantitative trait loci (eQTL) analysis**

Association of the common variants of the target genes with AD were retrieved from the summary statistics (7,055,881 SNPs) of IGAP, which is the most recent and largest GWAS study of AD based on 17,008 AD cases and 37,154 controls of European ancestry [45]. The IGAP dataset acts as a reliable and comprehensive resource for genetic association in AD research. Considering the fact that there were only 20 genome-wide significant loci surviving the multiple testing corrections, no novel genes would be identified with a cutoff of the genome-wide  $P$ -value. We therefore arbitrarily set the cutoff value of significant  $P$ -value at 0.001 for our CFG integration. One point was assigned to the target gene if at least one locus within that gene was associated with AD in IGAP data based on our cutoff  $P$ -value; otherwise zero point.

Expression data and genotyping data from Braincloud, which contained post-mortem brain tissues of 269 subjects spanning the majority of human lifespan, were used to compute eQTL [46]. Gene expression data was downloaded from GEO (accession ID: GSE30272 [46]) and was pre-processed as described in the above section 2. Two surrogate variables were adjusted as recommended by the authors of Braincloud [46]. Genotyping data was taken from the database of Genotypes and Phenotypes (dbGAP, <https://www.ncbi.nlm.nih.gov/gap>) (accession ID: phs000417.v1.p1). Infants (age < 0 year old) were excluded from the analysis according to PCA [46]. Finally, a total of 654,333 SNPs were tested for association with expression of 17160 genes using Plink v1.07 (<http://pngu.mgh.harvard.edu/purcell/plink/>) [50] by a linear regression model, and adjusted for covariates age and gender. The eQTLs were determined by SNPs showing a significant association with gene expression at a cutoff  $P < 0.001$ , to capture all suggestive targets. One point was assigned to the target gene if its expression was **associated with** ( $P_{\text{eQTL}} < 0.001$ ) at least one AD-related locus ( $P_{\text{GWAS}} < 0.001$ ); otherwise zero point.

### **5.2. Biological distance between target genes and AD core genes**

To prioritize the DEGs, protein-protein interaction (PPI) based biological distance was introduced in the convergent approach. The human gene connectome (HGC) provides all plausibly biological routes, distances, and degrees of separation between all pairs of human genes, which can be used to prioritize a list of target genes according to their biological proximity to core genes of interest [47, 48]. Gene specific human connectome data was downloaded from the Human Gene Connectome Server (<http://hgc.rockefeller.edu>). Biological distances based on PPI and connectivity  $P$ -values between each pair of target gene and AD core gene (*APP*, *PSEN1*, *PSEN2*, *APOE*, and *MAPT*) were extracted by an in-house Perl script. One point was assigned to the target gene if it showed a significant PPI ( $P < 0.05$ ) with any of the AD core genes; otherwise zero point.

### **5.3. AD mouse and cellular models**

In addition to the expression profiling data of human brain, we explored the spatial-temporal expression pattern of AD mouse models. Expression data and pathological features of AD transgenic and wide-type mice, including 219 brain tissues for five kinds of AD mouse models (transgenic mice with human mutant *APP* [K670N/M671L, TAS10], *PSEN1* [M146V, TPM], *APP/PSEN1* double mutant [homozygous and heterozygous TASTPM, HO/HET\_TASTPM], and human mutant *MAPT* [P301L, TAU] gene) and 114 brain tissues of age-matched wild-type (WT)

mice, covering three brain regions (hippocampus, cerebrum cortex, and cerebellum) and four life stages (2, 4, 8, and 18 months), were downloaded from Mouseac (<http://www.mouseac.org>) [49]. Those transgenic mice presented pathological characters (plaques and tangles) at or after 4 months old as described in the original paper [49]. Obvious A $\beta$  plaques did not form in 2 month-old AD mice of any type and AD pathology started earlier in hippocampus than in cortex, therefore genes with expression changes in hippocampus from 2-month old animals were thought to be early-changed genes in AD. Because TPM mice showed no amyloid deposition by 18 months old, we did not include mice of this model in the downstream analysis. DEGs between 2 month-old AD and WT mice were detected for each line of transgenic mouse (HO-TASTPM, HE-TASTPM, TAS10, TPM, and TAU) in hippocampus tissue as described in the above section 3. One point was assigned to the target gene if it showed a significant early alteration in hippocampus from 2-month old AD mice; otherwise zero point. Pearson correlations of gene expression and pathology for A $\beta$  line mice (HO-TASTPM, HE-TASTPM, TAS10 mice) and Tau mice in hippocampus were calculated by R package *psych* [51]. One point was assigned to the target gene if it showed a significant correlation with either A $\beta$  or Tau pathology; otherwise zero point.

To cross-validate the early alteration, expression profiles from additional AD mouse and cellular models were also retrieved. Expression data of mouse neonatal or adult astrocytes cultured on brain sections from wild-type/APdE9 (*APP/PSEN1* double mutant) mice (GSE29317) [52] and another dataset of AD mouse models (GSE31372, <https://www.ncbi.nlm.nih.gov/geo/query/acc.cgi?acc=GSE31372>) were downloaded from GEO and were pre-processed. DEGs were detected in neonatal astrocytes with or without A $\beta$  treatment, in 70-day old TgCRND8 (Transgenic *APP*, GSE31372) mice versus age-matched controls, using the same methods as described in the above section 3.

## 6. Cell cultures, RNA interference and transfections

U251 cells with stable expression of mutant APP (K670N/M671L, marked as U251-APP) were cultured in Roswell RPMI-1640 medium (HyClone, C11875500BT) supplemented with 10% fetal bovine serum at 37 °C in a humidified atmosphere incubator with 5% CO<sub>2</sub>, as described in our previous studies [53, 54]. Transfection with siRNA or plasmid DNA was performed using an electroporator (CUY21EDIT, Nepa gene, Japan) and electroporation cuvettes (EC-002S, Nepa gene, Japan) following manufactures' instructions. U251-APP cells were harvested by trypsinization and washed three times with Opti-MEM medium. After cell counting,  $1 \times 10^6$  cells were resuspended in 100  $\mu$ L Opti-MEM medium, then added 2.5  $\mu$ L siRNA (20  $\mu$ M) or 10  $\mu$ g plasmid DNA. After dispensing 100  $\mu$ L mixture into a cuvette, electroporation was carried out. After electroporation, cells were seeded in pre-warmed growth medium in 6-well plates. Supernatant in each well was replaced with equal volume of new growth medium after 24 h, and 1  $\mu$ g/mL doxycycline (Sigma; D9891) was added to induce *APP* expression. Cells were harvested at 72 h after transfection.

## 7. RNA extraction, RNA sequencing (RNA-seq) and Western blot (WB)

Total RNA was extracted by using the RNAeasy kit (TianGen, co.td.) according to the manufacturer's instructions. The A260/A280 ratio of total RNA was measured on a NanoDrop biophotometer (Thermo Fisher Scientific), and only samples with a value of 1.8–2.0 were used for subsequent experiments. Quality and integrity of RNA samples were also evaluated based on the 28S and 18S rRNA bands on a 1% agarose gel.

About 1.5  $\mu$ g total RNA per sample was used to prepare library for RNA-seq. Sequencing libraries were generated using the NEBNextUltra™ RNA Library Prep kit for Illumina (NEB, USA) following the manufacturer's recommendation and index codes were added to attribute sequence to each sample. The processed final library was sequenced on an IlluminaHiSeq 4000 platform, and 150 bp paired-ends reads were generated. Raw RNA-seq reads were trimmed to remove sequencing adapters and low quality reads. The clean reads were then aligned to the reference genome (GRCh38.p7) sequence using Tophat [55]. HTSeq-count [56] was used to count aligned reads that mapped to the annotated human genes (GRCh38.p7). Gene-level differential expression analyses were performed using DESeq2 [41]. Gene-level differential expression analyses and PCA (Fig. S9) analysis were performed using DESeq2 [41]. The RNA-seq data were uploaded to our database (<http://www.alzdata.org/download.html>) and GEO ([GSE100891](https://www.ncbi.nlm.nih.gov/geo/query/acc.cgi?acc=GSE100891), <https://www.ncbi.nlm.nih.gov/geo/query/acc.cgi?acc=GSE100891>).

Cell lysates of cells with *YAP1* overexpression, knockdown and scramble were prepared using the protein lysis buffer (Beyotime Institute of Biotechnology, P0013). Protein concentration was determined using BCA protein assay kit (Beyotime Institute of Biotechnology, P0012). Primary antibodies of GAPDH (proteintech group, #60004-I-IG), YAP1 (Cell Signaling Technology, #14074p), Tau (abcam, #ab80579), phosphorylated tau at threonine 181 (pTau181, SAB, #11107), phosphorylated tau at serine 396 (pTau396, Cell Signaling Technology, #9632s), APP (Cell Signaling Technology, #2450s), PSEN1 (Cell Signaling Technology, #5643), PSEN2 (Cell Signaling Technology, #9979), BACE1 (Cell Signaling Technology, #5606p), Nicastrin (Cell Signaling Technology, 5665), CDK5 (Santa Cruz Biotechnology, sc-6247), GSK3 $\alpha/\beta$  (Cell Signaling Technology, #5676), and A $\beta$  (1-42 Specific, Cell Signaling Technology, #14974) were used. The WB was performed according to routine procedure as described in our recent studies [57, 58]. In brief, 20  $\mu$ g proteins were separated by 12% SDS-PAGE, transferred to polyvinylidene fluoride membranes (Bio-Rad, #L1620177 Rev D). The membrane was soaked with 5% (w/v) skim milk for 2 h at room temperature, and then was incubated with the respective primary antibody overnight at 4°C. The membranes were washed 3 times with TBST (Tris Buffered Saline [Cell Signaling Technology, #9997] with Tween 20 [0.1%; Sigma, #P1379]), each time 5 min, followed by incubation with the peroxidase-conjugated secondary antibodies (anti-mouse [KPL, #474-1806] or anti-rabbit [KPL, #474-1506] IgG) for 1 h at room temperature. The membrane was visualized using enhanced chemiluminescence reagents (Millipore, #WBKLS0500) on the ChemiDoc MP Imaging system (Bio-Rad). For the targeted proteins with different molecular weights that could be well separated from each other on the gel,

we cut the transferred membrane into slices, each containing one target, and performed the WB using the respective antibody. For the targeted proteins with similar molecular weights, we run each target in separate gel electrophoresis and GAPDH in the same run was used as the loading control.

## 8. Construction of AlzData.org database

The AlzData.org webserver was constructed following the pipeline as described in our previous study [59]. Briefly, the database was based on LAMP (Linux-Apache-MySQL-PHP) software stack. Data were stored in MySQL and managed with phpMyAdmin. Web interfaces were shaped and developed by Javascript, Cascading Style Sheet (CSS), AJAX and jQuery plugins like Echarts and plotly. Data analysis module was written with PHP.

## Supplementary References

- [1] Williams C, Mehrian Shai R, Wu Y, Hsu YH, Sitzer T, Spann B, et al. Transcriptome analysis of synaptoneurosome identifies neuroplasticity genes overexpressed in incipient Alzheimer's disease. *PLoS One* 2009;4:e4936.
- [2] Berchtold NC, Cribbs DH, Coleman PD, Rogers J, Head E, Kim R, et al. Gene expression changes in the course of normal brain aging are sexually dimorphic. *Proc Natl Acad Sci U S A* 2008;105:15605-10.
- [3] Simpson JE, Ince PG, Minett T, Matthews FE, Heath PR, Shaw PJ, et al. Neuronal DNA damage response-associated dysregulation of signalling pathways and cholesterol metabolism at the earliest stages of Alzheimer-type pathology. *Neuropathol Appl Neurobiol* 2016;42:167-79.
- [4] Lu T, Aron L, Zullo J, Pan Y, Kim H, Chen Y, et al. REST and stress resistance in ageing and Alzheimer's disease. *Nature* 2014;507:448-54.
- [5] Hokama M, Oka S, Leon J, Ninomiya T, Honda H, Sasaki K, et al. Altered expression of diabetes-related genes in Alzheimer's disease brains: the Hisayama study. *Cereb Cortex* 2014;24:2476-88.
- [6] Silva AR, Grinberg LT, Farfel JM, Diniz BS, Lima LA, Silva PJ, et al. Transcriptional alterations related to neuropathology and clinical manifestation of Alzheimer's disease. *PLoS One* 2012;7:e48751.
- [7] Webster JA, Gibbs JR, Clarke J, Ray M, Zhang W, Holmans P, et al. Genetic control of human brain transcript expression in Alzheimer disease. *Am J Hum Genet* 2009;84:445-58.
- [8] Liang WS, Dunckley T, Beach TG, Grover A, Mastroeni D, Walker DG, et al. Gene expression profiles in anatomically and functionally distinct regions of the normal aged human brain. *Physiol Genomics* 2007;28:311-22.
- [9] Liang WS, Reiman EM, Valla J, Dunckley T, Beach TG, Grover A, et al. Alzheimer's disease is associated with reduced expression of energy metabolism genes in posterior cingulate neurons. *Proc Natl Acad Sci U S A* 2008;105:4441-6.
- [10] Zhang B, Gaiteri C, Bodea LG, Wang Z, McElwee J, Podtelezhnikov AA, et al. Integrated systems approach identifies genetic nodes and networks in late-onset Alzheimer's disease. *Cell* 2013;153:707-20.
- [11] Narayanan M, Huynh JL, Wang K, Yang X, Yoo S, McElwee J, et al. Common dysregulation network in the human prefrontal cortex underlies two neurodegenerative diseases. *Mol Syst Biol* 2014;10:743.

- [12] Liang WS, Dunckley T, Beach TG, Grover A, Mastroeni D, Ramsey K, et al. Neuronal gene expression in non-demented individuals with intermediate Alzheimer's Disease neuropathology. *Neurobiol Aging* 2010;31:549-66.
- [13] Lai MK, Esiri MM, Tan MG. Genome-wide profiling of alternative splicing in Alzheimer's disease. *Genom Data* 2014;2:290-2.
- [14] Tan MG, Chua WT, Esiri MM, Smith AD, Vinters HV, Lai MK. Genome wide profiling of altered gene expression in the neocortex of Alzheimer's disease. *J Neurosci Res* 2010;88:1157-69.
- [15] Simpson JE, Ince PG, Shaw PJ, Heath PR, Raman R, Garwood CJ, et al. Microarray analysis of the astrocyte transcriptome in the aging brain: relationship to Alzheimer's pathology and APOE genotype. *Neurobiol Aging* 2011;32:1795-807.
- [16] Blalock EM, Buechel HM, Popovic J, Geddes JW, Landfield PW. Microarray analyses of laser-captured hippocampus reveal distinct gray and white matter signatures associated with incipient Alzheimer's disease. *J Chem Neuroanat* 2011;42:118-26.
- [17] Blalock EM, Geddes JW, Chen KC, Porter NM, Markesbery WR, Landfield PW. Incipient Alzheimer's disease: microarray correlation analyses reveal major transcriptional and tumor suppressor responses. *Proc Natl Acad Sci U S A* 2004;101:2173-8.
- [18] Miller JA, Woltjer RL, Goodenbour JM, Horvath S, Geschwind DH. Genes and pathways underlying regional and cell type changes in Alzheimer's disease. *Genome Med* 2013;5:48.
- [19] Durrenberger PF, Fernando FS, Magliozzi R, Kashefi SN, Bonnert TP, Ferrer I, et al. Selection of novel reference genes for use in the human central nervous system: a BrainNet Europe Study. *Acta Neuropathol* 2012;124:893-903.
- [20] Durrenberger PF, Fernando FS, Kashefi SN, Bonnert TP, Seilhean D, Nait-Oumesmar B, et al. Common mechanisms in neurodegeneration and neuroinflammation: a BrainNet Europe gene expression microarray study. *J Neural Transm (Vienna)* 2015;122:1055-68.
- [21] Berson A, Barbash S, Shaltiel G, Goll Y, Hanin G, Greenberg DS, et al. Cholinergic-associated loss of hnRNP-A/B in Alzheimer's disease impairs cortical splicing and cognitive function in mice. *EMBO Mol Med* 2012;4:730-42.
- [22] Dunckley T, Beach TG, Ramsey KE, Grover A, Mastroeni D, Walker DG, et al. Gene expression correlates of neurofibrillary tangles in Alzheimer's disease. *Neurobiol Aging* 2006;27:1359-71.
- [23] Gautier L, Cope L, Bolstad BM, Irizarry RA. affy--analysis of Affymetrix GeneChip data at the probe level. *Bioinformatics* 2004;20:307-15.
- [24] Taminau J, Lazar C, Meganck S, Nowe A. Comparison of merging and meta-analysis as alternative approaches for integrative gene expression analysis. *ISRN Bioinform* 2014;2014:345106.
- [25] Mecham BH, Klus GT, Strovel J, Augustus M, Byrne D, Bozso P, et al. Sequence-matched probes produce increased cross-platform consistency and more reproducible biological results in microarray-based gene expression measurements. *Nucleic Acids Res* 2004;32:e74.
- [26] Zhou XJ, Kao MC, Huang H, Wong A, Nunez-Iglesias J, Primig M, et al. Functional annotation and network reconstruction through cross-platform integration of microarray data. *Nat Biotechnol* 2005;23:238-43.
- [27] Chen C, Grennan K, Badner J, Zhang D, Gershon E, Jin L, et al. Removing batch effects in analysis of expression microarray data: an evaluation of six batch adjustment methods. *PLoS One* 2011;6:e17238.



- [28] Luo J, Schumacher M, Scherer A, Sanoudou D, Megherbi D, Davison T, et al. A comparison of batch effect removal methods for enhancement of prediction performance using MAQC-II microarray gene expression data. *Pharmacogenomics J* 2010;10:278-91.
- [29] Taminau J, Meganck S, Lazar C, Steenhoff D, Coletta A, Molter C, et al. Unlocking the potential of publicly available microarray data using inSilicoDb and inSilicoMerging R/Bioconductor packages. *BMC Bioinformatics* 2012;13:335.
- [30] Johnson WE, Li C, Rabinovic A. Adjusting batch effects in microarray expression data using empirical Bayes methods. *Biostatistics* 2007;8:118-27.
- [31] Bushel P. pvca: Principal Variance Component Analysis (PVCA). R package version 1100 2013.
- [32] Ritchie ME, Phipson B, Wu D, Hu Y, Law CW, Shi W, et al. limma powers differential expression analyses for RNA-sequencing and microarray studies. *Nucleic Acids Res* 2015;43:e47.
- [33] Huang da W, Sherman BT, Lempicki RA. Systematic and integrative analysis of large gene lists using DAVID bioinformatics resources. *Nat Protoc* 2009;4:44-57.
- [34] Zhang B, Horvath S. A general framework for weighted gene co-expression network analysis. *Stat Appl Genet Mol Biol* 2005;4:Article17.
- [35] Langfelder P, Horvath S. WGCNA: an R package for weighted correlation network analysis. *BMC Bioinformatics* 2008;9:559.
- [36] Langfelder P, Zhang B, Horvath S. Defining clusters from a hierarchical cluster tree: the Dynamic Tree Cut package for R. *Bioinformatics* 2008;24:719-20.
- [37] Langfelder P, Horvath S. Fast R Functions for Robust Correlations and Hierarchical Clustering. *J Stat Softw* 2012;46:i11.
- [38] Langfelder P, Luo R, Oldham MC, Horvath S. Is my network module preserved and reproducible? *PLoS Comput Biol* 2011;7:e1001057.
- [39] Horvath S, Dong J. Geometric Interpretation of Gene Co-Expression Network Analysis. *PLoS Comput Biol* 2008;4:e1000117.
- [40] Darmanis S, Sloan SA, Zhang Y, Enge M, Caneda C, Shuer LM, et al. A survey of human brain transcriptome diversity at the single cell level. *Proc Natl Acad Sci U S A* 2015;112:7285-90.
- [41] Love MI, Huber W, Anders S. Moderated estimation of fold change and dispersion for RNA-seq data with DESeq2. *Genome Biol* 2014;15:550.
- [42] Zhang Y, Chen K, Sloan SA, Bennett ML, Scholze AR, O'Keefe S, et al. An RNA-sequencing transcriptome and splicing database of glia, neurons, and vascular cells of the cerebral cortex. *J Neurosci* 2014;34:11929-47.
- [43] Niculescu AB, Le-Niculescu H. Convergent Functional Genomics: what we have learned and can learn about genes, pathways, and mechanisms. *Neuropsychopharmacology* 2010;35:355-6.
- [44] Niculescu AB, 3rd, Segal DS, Kuczenski R, Barrett T, Hauger RL, Kelsoe JR. Identifying a series of candidate genes for mania and psychosis: a convergent functional genomics approach. *Physiol Genomics* 2000;4:83 - 91.
- [45] Lambert JC, Ibrahim-Verbaas CA, Harold D, Naj AC, Sims R, Bellenguez C, et al. Meta-analysis of 74,046 individuals identifies 11 new susceptibility loci for Alzheimer's disease. *Nat Genet* 2013;45:1452-8.
- [46] Colantuoni C, Lipska BK, Ye T, Hyde TM, Tao R, Leek JT, et al. Temporal dynamics and genetic control of transcription in the human prefrontal cortex. *Nature* 2011;478:519-23.
- [47] Itan Y, Mazel M, Mazel B, Abhyankar A, Nitschke P, Quintana-Murci L, et al. HGCS: an online tool for prioritizing disease-causing gene variants by biological distance. *BMC Genomics* 2014;15:256.

- [48] Itan Y, Zhang SY, Vogt G, Abhyankar A, Herman M, Nitschke P, et al. The human gene connectome as a map of short cuts for morbid allele discovery. *Proc Natl Acad Sci U S A* 2013;110:5558-63.
- [49] Matarin M, Salih DA, Yasvoina M, Cummings DM, Guelfi S, Liu W, et al. A genome-wide gene-expression analysis and database in transgenic mice during development of amyloid or tau pathology. *Cell Rep* 2015;10:633-44.
- [50] Purcell S, Neale B, Todd-Brown K, Thomas L, Ferreira MA, Bender D, et al. PLINK: a tool set for whole-genome association and population-based linkage analyses. *Am J Hum Genet* 2007;81:559-75.
- [51] Revelle W. *psych: Procedures for Personality and Psychological Research*. Northwestern University, Evanston, Illinois, USA, <https://CRANR-project.org/package=psych> Version = 1612 2016.
- [52] Kurronen A, Pihlaja R, Pollari E, Kanninen K, Storvik M, Wong G, et al. Adult and neonatal astrocytes exhibit diverse gene expression profiles in response to beta amyloid ex vivo. *World J Neurosci* 2012;2:57-67.
- [53] Zhang DF, Li J, Wu H, Cui Y, Bi R, Zhou HJ, et al. CFH variants affect structural and functional brain changes and genetic risk of Alzheimer's disease. *Neuropsychopharmacology* 2016;41:1034-45.
- [54] Xiang Q, Bi R, Xu M, Zhang DF, Tan L, Zhang C, et al. Rare Genetic Variants of the Transthyretin Gene Are Associated with Alzheimer's Disease in Han Chinese. *Mol Neurobiol* 2016.
- [55] Trapnell C, Pachter L, Salzberg SL. TopHat: discovering splice junctions with RNA-Seq. *Bioinformatics* 2009;25:1105-11.
- [56] Anders S, Pyl PT, Huber W. HTSeq--a Python framework to work with high-throughput sequencing data. *Bioinformatics* 2015;31:166-9.
- [57] Su LY, Li H, Lv L, Feng YM, Li GD, Luo R, et al. Melatonin attenuates MPTP-induced neurotoxicity via preventing CDK5-mediated autophagy and SNCA/alpha-synuclein aggregation. *Autophagy* 2015;11:1745-59.
- [58] Feng YM, Jia YF, Su LY, Wang D, Lv L, Xu L, et al. Decreased mitochondrial DNA copy number in the hippocampus and peripheral blood during opiate addiction is mediated by autophagy and can be salvaged by melatonin. *Autophagy* 2013;9:1395-406.
- [59] Wu Y, Yao YG, Luo XJ. SZDB: a database for schizophrenia genetic research. *Schizophr Bull* 2016;43:459-71.

**Table S1. Sample information of curated individual expression datasets of entorhinal cortex (EC), hippocampus (HP), temporal cortex (TC), and frontal cortex (FC).**

Brain region	Study (Reference)	Number of AD patients	Number of controls	Total number of samples	Platform	Total number of genes	RIN (mean±sd)
EC	GSE26927 [19, 20]	11	4	15	GPL6255	17189	7.3±0.7
	GSE48350 [2]	15	19	34	GPL570	20283	8.6±0.5
	GSE26972 [21]	3	3	6	GPL5188	22357	6.3±0.7
	GSE5281 [8, 9]	10	13	23	GPL570	20283	NA
HP	GSE28146 [16]	22	8	30	GPL570	20283	NA
	GSE48350 [2]	19	19	38	GPL570	20283	8.4±0.7
	GSE5281 [8, 9]	10	12	22	GPL570	20283	NA
	GSE29378 [18]	16	16	32	GPL6947	24384	6.3±1.2
	GSE36980 [5]	7	10	17	GPL6244	18725	7.4±0.4
TC	GSE37263 [14]	8	8	16	GPL5175	17168	NA
	GSE29652 [15]	18	0	18	GPL570	20283	NA
	GSE36980 [5]	10	19	29	GPL6244	18725	7.4±0.4
	GSE5281 [8, 9]	16	12	28	GPL570	20283	NA
	GSE15222 [7]	106	135	241	GPL2700	7715	NA
FC	GSE48350 [2]	21	27	48	GPL570	20283	8.4±0.6
	GSE66333 [3]	8	0	8	GPL570	20283	3.5±1.3*
	GSE53890 [4]	0	24	24	GPL570	20283	NA
	GSE5281 [8, 9]	23	11	34	GPL570	20283	NA
	GSE36980 [5]	15	18	33	GPL6244	18725	7.3±0.37
	GSE12685 [1]	6	8	14	GPL96	12752	NA
	GSE15222 [7]	31	40	71	GPL2700	7715	NA
	GSE33000 [11]	309	156	465	GPL4372	15586	6.8±0.8
<b>Total</b>	<b>14</b>	<b>684</b>	<b>562</b>	<b>1246</b>	<b>8</b>	-	-

EC - entorhinal cortex; HP – hippocampus; TC - temporal cortex; FC - frontal cortex.

Data were retrieved from the NCBI Gene Expression Omnibus

(GEO, <https://www.ncbi.nlm.nih.gov/geo>). Datasets GSE15222 [7] and GSE33000 [11] were used as stage 2 dataset, whereas the other datasets were merged as stage 1 dataset.

RIN, RNA integrity number; NA, not available.

\* Dataset GSE66333 has abnormal RIN, however, including or removal of GSE66333 has little effect on differentially expressed genes (DEGs) detection. DEGs identified by the six datasets excluding GSE66333 could capture a quite large proportion (910/1221) of DEGs that were identified by using all seven datasets. To keep the sample size as large as possible, we retained dataset GSE66333 in the analysis.

**Table S2. Number of DEGs in merged datasets of the four brain regions defined by different fold change cutoff values**

Fold change (log2)	Total number of DEGs (%) <sup>a</sup>					
	EC	HP	TC (stage 1)	TC (stage 2)	FC (stage 1)	FC (stage 2)
<b>1.07 (0.1)</b>	2330 (15.17%)	1508 (9.24%)	3101 (20.05%)	5185 (67.21%)	1221 (10.37%)	2675 (17.16%)
<b>1.2 (0.26)</b>	2236 (14.55%)	1237 (7.58%)	3057 (19.77%)	2836 (36.76%)	399 (3.39%)	175 (1.12%)
<b>1.5 (0.58)</b>	517 (3.37%)	123 (0.75%)	1168 (7.55%)	542 (7.03%)	2 (0.02%)	1 (0.01%)
<b>2.0 (1.0)</b>	34 (0.22%)	2 (0.01%)	89 (0.58%)	20 (0.26%)	0 (0.00%)	0 (0.00%)

EC - entorhinal cortex; HP – hippocampus; TC - temporal cortex; FC - frontal cortex

DEGs, differentially expressed genes in AD patients compared with controls, with absolute value of log2 fold change at different cutoffs and FDR smaller than 0.05.

<sup>a</sup>The percentage (%) = number of DEGs in the merged datasets / total number of genes in the merged datasets.

**Table S3. Number of DEGs in merged datasets of four brain regions and validation rate of stage 1 DEGs in stage 2 datasets of TC and FC**

Brain region	Total number of genes	DEGs				
		Up <sup>a</sup>	Down <sup>b</sup>	Total (%) <sup>c</sup>	Captured (%) <sup>d</sup>	Newly found (%) <sup>e</sup>
EC	15363	1010	1320	2330 (15.17%)	1385 (59.44%)	945 (40.56%)
HP	16315	631	877	1508 (9.24%)	489 (32.49%)	1019 (67.51%)
TC (stage 1)	15465	1067	2034	3101 (20.05%)	2405 (77.56%)	696 (22.44%)
FC (stage 1)	11779	697	525	1222 (10.37%)	1028 (84.12%)	194 (15.88%)
TC (stage 1 vs. stage 2) <sup>1</sup>	6835	477	991	1468 (21.47%)	-	-
FC (stage 1 vs. stage 2) <sup>1</sup>	8657	434	401	835 (9.65%)	-	-

EC - entorhinal cortex; HP – hippocampus; TC - temporal cortex; FC - frontal cortex.

DEGs, differentially expressed genes in AD patients compared with controls, with absolute value of log<sub>2</sub> fold change larger than 0.1 and FDR smaller than 0.05.

<sup>a</sup>Number of upregulated DEGs in AD patients versus controls.

<sup>b</sup>Number of downregulated DEGs in AD patients versus controls.

<sup>c</sup>Total number of DEGs in AD patients versus controls. The percentage (%) = total number of DEGs / total number of genes in the merged datasets.

<sup>d</sup>Number of DEGs captured in the original studies. The percentage (%) = number of captured DEGs in the original studies / total number of DEGs in the merged datasets.

<sup>e</sup>Number of DEGs newly found in the merged datasets. The percentage (%) = number of newly found DEGs in the merged datasets / total number of DEGs in the merged datasets.

<sup>1</sup>The results were based on the shared genes of stage 1 and stage 2 datasets. A very high proportion of DEGs in stage 1 dataset (TC: 1468/2028 = 72.39%; FC: 835/941 = 88.74%) could be successfully replicated by stage 2 dataset.

**Table S4. Proportion of DEGs in the original studies that were covered by the DEGs of the merged datasets**

Brain region	Study	$P < 0.05$ <sup>1</sup>		$FDR < 0.05$ <sup>2</sup>	
		Total number of DEGs	Coverage (%)	Total number of DEGs	Coverage (%)
EC	GSE26927	1392	624 (44.83%)	0	NA
	GSE48350	1473	933 (63.34%)	31	11 (35.48%)
	GSE26972	2395	1285 (53.65%)	0	NA
	GSE5281	4904	3082 (62.85%)	2610	1374 (52.64%)
HP	GSE28146	1150	582 (50.61%)	0	NA
	GSE48350	1199	808 (67.39%)	11	6 (54.55%)
	GSE5281	3554	1511 (42.52%)	1007	315 (31.28%)
	GSE29378	2647	1290 (48.73%)	407	180 (44.23%)
	GSE36980	1541	627 (40.69%)	0	0 (NA)
TC	GSE37263	3295	1570 (47.65%)	0	NA
	GSE29652 <sup>3</sup>	NA	NA	NA	NA
	GSE36980	1582	1097 (69.34%)	0	NA
	GSE5281	5485	3285 (59.89%)	3412	2006 (58.79%)
FC	GSE48350	1015	348 (34.29%)	46	5 (10.87%)
	GSE66333 <sup>3</sup>	NA	NA	NA	NA
	GSE53890 <sup>3</sup>	NA	NA	NA	NA
	GSE5281	2193	1082 (49.34%)	556	213 (38.31%)
	GSE36980	1329	370 (27.84%)	0	NA
	GSE12685	1834	240 (13.09%)	2	0
	GSE15222	2340	1468 (62.74%)	1595	875 (54.86%)

EC - entorhinal cortex; HP – hippocampus; TC - temporal cortex; FC - frontal cortex; NA, not applicable.

<sup>1</sup>Total number of differentially expressed genes (DEGs) in AD patients compared with controls in individual datasets with a  $P$ -value  $< 0.05$  without adjustment for multiple comparisons. Coverage - number of DEGs in a single dataset that was covered by the merged datasets; (%) - proportion of DEGs in the original studies that were covered by the DEGs of the merged datasets.

<sup>2</sup>Total number of differentially expressed genes (DEGs) in AD patients compared with controls in individual datasets with a  $FDR < 0.05$  (adjusted for multiple comparisons by the Benjamini-Hochberg's (BH) method); (%) - proportion of DEGs in the original studies that were covered by the DEGs of the merged datasets.

<sup>3</sup>No DEGs in the original datasets were detected for a lack of cases or controls in these three datasets.

**Table S5. 139 genes are differently expressed in all four brain regions**

Gene	EC		HP		TC		FC	
	logFC	FDR	logFC	FDR	logFC	FDR	logFC	FDR
<i>CHGB</i>	-1.003	6.26E-03	-0.920	7.35E-04	-1.253	1.62E-05	-0.476	5.18E-03
<i>APLNR</i>	1.349	6.81E-04	0.613	9.59E-03	1.295	2.58E-04	0.366	4.27E-02
<i>INA</i>	-1.007	6.62E-04	-0.841	2.38E-04	-1.342	7.11E-06	-0.289	4.08E-02
<i>NEFL</i>	-1.002	4.38E-03	-0.808	2.48E-04	-1.248	3.95E-04	-0.403	3.58E-02
<i>CALY</i>	-0.928	2.67E-03	-0.906	2.48E-04	-1.225	6.31E-05	-0.344	9.63E-03
<i>GFAP</i>	0.784	9.48E-03	0.487	8.13E-03	1.300	3.62E-05	0.612	2.27E-04
<i>GABRG2</i>	-0.862	7.11E-03	-0.783	7.35E-04	-1.170	3.62E-05	-0.367	2.58E-02
<i>SV2B</i>	-0.929	3.36E-03	-0.530	6.97E-03	-1.379	3.74E-06	-0.298	2.48E-02
<i>ATPIA3</i>	-0.746	5.86E-03	-0.694	7.59E-04	-1.250	7.84E-05	-0.345	6.22E-03
<i>MLLT11</i>	-0.929	6.30E-04	-0.618	7.14E-04	-1.156	1.62E-05	-0.326	1.06E-02
<i>PSMD8</i>	-1.132	3.94E-03	-0.688	1.99E-03	-0.976	1.99E-04	-0.224	3.53E-02
<i>SSSCA1</i>	-1.061	1.64E-03	-0.517	8.69E-03	-1.029	5.81E-04	-0.351	4.40E-03
<i>GNG3</i>	-1.075	4.47E-04	-0.656	2.38E-04	-0.966	1.62E-05	-0.259	4.29E-02
<i>NRN1</i>	-0.784	9.97E-03	-0.523	1.30E-03	-1.162	3.06E-06	-0.478	1.36E-03
<i>RPH3A</i>	-0.925	1.64E-03	-0.518	1.94E-03	-1.078	1.62E-05	-0.366	4.44E-03
<i>AEBP1</i>	0.725	1.92E-02	0.625	2.35E-03	0.999	4.67E-04	0.507	1.23E-03
<i>GOT1</i>	-0.829	7.12E-03	-0.512	5.21E-03	-1.165	2.27E-05	-0.325	2.64E-02
<i>NRXN3</i>	-0.700	1.25E-02	-0.573	7.35E-04	-1.211	1.62E-05	-0.340	4.08E-03
<i>RASL12</i>	0.717	3.75E-02	0.534	2.07E-02	1.230	9.50E-05	0.306	3.57E-02
<i>SNX10</i>	-0.803	1.15E-03	-0.449	2.10E-02	-0.979	2.80E-04	-0.468	4.25E-04
<i>PLSCR4</i>	0.821	9.39E-04	0.503	1.62E-03	1.060	2.84E-05	0.307	2.81E-02
<i>CA10</i>	-0.703	3.53E-03	-0.580	1.50E-03	-1.017	5.11E-05	-0.387	5.38E-04
<i>CITED1</i>	-1.080	9.46E-04	-0.487	4.48E-02	-0.828	1.25E-03	-0.248	1.98E-02
<i>GABRD</i>	-0.818	1.35E-02	-0.557	1.26E-02	-0.898	1.46E-03	-0.351	4.51E-03
<i>CRYM</i>	-0.668	9.48E-03	-0.543	2.62E-03	-0.999	1.09E-04	-0.389	2.85E-03
<i>SERPINI1</i>	-0.661	4.12E-02	-0.427	2.95E-02	-1.109	9.48E-04	-0.375	2.65E-02
<i>CACNG3</i>	-0.683	1.31E-02	-0.497	1.06E-02	-0.986	7.10E-05	-0.345	1.23E-03
<i>FIG4</i>	-0.788	5.30E-04	-0.482	5.19E-03	-0.997	1.66E-05	-0.235	9.73E-03
<i>KIFAP3</i>	-0.653	2.09E-02	-0.537	2.98E-03	-0.957	1.41E-04	-0.340	1.58E-02
<i>AP2M1</i>	-1.038	5.30E-04	-0.314	2.43E-02	-0.911	1.70E-04	-0.216	3.50E-02
<i>HMP19</i>	-0.638	1.07E-02	-0.536	7.97E-03	-0.999	4.84E-04	-0.303	2.02E-02
<i>ATP6V1B2</i>	-0.486	4.74E-02	-0.540	3.58E-03	-1.086	1.55E-05	-0.361	5.66E-03
<i>TAGLN3</i>	-0.461	2.72E-02	-0.563	1.36E-03	-1.138	6.59E-06	-0.309	3.21E-03
<i>GRAMD3</i>	0.724	2.82E-03	0.380	2.42E-02	1.006	5.11E-05	0.356	2.17E-03
<i>MEF2C</i>	-0.722	2.33E-02	-0.562	2.01E-03	-0.912	3.16E-04	-0.248	4.88E-02
<i>RIT2</i>	-0.761	5.22E-03	-0.640	3.89E-03	-0.658	4.20E-02	-0.369	1.13E-02
<i>FABP3</i>	-0.740	7.04E-03	-0.610	9.02E-04	-0.812	4.63E-04	-0.264	5.91E-03
<i>PPM1E</i>	-0.595	3.73E-02	-0.617	1.04E-02	-0.802	3.32E-04	-0.406	1.48E-03
<i>CXCR4</i>	0.803	8.48E-03	0.561	1.71E-02	0.549	2.07E-02	0.501	1.51E-03
<i>PNMAL1</i>	-0.690	1.50E-02	-0.530	8.11E-04	-0.887	2.23E-03	-0.283	4.06E-02
<i>ATP5B</i>	-0.632	2.88E-03	-0.508	1.62E-03	-0.946	8.43E-05	-0.251	1.31E-02

---

<i>ST8SIA5</i>	-0.663	1.55E-02	-0.518	2.47E-02	-0.833	1.94E-03	-0.309	2.22E-03
<i>SYP</i>	-0.431	4.67E-02	-0.554	7.97E-03	-1.045	1.62E-05	-0.269	1.11E-02
<i>RALYL</i>	-0.544	6.30E-03	-0.635	4.83E-03	-0.847	5.40E-04	-0.266	2.74E-02
<i>TGFBR3</i>	0.585	3.60E-03	0.583	2.48E-04	0.721	9.74E-05	0.371	2.77E-03
<i>ATP6VIA</i>	-0.589	2.12E-02	-0.490	2.30E-03	-0.819	5.72E-04	-0.360	5.49E-03
<i>GAD1</i>	-0.541	4.49E-02	-0.514	1.91E-02	-0.864	8.32E-04	-0.320	3.78E-02
<i>ERBIN</i>	0.578	1.30E-02	0.290	1.74E-02	0.956	3.66E-05	0.404	3.79E-04
<i>ATP5C1</i>	-0.586	7.64E-03	-0.371	1.24E-02	-0.968	4.38E-05	-0.276	7.35E-03
<i>GAP43</i>	-0.651	3.91E-03	-0.581	2.14E-03	-0.614	1.30E-04	-0.325	7.65E-03
<i>REEP1</i>	-0.499	2.70E-02	-0.453	2.43E-03	-0.863	9.74E-05	-0.349	4.02E-03
<i>UCHL1</i>	-0.511	1.03E-02	-0.481	9.99E-04	-0.906	4.99E-04	-0.231	3.89E-02
<i>SLC9A6</i>	-0.491	1.11E-02	-0.350	3.45E-03	-1.012	2.81E-04	-0.261	2.51E-02
<i>PCYOX1L</i>	-0.567	1.01E-02	-0.392	2.44E-02	-0.568	2.60E-03	-0.549	5.60E-06
<i>SLC25A4</i>	-0.438	2.26E-02	-0.432	3.49E-03	-0.916	4.77E-06	-0.273	9.99E-03
<i>FGF12</i>	-0.660	1.35E-02	-0.346	2.85E-02	-0.657	1.62E-04	-0.393	7.01E-03
<i>SLIRP</i>	-0.703	1.13E-03	-0.401	3.19E-03	-0.658	1.57E-03	-0.290	1.70E-02
<i>FHL2</i>	-0.633	2.49E-02	-0.486	7.44E-03	-0.675	1.77E-03	-0.224	2.96E-02
<i>EFHD1</i>	0.464	1.51E-02	0.322	2.93E-02	0.769	3.04E-04	0.455	2.42E-04
<i>ITGB5</i>	0.527	8.72E-03	0.380	5.76E-03	0.843	2.06E-04	0.252	3.04E-03
<i>PALLD</i>	0.500	5.18E-03	0.473	8.11E-04	0.686	6.48E-05	0.332	2.09E-03
<i>NUDT2</i>	-0.515	2.98E-02	-0.516	3.10E-02	-0.613	6.43E-03	-0.323	8.27E-04
<i>TBLIX</i>	0.514	2.64E-02	0.417	8.99E-03	0.643	4.30E-04	0.387	9.90E-04
<i>SASH1</i>	0.452	5.11E-03	0.247	2.55E-02	0.723	1.89E-04	0.534	1.63E-05
<i>CD200</i>	-0.384	4.82E-02	-0.385	1.16E-02	-0.895	2.39E-04	-0.281	4.08E-02
<i>PTPRR</i>	-0.578	1.85E-02	-0.474	2.44E-02	-0.696	7.92E-05	-0.193	4.67E-02
<i>MTX2</i>	-0.429	3.19E-02	-0.379	1.26E-02	-0.873	1.32E-04	-0.256	3.01E-02
<i>VCAN</i>	0.648	1.03E-02	0.332	1.28E-02	0.695	7.78E-04	0.261	3.07E-02
<i>PTPRN2</i>	-0.513	2.66E-02	-0.349	3.30E-02	-0.817	1.03E-04	-0.249	4.16E-03
<i>UBE2N</i>	-0.363	1.99E-02	-0.393	1.16E-02	-0.783	9.15E-05	-0.388	8.95E-04
<i>MRPL15</i>	-0.381	2.02E-02	-0.713	7.35E-04	-0.519	7.46E-03	-0.305	1.57E-03
<i>COPS3</i>	-0.340	3.60E-02	-0.447	1.26E-02	-0.856	1.99E-04	-0.264	7.58E-03
<i>ATP5G1</i>	-0.782	4.47E-04	-0.318	2.18E-03	-0.533	1.62E-04	-0.258	3.98E-03
<i>CDC42EP4</i>	0.337	3.53E-02	0.424	1.56E-02	0.862	1.91E-04	0.267	2.88E-03
<i>ITPKB</i>	0.486	1.81E-02	0.432	1.28E-02	0.580	8.78E-03	0.385	2.27E-04
<i>YWHAZ</i>	-0.522	1.30E-02	-0.405	1.13E-02	-0.717	3.19E-04	-0.233	3.68E-02
<i>ACTR10</i>	-0.428	3.64E-02	-0.420	3.58E-03	-0.733	2.60E-03	-0.290	5.74E-03
<i>C14orf2</i>	-0.514	3.19E-03	-0.380	6.24E-04	-0.727	3.04E-04	-0.223	1.01E-02
<i>ANP32B</i>	0.532	9.84E-03	0.253	2.38E-02	0.757	1.37E-04	0.299	5.74E-03
<i>AK5</i>	-0.443	3.38E-02	-0.274	4.72E-02	-0.823	1.86E-03	-0.293	1.14E-02
<i>NDRG4</i>	-0.408	3.34E-02	-0.408	2.02E-03	-0.758	6.48E-05	-0.254	2.12E-02
<i>PPME1</i>	-0.582	1.70E-03	-0.292	8.69E-03	-0.740	2.17E-05	-0.207	9.63E-03
<i>CPQ</i>	0.391	4.56E-02	0.386	4.02E-03	0.684	1.41E-03	0.346	6.68E-04
<i>RIN2</i>	0.525	7.68E-03	0.291	4.85E-02	0.652	6.44E-04	0.337	2.17E-03
<i>HSPB8</i>	0.437	3.68E-02	0.583	8.11E-04	0.590	4.93E-05	0.182	2.82E-02



<i>BAZIA</i>	0.480	3.46E-02	0.406	6.30E-03	0.618	9.42E-04	0.286	7.46E-03
<i>SRD5A1</i>	-0.486	1.92E-02	-0.438	8.27E-03	-0.572	8.44E-03	-0.288	2.42E-03
<i>PGK1</i>	-0.457	4.71E-02	-0.375	9.97E-03	-0.684	3.95E-04	-0.248	1.31E-02
<i>VEZF1</i>	0.668	2.69E-03	0.273	3.02E-02	0.448	2.58E-03	0.366	1.99E-04
<i>FIBP</i>	-0.458	1.12E-02	-0.538	7.59E-04	-0.562	8.19E-04	-0.192	4.57E-02
<i>SEZ6L2</i>	-0.747	9.39E-04	-0.235	4.96E-02	-0.587	5.31E-05	-0.180	2.07E-02
<i>GHITM</i>	-0.583	9.98E-03	-0.347	2.10E-02	-0.561	1.58E-03	-0.251	1.22E-02
<i>ADD3</i>	0.640	4.26E-03	0.246	3.44E-02	0.528	1.59E-03	0.327	4.38E-03
<i>MAGED1</i>	-0.395	4.94E-02	-0.397	2.41E-02	-0.690	1.34E-04	-0.256	1.37E-02
<i>RPP40</i>	-0.322	4.69E-02	-0.472	2.68E-02	-0.702	8.77E-03	-0.234	1.28E-02
<i>IMP4</i>	-0.530	7.38E-03	-0.356	2.79E-02	-0.667	5.17E-04	-0.177	2.48E-02
<i>NDUFB5</i>	-0.514	7.93E-03	-0.248	4.55E-02	-0.695	4.00E-04	-0.271	1.74E-03
<i>MECR</i>	-0.492	4.18E-02	-0.397	3.28E-02	-0.582	1.01E-02	-0.253	5.41E-03
<i>MICU1</i>	-0.387	4.28E-03	-0.532	3.93E-03	-0.673	3.55E-04	-0.122	2.96E-02
<i>PSMB3</i>	-0.479	7.20E-03	-0.377	3.23E-02	-0.646	3.70E-04	-0.192	7.13E-03
<i>ADAM23</i>	-0.447	7.11E-03	-0.377	2.33E-03	-0.652	1.32E-04	-0.203	4.18E-02
<i>CPM</i>	0.571	6.84E-03	0.330	2.34E-02	0.506	5.39E-03	0.269	7.84E-03
<i>PORCN</i>	-0.438	9.25E-03	-0.509	9.99E-04	-0.528	1.19E-02	-0.184	4.42E-03
<i>NDUFA9</i>	-0.368	9.56E-03	-0.347	2.02E-03	-0.723	6.31E-05	-0.216	2.19E-03
<i>TNS3</i>	0.461	2.27E-02	0.434	1.08E-02	0.443	3.84E-02	0.275	1.32E-02
<i>HPS5</i>	0.472	4.15E-02	0.393	1.62E-02	0.555	1.26E-02	0.182	2.38E-02
<i>LSM4</i>	-0.722	9.39E-04	-0.254	3.63E-02	-0.465	3.68E-03	-0.156	2.26E-02
<i>COPG1</i>	-0.296	4.90E-02	-0.419	9.02E-04	-0.707	1.32E-03	-0.168	3.53E-02
<i>ACLY</i>	-0.440	2.95E-02	-0.231	3.13E-02	-0.625	1.18E-03	-0.276	1.01E-03
<i>NARS</i>	-0.515	9.39E-04	-0.195	4.44E-02	-0.669	1.46E-03	-0.192	2.17E-02
<i>GABARAPLI</i>	-0.393	3.71E-02	-0.255	4.52E-02	-0.615	1.00E-03	-0.306	2.09E-03
<i>POLB</i>	-0.459	2.90E-03	-0.355	4.43E-03	-0.586	7.58E-03	-0.167	4.29E-02
<i>PDHB</i>	-0.371	3.66E-02	-0.305	1.57E-02	-0.678	8.32E-04	-0.197	9.71E-03
<i>STAU2</i>	-0.378	1.62E-02	-0.313	7.17E-03	-0.646	2.87E-04	-0.212	3.39E-02
<i>BCAR3</i>	0.461	3.66E-02	0.307	4.51E-02	0.555	1.22E-02	0.205	2.29E-02
<i>PEX11B</i>	-0.398	1.89E-02	-0.341	6.73E-03	-0.475	1.52E-02	-0.300	4.02E-03
<i>FAM216A</i>	-0.332	1.76E-02	-0.485	7.40E-03	-0.423	3.12E-03	-0.272	7.40E-03
<i>SEH1L</i>	-0.478	1.26E-02	-0.295	2.10E-02	-0.462	3.50E-02	-0.247	1.14E-02
<i>IQGAP1</i>	0.357	4.52E-02	0.288	3.16E-02	0.461	4.57E-03	0.365	2.14E-04
<i>MXII</i>	0.370	7.59E-03	0.200	4.25E-02	0.509	3.04E-04	0.384	2.54E-04
<i>CAPN2</i>	0.437	5.83E-03	0.244	3.45E-02	0.569	4.63E-04	0.187	6.66E-03
<i>PPIH</i>	-0.382	2.96E-02	-0.385	8.97E-03	-0.469	3.02E-02	-0.177	2.36E-02
<i>C3orf14</i>	-0.358	2.88E-02	-0.235	4.18E-02	-0.568	3.40E-04	-0.247	3.04E-03
<i>OLA1</i>	-0.486	6.61E-03	-0.218	3.84E-02	-0.429	3.28E-02	-0.245	1.12E-02
<i>RNMT</i>	-0.345	3.49E-02	-0.268	2.54E-02	-0.448	2.82E-02	-0.282	8.11E-04
<i>COX5B</i>	-0.413	5.65E-03	-0.256	1.48E-02	-0.526	4.56E-04	-0.140	4.57E-02
<i>AGK</i>	-0.263	4.08E-02	-0.295	1.21E-02	-0.537	7.17E-03	-0.228	3.32E-03
<i>POLR2K</i>	-0.398	1.68E-02	-0.249	8.13E-03	-0.396	2.50E-02	-0.239	7.17E-03
<i>GSS</i>	-0.528	1.14E-03	-0.253	3.19E-02	-0.293	1.47E-02	-0.205	9.90E-04

<i>COQ3</i>	-0.360	2.48E-02	-0.324	5.01E-03	-0.405	4.71E-02	-0.187	9.81E-03
<i>SRM</i>	-0.386	8.20E-03	-0.397	3.65E-02	-0.325	3.12E-02	-0.114	4.90E-02
<i>CD2BP2</i>	-0.301	3.38E-02	-0.312	3.20E-03	-0.412	2.96E-03	-0.187	5.51E-03
<i>C16orf45</i>	-0.427	1.11E-02	-0.247	3.17E-02	-0.365	1.19E-02	-0.161	2.17E-02
<i>CTDSP2</i>	0.299	1.99E-02	0.224	2.08E-02	0.376	4.96E-03	0.289	7.42E-05
<i>VPS33B</i>	-0.294	3.79E-02	-0.262	4.32E-02	-0.437	1.36E-02	-0.196	6.77E-03
<i>SPEN</i>	0.300	3.11E-02	0.241	3.02E-02	0.430	4.82E-03	0.208	1.60E-03
<i>SGPL1</i>	0.281	3.29E-02	0.215	4.18E-02	0.388	1.49E-02	0.200	1.77E-03
<i>ZHX3</i>	0.243	3.67E-02	0.311	4.35E-03	0.335	1.62E-02	0.190	1.87E-03
<i>HABP4</i>	-0.308	5.86E-03	-0.215	3.05E-02	-0.410	3.93E-04	-0.130	4.00E-02

EC - entorhinal cortex; HP – hippocampus; TC - temporal cortex; FC - frontal cortex.

logFC - log2 fold change of gene expression in AD patients compared with controls.

FDR - *P*-value of differential expression with adjustment for multiple comparisons by the Benjamini-Hochberg's (BH) method.

**Table S6. Expression, connectivity, and CFG score of AD core genes in four brain regions**

Gene	EC		HP		TC		FC		Connectivity		CFG <sup>1</sup>
	logFC	FDR	logFC	FDR	logFC	FDR	logFC	FDR	k <sub>AD</sub>	k <sub>CTL</sub>	
<i>APP</i>	-0.055	0.738	-0.108	0.376	-0.261	0.085	-0.234	0.015	0.19	0.25	4
<i>PSENI</i>	0.382	0.03	0.179	0.144	-0.056	0.848	0.038	0.893	0.49	0.32	2
<i>PSEN2</i>	-0.222	0.163	-0.041	0.861	-0.06	0.81	-0.147	0.019	0.09	0.13	2
<i>APOE</i>	-0.089	0.662	0.05	0.814	0.265	0.184	0.063	0.578	0.47	0.57	5
<i>MAPT</i>	-0.205	0.097	-0.122	0.162	-0.127	0.385	0.068	0.505	0.24	0.22	5
<i>ABCA7</i>	-0.231	0.06	-0.046	0.805	0.251	0.361	0.109	0.64	0.41	0.44	3
<i>BINI</i>	-0.118	0.452	-0.259	0.028	-0.092	0.67	0.109	0.268	0.30	0.43	4
<i>CASS4</i>	0.17	0.336	-0.005	0.984	0.099	0.702	-0.009	0.986	0.39	0.40	1
<i>CD2AP</i>	0.309	0.051	0.226	0.105	0.363	0.048	0.112	0.429	0.27	0.32	2
<i>CD33</i>	0.178	0.431	0.29	0.114	0.204	0.567	0.013	0.976	0.56	0.45	3
<i>CELF1</i>	NA	NA	0.03	0.823	-0.347	0.015	0.061	0.723	NA	NA	NA
<i>CLU</i>	-0.063	0.647	0.1	0.346	0.313	0.09	0.157	0.122	0.40	0.26	4
<i>CRI</i>	0.225	0.197	-0.012	0.954	0.388	0.118	-0.04	0.906	0.45	0.22	2
<i>DSG2</i>	0.305	0.087	0.088	0.708	-0.26	0.491	-0.231	0.496	0.22	0.90	3
<i>EPHA1</i>	0.22	0.131	0.075	0.706	-0.081	0.816	0.043	0.875	0.71	0.69	3
<i>FERMT2</i>	0.328	0.037	0.164	0.187	0.613	2.05E-03	0.11	0.302	0.69	0.88	2
<i>HLA-DRB5</i>	NA	NA	NA	NA	NA	NA	NA	NA	NA	NA	NA
<i>INPP5D</i>	0.494	0.031	0.051	0.788	0.25	0.304	0.308	1.34E-03	0.67	0.53	4
<i>MEF2C</i>	-0.722	0.023	-0.562	2.01E-03	-0.912	3.16E-04	-0.248	0.049	0.67	0.50	4
<i>MS4A6A</i>	0.414	0.173	0.272	0.224	0.207	0.5	0.278	0.053	0.93	0.76	2
<i>NME8</i>	0.173	0.495	0.009	0.976	0.071	0.894	0.254	0.338	0.13	0.35	1
<i>PICALM</i>	0.194	0.253	-0.078	0.665	-0.123	0.55	-0.047	0.665	0.36	0.27	3
<i>PTK2B</i>	-0.352	0.066	-0.268	0.121	-0.726	2.71E-04	-0.159	0.109	0.26	0.27	3
<i>SLC24A4</i>	0.114	0.681	0.113	0.622	-0.131	0.541	NA	NA	NA	NA	NA
<i>RIN3</i>	-0.019	0.94	0.223	0.117	0.145	0.637	-0.099	0.667	0.29	0.40	1
<i>SORL1</i>	0.064	0.676	0.045	0.806	-0.36	0.016	0.05	0.635	0.13	0.13	3
<i>ZCWPWI</i>	0.072	0.649	-0.087	0.637	0.215	0.259	-0.008	0.934	0.24	0.18	3

EC - entorhinal cortex; HP – hippocampus; TC - temporal cortex; FC - frontal cortex; AD – AD patients; CT - controls.

<sup>1</sup> CFG: convergent functional genomics score based on the lines of AD-related evidence.

logFC, log<sub>2</sub> fold change of gene expression in AD patients compared with controls.

FDR, *P*-value of differential expression with adjustment for multiple comparisons by the Benjamini-Hochberg’s (BH) method. FDR < 0.05 was marked in red.

“NA”, not applicable due to missing related data for the target gene.

k<sub>AD</sub>: connectivity of a gene in the AD network; k<sub>CTL</sub>: connectivity of a gene in the control network.

**Table S7. Top 30 DEGs in four brain regions**

Gene	Official descriptions	logFC	FDR
<b>Entorhinal cortex (EC)</b>			
<i>APLNR</i>	apelin receptor	1.349	6.81E-04
<i>SLC17A6</i>	solute carrier family 17 member 6	-1.295	1.84E-03
<i>CIQTNF4</i>	C1q and tumor necrosis factor related protein 4	-1.270	6.10E-03
<i>ACTL6B</i>	actin like 6B	-1.226	1.44E-03
<i>PCSK1</i>	proprotein convertase subtilisin/kexin type 1	-1.207	8.20E-03
<i>RSPO2</i>	R-spondin 2	-1.205	0.010
<i>STMN2</i>	stathmin 2	-1.132	6.63E-04
<i>PSMD8</i>	proteasome 26S subunit, non-ATPase 8	-1.132	3.94E-03
<i>MAST1</i>	microtubule associated serine/threonine kinase 1	-1.117	7.41E-04
<i>GABRA1</i>	gamma-aminobutyric acid type A receptor alpha1 subunit	-1.096	9.53E-03
<i>EEF1A2</i>	eukaryotic translation elongation factor 1 alpha 2	-1.093	1.02E-03
<i>MLIP</i>	muscular LMNA-interacting protein	-1.087	1.08E-03
<i>CITED1</i>	Cbp/p300 interacting transactivator with Glu/Asp rich carboxy-terminal domain 1	-1.080	9.46E-04
<i>GNG3</i>	G protein subunit gamma 3	-1.075	4.47E-04
<i>FSD1</i>	fibronectin type III and SPRY domain containing 1	-1.074	4.64E-04
<i>CPLX1</i>	complexin 1	-1.074	1.13E-03
<i>FAM107B</i>	family with sequence similarity 107 member B	1.070	2.53E-03
<i>ENDOG</i>	endonuclease G	-1.064	9.39E-04
<i>VSNL1</i>	visinin like 1	-1.061	3.86E-03
<i>SSSCA1</i>	Sjogren syndrome/scleroderma autoantigen 1	-1.061	1.64E-03
<i>ANGPT1</i>	angiopoietin 1	1.051	1.14E-03
<i>MIF</i>	macrophage migration inhibitory factor (glycosylation-inhibiting factor)	-1.046	2.00E-04
<i>AP2M1</i>	adaptor related protein complex 2 mu 1 subunit	-1.038	5.30E-04
<i>FAM19A1</i>	family with sequence similarity 19 (chemokine (C-C motif)-like), member A1	-1.034	9.05E-03
<i>WWTR1</i>	WW domain containing transcription regulator 1	1.034	5.30E-04
<i>RTBDN</i>	retbindin	-1.020	7.26E-04
<i>CHST6</i>	carbohydrate sulfotransferase 6	1.009	5.21E-03
<i>SLC16A9</i>	solute carrier family 16 member 9	1.009	1.53E-03
<i>ANLN</i>	anillin actin binding protein	1.008	5.50E-03
<i>INA</i>	internexin neuronal intermediate filament protein alpha	-1.007	6.62E-04
<b>Hippocampus (HP)</b>			
<i>SLC47A2</i>	solute carrier family 47 member 2	1.235	7.35E-04
<i>C1orf87</i>	chromosome 1 open reading frame 87	1.061	2.38E-04
<i>CFAP126</i>	cilia and flagella associated protein 126	0.996	7.35E-04
<i>LTF</i>	lactotransferrin	0.988	5.01E-03
<i>CHGB</i>	chromogranin B	-0.920	7.35E-04
<i>PDYN</i>	prodynorphin	-0.918	0.015
<i>CALY</i>	calcyon neuron specific vesicular protein	-0.906	2.48E-04
<i>SNCB</i>	synuclein beta	-0.875	9.99E-04
<i>FOXJ1</i>	forkhead box J1	0.846	7.67E-04
<i>INA</i>	internexin neuronal intermediate filament protein alpha	-0.841	2.38E-04

<i>PROK2</i>	prokineticin 2	0.832	1.22E-03
<i>SNX31</i>	sorting nexin 31	0.826	8.97E-03
<i>CCDC81</i>	coiled-coil domain containing 81	0.819	8.32E-04
<i>PVALB</i>	parvalbumin	-0.808	0.011
<i>NEFL</i>	neurofilament, light polypeptide	-0.808	2.48E-04
<i>SLC17A6</i>	solute carrier family 17 member 6	-0.807	0.019
<i>PLEKHA7</i>	pleckstrin homology domain containing A7	0.800	7.35E-04
<i>C21orf62</i>	chromosome 21 open reading frame 62	0.799	2.38E-04
<i>OGDHL</i>	oxoglutarate dehydrogenase-like	-0.786	6.24E-04
<i>GABRG2</i>	gamma-aminobutyric acid type A receptor gamma2 subunit	-0.783	7.35E-04
<i>FOS</i>	FBJ murine osteosarcoma viral oncogene homolog	0.778	0.024
<i>CCK</i>	cholecystokinin	-0.767	1.70E-03
<i>ANGPT1</i>	angiotensinogen 1	0.763	1.20E-03
<i>CD163</i>	CD163 molecule	0.754	0.036
<i>STMN2</i>	stathmin 2	-0.752	7.14E-04
<i>RGS1</i>	regulator of G-protein signaling 1	0.747	0.029
<i>TGFB111</i>	transforming growth factor beta 1 induced transcript 1	0.747	1.50E-03
<i>CPLX1</i>	complexin 1	-0.746	3.05E-04
<i>NRIP3</i>	nuclear receptor interacting protein 3	-0.744	1.22E-03
<i>SEMA5B</i>	semaphorin 5B	-0.736	7.90E-04

**Temporal cortex (TC)**

<i>PCSK1</i>	proprotein convertase subtilisin/kexin type 1	-1.751	3.50E-05
<i>SST</i>	somatostatin	-1.428	7.48E-05
<i>ADCYAP1</i>	adenylate cyclase activating polypeptide 1	-1.418	1.75E-06
<i>GABRA1</i>	gamma-aminobutyric acid type A receptor alpha1 subunit	-1.402	1.62E-05
<i>SLC14A1</i>	solute carrier family 14 member 1 (Kidd blood group)	1.400	3.25E-04
<i>SV2B</i>	synaptic vesicle glycoprotein 2B	-1.379	3.74E-06
<i>GABRA5</i>	gamma-aminobutyric acid type A receptor alpha5 subunit	-1.374	4.53E-04
<i>ENC1</i>	ectodermal-neural cortex 1	-1.356	2.27E-05
<i>VSNL1</i>	visinin like 1	-1.356	1.03E-04
<i>MAL2</i>	mal, T-cell differentiation protein 2 (gene/pseudogene)	-1.343	3.62E-05
<i>INA</i>	internexin neuronal intermediate filament protein alpha	-1.342	7.11E-06
<i>NPTX2</i>	neuronal pentraxin 2	-1.330	3.76E-06
<i>HSPB3</i>	heat shock protein family B (small) member 3	-1.329	1.62E-05
<i>ATP6V1E1</i>	ATPase H <sup>+</sup> transporting V1 subunit E1	-1.313	5.91E-06
<i>GFAP</i>	glial fibrillary acidic protein	1.300	3.62E-05
<i>APLNR</i>	apelin receptor	1.295	2.58E-04
<i>NELL2</i>	neural EGFL like 2	-1.269	1.03E-04
<i>STMN2</i>	stathmin 2	-1.260	8.37E-05
<i>CDK5</i>	cyclin-dependent kinase 5	-1.259	5.91E-06
<i>ID3</i>	inhibitor of DNA binding 3, HLH protein	1.256	8.01E-05
<i>PHYHD1</i>	phytanoyl-CoA dioxygenase domain containing 1	1.255	1.19E-04
<i>CHGB</i>	chromogranin B	-1.253	1.62E-05
<i>ATPIA3</i>	ATPase Na <sup>+</sup> /K <sup>+</sup> transporting subunit alpha 3	-1.250	7.84E-05

<i>NEFL</i>	neurofilament, light polypeptide	-1.248	3.95E-04
<i>CALB1</i>	calbindin 1	-1.242	2.84E-05
<i>RASL12</i>	RAS like family 12	1.230	9.50E-05
<i>CALY</i>	calcyon neuron specific vesicular protein	-1.225	6.31E-05
<i>NRXN3</i>	neurexin 3	-1.211	1.62E-05
<i>GJA1</i>	gap junction protein alpha 1	1.211	6.48E-05
<i>NECAB1</i>	N-terminal EF-hand calcium binding protein 1	-1.171	1.87E-04
<b>Frontal cortex (FC)</b>			
<i>GFAP</i>	glial fibrillary acidic protein	0.612	2.27E-04
<i>SCG2</i>	secretogranin II	-0.585	3.94E-04
<i>PLPP2</i>	phospholipid phosphatase 2	0.565	6.78E-04
<i>C21orf62</i>	chromosome 21 open reading frame 62	0.556	4.10E-06
<i>PCYOX1L</i>	prenylcysteine oxidase 1 like	-0.549	5.60E-06
<i>SASH1</i>	SAM and SH3 domain containing 1	0.534	1.63E-05
<i>PCSK1</i>	proprotein convertase subtilisin/kexin type 1	-0.518	5.49E-03
<i>NEUROD6</i>	neuronal differentiation 6	-0.511	3.96E-04
<i>AEBP1</i>	AE binding protein 1	0.507	1.23E-03
<i>ID3</i>	inhibitor of DNA binding 3, HLH protein	0.505	5.33E-03
<i>MID1IP1</i>	MID1 interacting protein 1	0.504	1.33E-04
<i>CXCR4</i>	C-X-C motif chemokine receptor 4	0.501	1.51E-03
<i>HSPA2</i>	heat shock protein family A (Hsp70) member 2	0.498	6.68E-04
<i>SLC30A3</i>	solute carrier family 30 member 3	-0.494	1.99E-04
<i>NRN1</i>	neuritin 1	-0.478	1.36E-03
<i>HSPB1</i>	heat shock protein family B (small) member 1	0.476	3.59E-03
<i>CHGB</i>	chromogranin B	-0.476	5.18E-03
<i>DDIT4</i>	DNA damage inducible transcript 4	0.475	1.23E-03
<i>SNX10</i>	sorting nexin 10	-0.468	4.25E-04
<i>MT1H</i>	metallothionein 1H	0.459	1.23E-03
<i>NFKBIA</i>	NFKB inhibitor alpha	0.456	3.72E-05
<i>EFHD1</i>	EF-hand domain family member D1	0.455	2.42E-04
<i>ZCCHC24</i>	zinc finger CCHC-type containing 24	0.455	3.30E-04
<i>EMP3</i>	epithelial membrane protein 3	0.454	8.60E-04
<i>MT1F</i>	metallothionein 1F	0.454	2.80E-03
<i>SEPP1</i>	selenoprotein P, plasma, 1	0.451	8.95E-04
<i>NDE1</i>	nudE neurodevelopment protein 1	0.451	1.50E-05
<i>SPP1</i>	secreted phosphoprotein 1	0.451	3.33E-03
<i>HIST1H2BD</i>	histone cluster 1, H2bd	0.450	5.31E-04
<i>MSX1</i>	mshhomeobox 1	0.447	1.22E-04

logFC, log<sub>2</sub> fold change of gene expression in AD patients compared with controls

FDR: *P*-value of differential expression with adjustment for multiple comparisons by the Benjamini-Hochberg's (BH) method.

**Table S8. Enriched pathways (Gene ontology, biological process) of DEGs in each brain region**

Term	Count	% <sup>1</sup>	Fold enrichment	<i>P</i> -value	FDR
<b>Entorhinal cortex (EC)</b>					
GO:0044237~cellular metabolic process	47	2.02	2.65	4.03E-10	7.67E-07
GO:0022904~respiratory electron transport chain	39	1.68	2.93	5.91E-10	1.12E-06
GO:0007269~neurotransmitter secretion	25	1.07	2.99	7.65E-07	1.46E-03
GO:0007268~synaptic transmission	87	3.74	1.69	9.28E-07	1.77E-03
GO:0035329~hippo signaling	14	0.60	4.09	7.45E-06	0.014
GO:0016079~synaptic vesicle exocytosis	11	0.47	4.82	1.74E-05	0.033
GO:0044281~small molecule metabolic process	272	11.69	1.26	2.50E-05	0.048
<b>Hippocampus (HP)</b>					
GO:0044237~cellular metabolic process	44	2.92	3.94	3.48E-15	6.34E-12
GO:0022904~respiratory electron transport chain	32	2.12	3.82	7.59E-11	1.40E-07
GO:0007268~synaptic transmission	68	4.52	2.09	8.58E-09	1.58E-05
GO:0015991~ATP hydrolysis coupled proton transport	14	0.93	5.49	4.07E-07	7.50E-04
GO:0033572~transferrin transport	13	0.86	4.53	1.29E-05	0.024
GO:0042776~mitochondrial ATP synthesis coupled proton transport	9	0.60	6.64	2.02E-05	0.037
GO:0006879~cellular iron ion homeostasis	18	1.20	3.22	2.58E-05	0.048
<b>Temporal cortex (TC)</b>					
GO:0007268~synaptic transmission	140	4.52	2.04	4.58E-18	8.85E-15
GO:0044237~cellular metabolic process	63	2.03	2.67	2.32E-14	4.49E-11
GO:0007411~axon guidance	150	4.84	1.66	9.32E-11	1.80E-07
GO:0048011~neurotrophin TRK receptor signaling pathway	112	3.62	1.68	1.11E-08	2.15E-05
GO:0022904~respiratory electron transport chain	43	1.39	2.43	1.43E-08	2.76E-05
GO:0006099~tricarboxylic acid cycle	18	0.58	3.68	4.53E-07	8.75E-04
GO:0044281~small molecule metabolic process	361	11.66	1.26	8.29E-07	1.60E-03
GO:0007173~epidermal growth factor receptor signaling pathway	89	2.87	1.63	1.52E-06	2.94E-03
GO:0000165~MAPK cascade	71	2.29	1.73	2.47E-06	4.79E-03
GO:0048010~vascular endothelial growth factor receptor signaling pathway	79	2.55	1.67	2.74E-06	5.29E-03
GO:0032543~mitochondrial translation	37	1.20	2.19	2.99E-06	5.78E-03
GO:0007269~neurotransmitter secretion	28	0.90	2.52	3.17E-06	6.13E-03
GO:0070125~mitochondrial translational elongation	33	1.07	2.30	3.48E-06	6.74E-03
GO:0043524~negative regulation of neuron apoptotic process	44	1.42	2.01	4.51E-06	8.73E-03
GO:0007399~nervous system development	75	2.42	1.67	5.18E-06	0.010
GO:0070124~mitochondrial translational initiation	32	1.03	2.26	7.94E-06	0.015
GO:0006521~regulation of cellular amino acid metabolic process	23	0.74	2.67	9.21E-06	0.018
GO:0006996~organelle organization	80	2.58	1.61	1.02E-05	0.020
GO:0060291~long-term synaptic potentiation	20	0.65	2.82	1.63E-05	0.032
GO:0051084~'de novo' posttranslational protein folding	20	0.65	2.82	1.63E-05	0.032
GO:0030036~actin cytoskeleton organization	41	1.32	1.96	1.87E-05	0.036
GO:0008543~fibroblast growth factor receptor signaling pathway	78	2.52	1.58	2.36E-05	0.046
<b>Frontal cortex (FC)</b>					

GO:0044281~small molecule metabolic process	175	14.32	1.49	3.37E-08	6.24E-05
GO:0034166~toll-like receptor 10 signaling pathway	19	1.55	4.01	6.05E-07	1.12E-03
GO:0034146~toll-like receptor 5 signaling pathway	19	1.55	4.01	6.05E-07	1.12E-03
GO:0048011~neurotrophin TRK receptor signaling pathway	55	4.50	2.03	9.12E-07	1.69E-03
GO:0034162~toll-like receptor 9 signaling pathway	19	1.55	3.69	2.26E-06	4.19E-03
GO:0038123~toll-like receptor TLR1:TLR2 signaling pathway	19	1.55	3.64	2.78E-06	5.14E-03
GO:0038124~toll-like receptor TLR6:TLR2 signaling pathway	19	1.55	3.64	2.78E-06	5.14E-03
GO:0002755~MyD88-dependent toll-like receptor signaling pathway	20	1.64	3.42	3.74E-06	6.91E-03
GO:0034134~toll-like receptor 2 signaling pathway	19	1.55	3.54	4.14E-06	7.65E-03
GO:0034138~toll-like receptor 3 signaling pathway	20	1.64	3.34	5.38E-06	9.95E-03
GO:0035666~TRIF-dependent toll-like receptor signaling pathway	19	1.55	3.41	7.30E-06	0.014
GO:0050790~regulation of catalytic activity	16	1.31	3.88	9.18E-06	0.017
GO:0002756~MyD88-independent toll-like receptor signaling pathway	19	1.55	3.33	1.05E-05	0.019
GO:0051403~stress-activated MAPK cascade	16	1.31	3.82	1.14E-05	0.021
GO:0007050~cell cycle arrest	26	2.13	2.65	1.33E-05	0.025
GO:0034142~toll-like receptor 4 signaling pathway	21	1.72	2.94	2.30E-05	0.042
GO:0006897~endocytosis	24	1.96	2.69	2.39E-05	0.044

<sup>1</sup> % (percentage) = the number of genes for each term / total number of differentially expressed genes (DEGs) in each brain region.

Count - number of DEGs that belongs to the term.

*P*-value: enrichment p-value measured by Fisher exact test.

FDR: adjusted for multiple comparisons by the Benjamini-Hochberg's (BH) method.



**Table S9. Enrichment of DEGs in 13 modules of the AD network**

Module	Module size	EC			HP			TC			FC		
		DEGs	Fold	FDR	DEGs	Fold	FDR	DEGs	Fold	FDR	DEGs	Fold	FDR
<b>DEGs cutoff:  logFC  &gt; 0.1 (fold change &gt; 1.07), FDR &lt; 0.05</b>													
black	358	73	1.30	0.03	1	0.07	1	5	0.15	1	6	0.37	1
blue	2050	119	0.37	1	8	0.41	1	14	0.32	1	27	1.25	1
brown	854	55	0.41	1	23	0.90	1	25	0.44	1	27	0.97	0.36
green	671	121	1.15	0.12	53	2.01	1	80	1.37	1	37	1.28	6.19E-16
green yellow	263	32	0.78	1	6	0.22	1	19	0.32	1	20	0.69	0.96
magenta	276	37	0.86	1	6	0.22	1	34	0.57	1	10	0.34	1
pink	281	11	0.25	1	14	0.40	1	41	0.54	1	33	0.87	1
purple	273	50	1.17	0.27	112	1.93	2.25E-06	248	1.93	4.95E-03	107	1.69	0.17
red	599	137	1.46	7.22E-06	11	0.17	1.37E-11	107	0.75	1.99E-29	142	2.01	1.15E-07
salmon	155	15	0.62	1	80	1.15	1	114	0.74	1	108	1.42	1
tan	204	28	0.88	1	53	0.64	1	104	0.57	1	98	1.09	0.28
turquoise	3626	789	1.39	3.43E-34	39	0.20	7.08E-60	34	0.08	2.07E-197	12	0.06	2.45E-07
yellow	722	149	1.32	5.51E-04	593	1.69	0.34	1386	1.79	1	463	1.21	2.75E-04
<b>DEGs cutoff:  logFC  &gt; 0.26 (fold change &gt; 1.2), FDR &lt; 0.05</b>													
black	358	68	1.27	0.07	1	0.08	1	5	0.15	1	0	0.00	1
blue	2050	118	0.38	1	3	0.19	1	14	0.33	1	2	0.28	1
brown	854	54	0.42	1	22	1.05	1	24	0.43	1	17	1.84	0.67
green	671	117	1.17	0.10	51	2.35	1	80	1.39	1	24	2.50	6.80E-16
green yellow	263	32	0.81	1	3	0.14	1	19	0.33	1	5	0.52	0.04
magenta	276	36	0.87	1	5	0.22	1	33	0.56	1	0	0.00	1
pink	281	10	0.24	1	11	0.39	1	41	0.54	1	3	0.24	1

<b>purple</b>	273	49	1.20	0.21	99	2.08	2.47E-08	248	1.97	2.98E-03	51	2.42	1.41E-04
<b>red</b>	599	132	1.47	8.228E-06	9	0.17	4.37E-12	103	0.73	1.28E-30	70	2.97	1.77E-08
<b>salmon</b>	155	12	0.52	1	60	1.05	1	110	0.72	1	29	1.14	1
<b>tan</b>	204	25	0.82	1	47	0.69	1	102	0.57	1	33	1.10	1
<b>turquoise</b>	3626	753	1.39	6.15E-32	38	0.23	2.16E-41	34	0.08	2.47E-192	2	0.03	1
<b>yellow</b>	722	140	1.30	2.08E-03	472	1.64	1	1362	1.78	1	127	1.00	0.65

Modules highlighted in yellow were DEG-enriched modules. EC - entorhinal cortex; HP – hippocampus; TC - temporal cortex; FC - frontal cortex. Fold, ratio of observed DEGs in the target module compared with the expected DEGs. FDR, Fisher’s exact test p-value adjusted for the number of modules.

**Table S10. Details about hub genes in the DEG-enriched modules**

Modules	Gene	Connectivity <sup>1</sup>			AD-related evidence							Expression change		Upstream regulator <sup>9</sup>
		k <sub>AD</sub>	k <sub>CTL</sub>	k <sub>AD</sub> -k <sub>CTL</sub> L	CFG <sup>2</sup>	eQTL <sup>3</sup>	GWAS <sup>4</sup>	PPI <sup>5</sup>	Pathology <sup>6</sup>		Early change <sup>7</sup>	in AD patients <sup>8</sup>		
									Aβ	Tau		EC/HP/TC/FC		
red	<i>ADD3</i>	0.88	0.90	-0.02	2	3	0	-	0.789,***	0.515,*	----	↑↑↑↑	no	
red	<i>AGT</i>	0.93	0.90	0.03	4	1	0	APP, PSEN1, APOE	-0.359,*	0.002,ns	↑↑--	--↑-	yes	
red	<i>ATPIA2</i>	0.82	0.71	0.11	3	1	0	-	0.460,**	-0.110,ns	-↓--	--↑-	yes	
red	<i>EPS8</i>	0.57	0.83	-0.26	2	1	0	MAPT	-0.228,ns	-0.376,ns	----	↑-↑-	no	
red	<i>GJA1</i>	0.80	0.81	-0.02	4	2	0	PSEN1, APOE, MAPT	0.388,**	0.131,ns	--↓-	-↑↑↑	yes	
red	<i>HDAC1</i>	0.56	0.98	-0.43	4	1	0	APP, PSEN2, MAPT	0.449,**	0.643,**	↓-↓-	--↑↑	yes	
red	<i>HSPB1</i>	0.18	0.82	-0.64	3	0	0	APP, PSEN1, MAPT	0.520,***	0.711,**	↓↓--	---↑	yes	
red	<i>MSN</i>	0.63	0.96	-0.33	3	0	NA	APOE	0.791,***	0.549,*	↓↓--	↑-↑↑	yes	
red	<i>NOTCH2</i>	0.80	0.58	0.22	2	3	0	PSEN1, PSEN2, APOE	NA,NA	NA,NA	NA	--↑-	no	
red	<i>PON2</i>	0.74	0.85	-0.11	3	2	0	-	0.697,***	0.760,**	-↓↓-	↑---	yes	
red	<i>SOX9</i>	0.81	0.79	0.01	2	3	0	-	0.671,***	0.539,*	----	↑↑↑-	no	
red	<i>SSPN</i>	0.82	0.70	0.13	3	3	0	-	0.543,***	0.179,ns	---↑	↑↑↑-	no	
red	<i>PRDX6</i>	1.00	0.74	0.26	2	2	0	-	0.749,***	0.841,***	----	↑-↑-	no	
red	<i>YAP1</i>	0.84	0.50	0.34	3	5	0	-	0.207,ns	0.563,*	↓--↓	↑↑↑-	yes	
red	<i>FERMT2</i>	0.69	0.88	-0.19	2	2	49	-	NA,NA	NA,NA	NA	↑-↑-	no	
red	<i>PBXIP1</i>	0.85	0.93	-0.07	2	0	0	-	0.758,***	0.190,ns	---↑	-↑↑↑	no	
green	<i>SLC31A2</i>	0.84	0.78	0.05	3	3	0	-	0.506,***	0.216,ns	--↓-	↑---	no	
green	<i>LPAR1</i>	0.85	0.97	-0.12	3	4	4	APP, APOE, MAPT	NA,NA	NA,NA	NA	↑---	no	
green	<i>ERBB3</i>	0.81	0.42	0.38	2	1	0	APP, PSEN1, MAPT	NA,NA	NA,NA	NA	----	no	
green	<i>HSPA2</i>	0.74	0.89	-0.15	2	1	0	-	0.132,ns	0.472,ns	↓---	↑-↑↑	yes	

green	<i>MAL</i>	0.78	0.80	-0.02	3	1	0	-	-0.253,ns	-0.692,**	---↑	--↑-	no
green	<i>KLK6</i>	0.79	0.91	-0.12	3	2	0	-	0.795,***	0.458,ns	-↓--	---↑	yes
green	<i>SOX10</i>	0.79	0.82	-0.02	2	2	0	PSEN2	NA,NA	NA,NA	NA	---↑	no
green	<i>TF</i>	0.80	0.78	0.02	2	1	0	APOE	NA,NA	NA,NA	NA	---↑	no
green	<i>UGT8</i>	0.94	0.91	0.03	2	0	0	-	0.102,ns	-0.523,*	--↓↑	↑---	no
green	<i>VEZF1</i>	0.88	0.68	0.20	2	1	0	-	-0.054,ns	-0.301,ns	---↑	↑↑↑↑	no
green	<i>ST18</i>	0.97	0.78	0.19	2	2	0	NA	0.272,ns	0.357,ns	↓---	↑---	no
green	<i>RASSF2</i>	0.73	1.00	-0.27	2	0	0	-	0.525,***	-0.118,ns	-↓-↑	↑---	no
green	<i>SLC44A1</i>	0.87	0.86	0.01	2	0	0	-	0.666,***	0.246,ns	-↓↓↑	↑--↑	yes
green	<i>DAAM2</i>	0.82	0.79	0.03	3	3	0	-	0.477,**	0.307,ns	---↑	↑-↑↑	no
green	<i>GLTP</i>	0.84	0.76	0.07	2	0	0	-	0.634,***	0.107,ns	---↑	↑-↑↑	no
green	<i>NDE1</i>	0.81	0.79	0.01	4	2	0	PSEN2, MAPT	0.626,***	0.297,ns	↓-↓-	---↑	yes
green	<i>FA2H</i>	0.91	0.85	0.05	2	0	1	-	0.007,ns	-0.496,ns	---↑	↑---	no
green	<i>TJAP1</i>	0.82	0.95	-0.13	3	1	0	-	0.481,***	0.008,ns	↓-↓↑	↑-↑↑	yes
purple	<i>CLIC1</i>	0.90	0.99	-0.10	2	0	0	NA	0.616,***	0.596,*	-↓--	--↑↑	no
purple	<i>COL1A2</i>	0.40	0.98	-0.58	3	0	0	PSEN2, MAPT	-0.473,**	0.163,ns	↓---	↑-↑-	no
purple	<i>ILAR</i>	0.95	0.61	0.34	2	1	0	PSEN1	NA,NA	NA,NA	NA	--↑-	no
purple	<i>OGN</i>	0.27	0.81	-0.54	2	3	NA	-	0.347,*	0.029,ns	----	----	no
purple	<i>STAT3</i>	0.46	0.86	-0.39	4	3	0	APP, PSEN2, APOE	0.873,***	0.572,*	-↓--	---↑	no
purple	<i>TIMP1</i>	0.61	0.85	-0.24	4	1	NA	APP, APOE, MAPT	0.872,***	0.765,***	-↓--	--↑-	no
purple	<i>TNFRSF1A</i>	1.00	1.00	0.00	3	2	0	APP, PSEN2, APOE, MAPT	0.860,***	0.511,ns	----	↑-↑↑	no
purple	<i>IFITM3</i>	0.64	0.86	-0.22	4	2	0	PSEN2, MAPT	0.863,***	0.615,*	-↓--	--↑↑	no
purple	<i>IFITM2</i>	0.82	0.82	0.00	4	2	0	PSEN2, MAPT	0.660,***	0.726,**	-↓--	--↑-	no
turquoise	<i>AMPH</i>	0.81	0.77	0.04	2	0	1	-	-0.327,*	-0.264,ns	----	↓↓↓-	no
turquoise	<i>ATP6V1B2</i>	0.90	0.88	0.02	2	1	0	-	-0.162,ns	-0.527,*	----	↓↓↓↓	no
turquoise	<i>ATP6V1C1</i>	0.76	0.86	-0.10	2	1	0	-	-0.169,ns	0.138,ns	---↓	--↓↓	no

turquoise	<i>ATP6V1E1</i>	0.84	0.85	-0.01	2	0	0	-	-0.534,***	-0.316,ns	---↓	↓↓↓-	no
turquoise	<i>DDX1</i>	0.66	0.81	-0.15	3	3	0	-	-0.351,*	-0.459,ns	---↑	-↓↓-	no
turquoise	<i>ENO2</i>	0.83	0.72	0.10	3	2	0	-	-0.022,ns	-0.547,*	---↓	↓↓↓-	no
turquoise	<i>GABRG2</i>	0.93	0.69	0.24	3	1	0	-	-0.441,**	-0.763,***	↓---	↓↓↓↓	no
turquoise	<i>GLRB</i>	0.90	0.74	0.16	2	1	0	-	-0.521,***	-0.766,***	----	↓↓↓-	no
turquoise	<i>GOT1</i>	0.76	0.87	-0.11	3	1	0	-	-0.472,**	-0.551,*	-↑--	↓↓↓↓	no
turquoise	<i>GUCY1B3</i>	0.65	0.83	-0.18	3	1	0	-	-0.246,ns	-0.581,*	-↑--	-↓↓-	no
turquoise	<i>PCMT1</i>	0.85	1.00	-0.15	2	0	0	-	-0.512,***	-0.630,*	---↑	↓↓↓-	no
turquoise	<i>PFN2</i>	0.81	0.89	-0.08	2	1	0	-	-0.339,*	-0.573,*	----	↓-↓↓	no
turquoise	<i>SERPINI1</i>	0.83	0.78	0.05	3	2	0	-	-0.356,*	-0.656,**	-↑--	↓↓↓↓	no
turquoise	<i>MAPK9</i>	0.88	0.86	0.02	2	0	0	APP, PSEN1, PSEN2, APOE	-0.364,*	-0.743,**	----	-↓↓-	no
turquoise	<i>PSMD1</i>	0.59	0.81	-0.22	2	1	0	PSEN1	-0.131,ns	-0.063,ns	----	↓↓↓-	no
turquoise	<i>SCG5</i>	0.82	0.79	0.03	2	1	1	-	NA,NA	NA,NA	NA	↓↓↓-	no
turquoise	<i>SH3GL2</i>	0.85	0.68	0.17	4	1	0	PSEN2	-0.365,*	-0.393,ns	↓--↓	↓↓↓-	yes
turquoise	<i>STXBP1</i>	0.86	0.73	0.14	4	1	0	MAPT	-0.429,**	-0.868,***	---↑	↓↓↓-	no
turquoise	<i>SYT1</i>	1.00	0.89	0.11	3	0	5	MAPT	-0.209,ns	-0.471,ns	-↑--	-↓↓-	no
turquoise	<i>TUBA4A</i>	0.68	0.81	-0.13	2	2	0	PSEN2, MAPT	NA,NA	NA,NA	NA	↓↓↓-	no
turquoise	<i>UCHL1</i>	0.83	0.49	0.34	3	1	0	-	-0.338,*	-0.209,ns	↑↑--	↓↓↓↓	yes
turquoise	<i>YWHAB</i>	0.78	0.91	-0.13	3	1	0	PSEN2, MAPT	-0.234,ns	-0.596,*	----	↓↓↓-	no
turquoise	<i>YWHAZ</i>	0.74	0.86	-0.12	3	2	0	MAPT	-0.391,**	-0.362,ns	----	↓↓↓↓	no
turquoise	<i>RBM10</i>	0.04	0.80	-0.76	2	1	NA	-	-0.166,ns	-0.692,**	----	----	no
turquoise	<i>SLC25A12</i>	0.81	0.70	0.12	2	5	0	-	-0.263,ns	-0.262,ns	--↓-	↓↓↓-	no
turquoise	<i>PEX11B</i>	0.82	0.86	-0.04	3	3	NA	-	-0.353,*	0.083,ns	↑---	↓↓↓↓	no
turquoise	<i>INA</i>	0.94	0.73	0.21	3	2	0	-	-0.268,ns	-0.860,***	---↑	↓↓↓↓	no
turquoise	<i>SNAP91</i>	0.83	0.76	0.08	2	2	0	-	-0.339,*	-0.527,*	----	↓↓↓-	no
turquoise	<i>CAP2</i>	0.85	0.72	0.13	2	2	0	APP, APOE, MAPT	NA,NA	NA,NA	NA	↓-↓-	no

turquoise	<i>MLLT11</i>	0.97	0.70	0.27	3	1	0	-	-0.445,**	-0.600,*	-↑--	↓↓↓↓	no
turquoise	<i>STMN2</i>	1.00	0.83	0.17	2	0	0	-	-0.662,***	-0.713,**	↑↑↑-	↓↓↓-	yes
turquoise	<i>GHITM</i>	0.52	0.88	-0.35	2	0	0	PSEN2	-0.287,ns	-0.372,ns	↑---	↓↓↓↓	no
turquoise	<i>TAGLN3</i>	0.87	0.63	0.24	2	1	0	-	0.291,ns	0.371,ns	↑---	↓↓↓↓	no
turquoise	<i>RAPGEFL1</i>	0.19	0.87	-0.68	2	1	0	NA	0.016,ns	-0.162,ns	↓---	↓-↓-	no
turquoise	<i>REEP1</i>	0.93	0.75	0.18	2	0	0	-	-0.621,***	-0.858,***	--↑↑	↓↓↓↓	yes
yellow	<i>VCAN</i>	0.99	0.76	0.23	2	4	0	PSEN1, APOE	NA,NA	NA,NA	NA	↑↑↑↑	no
yellow	<i>CTNNA1</i>	0.80	0.56	0.24	3	0	0	PSEN1	0.665,***	0.141,ns	-↓--	----	no
yellow	<i>SMAD5</i>	0.81	0.47	0.34	3	0	0	APP, APOE	0.531,***	0.216,ns	--↓-	↑-↑-	no
yellow	<i>SPI</i>	0.68	0.82	-0.14	2	1	0	APP, PSEN1, PSEN2, APOE, MAPT	0.020,ns	0.079,ns	----	--↑↑	no
yellow	<i>SYPL1</i>	0.92	0.60	0.32	2	4	2	-	NA,NA	NA,NA	NA	↑-↑-	no
yellow	<i>TJP1</i>	0.87	0.70	0.16	2	4	0	PSEN1	0.100,ns	-0.047,ns	----	↑---	no
yellow	<i>TYK2</i>	0.29	0.82	-0.53	4	1	0	APOE	0.440,**	0.163,ns	↓---	--↑↑	no
yellow	<i>SNAP23</i>	0.73	0.83	-0.11	3	1	0	-	0.657,***	0.433,ns	↓---	--↑-	no
yellow	<i>IQGAP1</i>	0.72	1.00	-0.28	4	1	0	PSEN1	0.310,*	0.282,ns	--↑-	↑↑↑↑	no
yellow	<i>KAT2B</i>	0.85	0.42	0.43	2	4	0	PSEN2	NA,NA	NA,NA	NA	--↑-	no
yellow	<i>BBX</i>	0.85	0.61	0.24	2	1	0	-	0.049,ns	-0.424,ns	↓--↑	↑↑↑-	no

<sup>1</sup>  $k_{AD}$ : connectivity of a gene in AD network;  $k_{CTL}$ : connectivity of a gene in control network.  $k_{AD}-k_{CTL}$ : an index to show the gain-of-connectivity (positive value) or loss-of-connectivity (negative value) in AD network compared to control network.

<sup>2</sup> CFG: convergent functional genomics score based on the total number of lines of AD-related evidence.

<sup>3</sup> eQTL: total number of genetic variants (IGAP GWAS [45],  $P < 0.001$ ) that showing significant associations with expression of the target gene (Braincloud [46],  $P < 0.001$ ).

<sup>4</sup> GWAS: total number of genetic variants in IGAP GWAS [45] ( $P < 0.001$ ).

<sup>5</sup> PPI: AD core genes (APP, PSEN1, PSEN2, MAPT and APOE) had significant protein-protein interaction ( $P < 0.05$ ) with the target gene [47, 48].

<sup>6</sup> Pathology: expression correlation ( $r$ ) and significance (P-value significance, \* $P < .05$ , \*\* $P < .01$ , \*\*\* $P < .001$ ) of the target gene and AD pathology in AD mice (Pearson's correlation,  $P < 0.05$ ), A $\beta$ : A $\beta$  line AD mice in Mouseac [49], Tau: tau line AD mice in Mouseac [49].

<sup>7</sup> Early change: expression alterations in hippocampus of 2 month-old AD mice (in order of: HO-TASTPM [homozygous APP/PSEN1 double mutant mice], HET-TASTPM [heterozygous APP/PSEN1 double mutant mice], TAS10 [human mutant APP mice], TAU [mutant human MAPT mice]) [49].

<sup>8</sup> Expression change of target genes in AD patients in renormalized datasets of entorhinal cortex (EC), hippocampus (HP), temporal cortex (TC), and frontal cortex (FC).

<sup>9</sup> Upstream regulator: hub genes showed consistent early expression alterations in Mouseac [49] or in other two replicating datasets (GSE29317 [52] and GSE31372). “ $\uparrow$ ”, upregulated; “ $\downarrow$ ”, downregulated; “-”, no significant PPI interaction, expression correlation or expression change; “NA”, related data were missing for the target gene. Genes highlighted in yellow have transcription factor activities; Genes highlighted in green are candidate upstream regulators, as indicated by early alteration.

**Table S11. Genetic variants regulating mRNA expression of *YAP1***

SNP ID	Chromosome	Position	GWAS		eQTL	
			<i>P</i>	OR	<i>P</i>	Beta
rs17093759	chr10	82382102	6.39E-04	1.07	9.03E-04	0.15
rs4500467	chr11	15401144	8.70E-04	1.06	4.66E-04	-0.18
rs10860303	chr12	98573602	5.91E-04	0.94	4.97E-05	0.19
rs7966704	chr12	98577304	2.65E-04	0.94	2.33E-04	0.16
rs12369175	chr12	98578617	8.40E-04	0.94	4.08E-04	0.17

GWAS data were taken from IGAP [45]; eQTL data were taken from the Braincloud [46]; OR: Odds ratio; beta: eQTL effect on *YAP1* expression.



**Table S12. YAP1-regulated genes (N = 455, identified by RNA-seq) in DEG-enriched modules**

Module	Gene	YAP1 interference			YAP1 overexpression		
		logFC	P	FDR	logFC	P	FDR
red	<i>USP53</i>	0.50	1.39E-04	3.85E-03	-0.61	3.45E-05	2.18E-03
red	<i>OGFRL1</i>	0.34	3.77E-04	8.09E-03	-0.34	1.15E-03	0.04
red	<i>YES1</i>	0.37	5.13E-04	0.01	-0.43	1.44E-04	6.92E-03
red	<i>LARP7</i>	0.43	1.32E-03	0.02	-0.46	1.88E-03	0.05
red	<i>FGF2</i>	0.35	1.93E-03	0.03	-0.41	9.62E-04	0.03
red	<i>TEAD1</i>	0.30	1.94E-03	0.03	-0.24	0.04	0.43
red	<i>ENAH</i>	0.29	2.66E-03	0.03	-0.21	0.05	0.48
red	<i>CD2AP</i>	0.36	2.89E-03	0.04	-0.50	1.51E-05	1.10E-03
red	<i>TMEM47</i>	0.35	3.11E-03	0.04	-0.37	4.67E-03	0.10
red	<i>ANP32E</i>	0.31	3.19E-03	0.04	-0.27	0.01	0.18
red	<i>PLOD2</i>	0.26	3.61E-03	0.04	-0.30	3.32E-03	0.08
red	<i>REST</i>	0.29	3.85E-03	0.04	-0.30	0.01	0.18
red	<i>YAP1</i>	-0.26	3.93E-03	0.04	0.46	6.44E-07	9.05E-05
red	<i>GOLIM4</i>	0.28	4.31E-03	0.05	-0.32	2.75E-03	0.07
red	<i>FGD6</i>	0.38	0.01	0.10	-0.36	0.03	0.35
red	<i>ITPR2</i>	0.32	0.01	0.11	-0.42	1.44E-03	0.04
red	<i>PRKD3</i>	0.26	0.02	0.11	-0.27	0.01	0.24
red	<i>RNF19A</i>	0.26	0.02	0.12	-0.24	0.04	0.43
red	<i>RYR3</i>	0.39	0.03	0.15	-0.34	0.03	0.37
red	<i>TLR4</i>	0.25	0.03	0.17	-0.29	0.04	0.41
red	<i>FAM184A</i>	0.31	0.04	0.18	-0.34	0.03	0.36
red	<i>LYRM2</i>	0.22	0.04	0.19	-0.24	0.03	0.35
red	<i>NEK1</i>	0.27	0.05	0.21	-0.48	3.80E-04	0.01
green	<i>ARID4B</i>	0.65	1.32E-08	3.09E-06	-0.63	9.57E-08	2.23E-05
green	<i>C21orf91</i>	0.47	1.02E-05	5.41E-04	-0.35	3.34E-03	0.08
green	<i>CARF</i>	0.33	0.02	0.11	-0.35	0.02	0.27
green	<i>CCDC102B</i>	0.36	0.04	0.18	-0.35	0.03	0.41
green	<i>CCDC88A</i>	0.60	5.76E-06	3.51E-04	-0.58	8.87E-06	7.24E-04
green	<i>CDK6</i>	0.57	1.63E-08	3.56E-06	-0.39	2.94E-03	0.07
green	<i>CENPU</i>	0.43	3.24E-04	7.21E-03	-0.36	5.93E-03	0.13
green	<i>CEP135</i>	0.57	1.22E-06	1.11E-04	-0.57	6.23E-06	5.43E-04
green	<i>CHD9</i>	0.80	1.03E-13	4.42E-10	-0.74	3.32E-09	1.90E-06
green	<i>DICER1</i>	0.42	2.09E-05	9.23E-04	-0.44	5.46E-04	0.02
green	<i>DOCK10</i>	0.42	1.58E-04	4.25E-03	-0.29	0.01	0.21
green	<i>EVI5</i>	0.31	2.95E-03	0.04	-0.28	0.03	0.35
green	<i>FBXO5</i>	0.33	3.80E-03	0.04	-0.44	2.38E-04	0.01
green	<i>FOXN2</i>	0.38	1.78E-03	0.03	-0.38	3.40E-03	0.08
green	<i>GCFC2</i>	0.33	3.06E-03	0.04	-0.27	0.04	0.45
green	<i>ICE2</i>	0.38	2.76E-04	6.40E-03	-0.41	3.86E-04	0.01
green	<i>IFIT2</i>	0.33	0.02	0.11	-0.31	0.02	0.32

green	<i>KIAA0586</i>	0.32	0.01	0.08	-0.41	9.67E-04	0.03
green	<i>MBNL2</i>	0.41	1.21E-04	3.44E-03	-0.47	1.60E-04	7.52E-03
green	<i>MOSPD2</i>	0.27	0.03	0.16	-0.47	1.57E-04	7.38E-03
green	<i>NIN</i>	0.44	5.57E-05	1.98E-03	-0.51	2.33E-05	1.56E-03
green	<i>PDE1C</i>	0.38	6.51E-05	2.22E-03	-0.29	5.86E-03	0.12
green	<i>RAI14</i>	0.23	0.01	0.10	-0.25	0.02	0.27
green	<i>RDX</i>	0.36	2.79E-04	6.43E-03	-0.25	0.01	0.20
green	<i>RIF1</i>	0.79	5.04E-10	2.50E-07	-0.66	1.22E-06	1.52E-04
green	<i>RUFY2</i>	0.31	7.31E-03	0.07	-0.33	6.66E-03	0.14
green	<i>SHTN1</i>	0.25	0.02	0.11	-0.25	0.01	0.21
green	<i>SLF2</i>	0.38	9.26E-05	2.84E-03	-0.28	0.02	0.25
green	<i>SOS2</i>	0.33	1.96E-03	0.03	-0.27	0.03	0.38
green	<i>STRN</i>	0.35	5.16E-04	0.01	-0.23	0.04	0.45
green	<i>TBC1D8B</i>	0.44	1.18E-03	0.02	-0.53	1.79E-04	8.30E-03
green	<i>TRMT13</i>	0.51	1.80E-04	4.59E-03	-0.55	3.09E-04	0.01
green	<i>TTN</i>	0.59	5.12E-04	0.01	-0.36	0.03	0.38
green	<i>UBA6</i>	0.43	1.84E-05	8.40E-04	-0.47	1.27E-05	9.53E-04
green	<i>USP34</i>	0.59	6.21E-08	1.08E-05	-0.60	2.77E-06	2.89E-04
green	<i>VPS13C</i>	0.76	1.13E-11	1.53E-08	-0.68	6.08E-08	1.64E-05
green	<i>ZBTB44</i>	0.25	0.02	0.14	-0.26	0.03	0.37
green	<i>ZFC3H1</i>	0.62	4.25E-08	7.94E-06	-0.45	2.24E-04	0.01
green	<i>ZFYVE16</i>	0.63	2.41E-09	8.12E-07	-0.63	1.43E-07	2.90E-05
green	<i>ZNF226</i>	0.25	0.04	0.19	-0.27	0.03	0.40
green	<i>ZNF253</i>	0.53	7.46E-04	0.01	-0.52	1.39E-03	0.04
green	<i>ZNF430</i>	0.53	1.45E-04	3.97E-03	-0.51	1.07E-03	0.03
green	<i>ZNF507</i>	0.34	3.29E-03	0.04	-0.33	6.62E-03	0.14
green	<i>ZNF614</i>	0.45	8.24E-04	0.01	-0.62	5.41E-06	4.91E-04
green	<i>ZNF721</i>	0.65	1.13E-06	1.05E-04	-0.55	2.36E-04	0.01
purple	<i>CALD1</i>	0.21	0.02	0.14	-0.32	5.01E-03	0.11
purple	<i>CFH</i>	0.56	1.83E-04	4.64E-03	-0.32	0.04	0.42
purple	<i>IFI16</i>	0.27	0.01	0.10	-0.49	6.63E-05	3.61E-03
purple	<i>IL4R</i>	-0.45	3.66E-03	0.04	0.33	0.04	0.45
purple	<i>LTBP1</i>	-0.21	0.03	0.17	0.25	0.01	0.21
purple	<i>MALT1</i>	0.39	4.09E-04	8.57E-03	-0.33	3.68E-03	0.09
purple	<i>PAWR</i>	0.31	3.88E-03	0.04	-0.33	3.25E-03	0.08
purple	<i>REL</i>	0.42	4.18E-03	0.05	-0.37	0.02	0.25
purple	<i>UTRN</i>	0.67	3.10E-10	1.74E-07	-0.59	1.34E-06	1.65E-04
red	<i>SCAF11</i>	0.65	1.67E-09	6.46E-07	-0.55	1.86E-05	1.32E-03
red	<i>ITGB8</i>	0.52	3.87E-08	7.55E-06	-0.59	5.49E-07	7.97E-05
red	<i>FAM111A</i>	0.51	1.67E-07	2.37E-05	-0.28	6.94E-03	0.14
red	<i>PIK3C2A</i>	0.55	3.52E-07	4.09E-05	-0.78	1.10E-09	8.41E-07
red	<i>IL6ST</i>	0.52	1.01E-06	9.51E-05	-0.81	1.59E-10	2.43E-07
red	<i>SLC7A11</i>	0.45	1.56E-06	1.36E-04	-0.67	2.21E-07	3.83E-05
red	<i>DDX60</i>	0.51	4.06E-06	2.65E-04	-0.55	4.09E-06	3.97E-04

red	<i>MKLN1</i>	0.46	5.93E-06	3.53E-04	-0.46	1.20E-04	5.97E-03
red	<i>ITGAV</i>	0.41	9.03E-06	4.95E-04	-0.24	0.01	0.21
turquoise	<i>ACSL3</i>	0.20	0.04	0.18	-0.19	0.05	0.49
turquoise	<i>ADAMTS3</i>	0.47	1.84E-03	0.03	-0.50	1.62E-03	0.05
turquoise	<i>AGGF1</i>	0.36	7.48E-04	0.01	-0.45	4.32E-05	2.56E-03
turquoise	<i>AGL</i>	0.45	1.76E-05	8.10E-04	-0.47	2.31E-04	0.01
turquoise	<i>AGTPBP1</i>	0.25	0.04	0.20	-0.35	7.29E-03	0.15
turquoise	<i>AH11</i>	0.35	3.74E-03	0.04	-0.47	2.71E-04	0.01
turquoise	<i>AKAP11</i>	0.60	1.76E-09	6.46E-07	-0.52	7.64E-05	4.06E-03
turquoise	<i>AKAP6</i>	0.23	0.03	0.17	-0.32	0.02	0.33
turquoise	<i>APC</i>	0.83	1.19E-11	1.53E-08	-0.48	3.72E-03	0.09
turquoise	<i>APPL1</i>	0.37	3.82E-04	8.13E-03	-0.37	8.64E-04	0.03
turquoise	<i>ARFGEF1</i>	0.44	1.04E-05	5.47E-04	-0.33	3.49E-03	0.08
turquoise	<i>ARGLU1</i>	0.30	1.33E-03	0.02	-0.19	0.05	0.49
turquoise	<i>ARID4A</i>	0.54	1.88E-04	4.72E-03	-0.60	9.63E-05	4.99E-03
turquoise	<i>ARL6IP1</i>	0.20	0.03	0.17	-0.19	0.05	0.48
turquoise	<i>ASCC3</i>	0.34	2.27E-03	0.03	-0.36	1.49E-03	0.04
turquoise	<i>ASNSD1</i>	0.29	0.01	0.10	-0.23	0.04	0.45
turquoise	<i>ATAD2</i>	0.65	1.13E-11	1.53E-08	-0.64	2.45E-08	8.23E-06
turquoise	<i>ATG2B</i>	0.30	3.91E-03	0.04	-0.26	0.02	0.33
turquoise	<i>ATP11B</i>	0.40	1.74E-05	8.07E-04	-0.32	2.39E-03	0.06
turquoise	<i>ATP2B1</i>	0.47	7.38E-05	2.43E-03	-0.48	1.26E-05	9.51E-04
turquoise	<i>ATP6VIC1</i>	0.23	0.04	0.19	-0.34	1.75E-03	0.05
turquoise	<i>ATR</i>	0.63	2.37E-08	4.85E-06	-0.57	2.43E-06	2.64E-04
turquoise	<i>ATRX</i>	0.83	3.47E-10	1.86E-07	-0.56	2.08E-05	1.44E-03
turquoise	<i>BCAP29</i>	0.28	0.01	0.08	-0.37	3.60E-04	0.01
turquoise	<i>BCAT1</i>	0.18	0.05	0.21	-0.40	3.00E-04	0.01
turquoise	<i>BICD1</i>	0.37	1.66E-04	4.38E-03	-0.21	0.05	0.49
turquoise	<i>BLZF1</i>	0.36	1.87E-03	0.03	-0.42	1.06E-03	0.03
turquoise	<i>BMPR2</i>	0.35	5.40E-04	0.01	-0.25	0.04	0.43
turquoise	<i>BRCC3</i>	0.34	8.23E-04	0.01	-0.58	1.18E-06	1.51E-04
turquoise	<i>BRIP1</i>	0.75	4.33E-11	4.29E-08	-0.59	8.88E-06	7.24E-04
turquoise	<i>BRWD1</i>	0.57	1.66E-06	1.43E-04	-0.59	6.45E-06	5.59E-04
turquoise	<i>C5orf42</i>	0.65	4.53E-07	4.99E-05	-0.66	1.07E-06	1.41E-04
turquoise	<i>CACNA2D1</i>	0.62	1.99E-06	1.63E-04	-0.51	3.50E-04	0.01
turquoise	<i>CAMK4</i>	0.53	7.01E-06	4.03E-04	-0.62	3.14E-05	2.03E-03
turquoise	<i>CAMSAP2</i>	0.47	4.71E-06	2.93E-04	-0.46	2.01E-04	0.01
turquoise	<i>CAND1</i>	0.30	1.35E-03	0.02	-0.20	0.04	0.46
turquoise	<i>CCNT2</i>	0.41	1.31E-04	3.67E-03	-0.47	5.79E-05	3.21E-03
turquoise	<i>CDC27</i>	0.30	3.76E-03	0.04	-0.31	6.34E-03	0.13
turquoise	<i>CDC5L</i>	0.36	1.78E-03	0.03	-0.41	6.29E-04	0.02
turquoise	<i>CDC7</i>	0.44	3.77E-04	8.09E-03	-0.29	0.02	0.27
turquoise	<i>CENPF</i>	0.57	1.12E-03	0.02	-0.72	3.73E-08	1.14E-05
turquoise	<i>CEP170</i>	0.38	1.30E-04	3.66E-03	-0.49	2.62E-05	1.74E-03

turquoise	<i>CEP57</i>	0.38	1.73E-04	4.47E-03	-0.34	9.48E-04	0.03
turquoise	<i>CEP83</i>	0.38	0.02	0.12	-0.36	0.03	0.36
turquoise	<i>CFAP44</i>	0.54	9.72E-04	0.02	-0.41	0.01	0.22
turquoise	<i>CHM</i>	0.40	9.80E-05	2.91E-03	-0.61	2.87E-08	9.19E-06
turquoise	<i>CHML</i>	0.63	9.33E-07	9.01E-05	-0.69	5.30E-06	4.87E-04
turquoise	<i>CHORDC1</i>	0.43	1.81E-04	4.60E-03	-0.40	3.50E-03	0.08
turquoise	<i>CKAP2</i>	0.56	9.78E-07	9.33E-05	-0.62	1.87E-06	2.16E-04
turquoise	<i>CKAP5</i>	0.29	1.45E-03	0.02	-0.25	0.01	0.21
turquoise	<i>CLIP1</i>	0.27	6.92E-03	0.06	-0.49	2.08E-05	1.44E-03
turquoise	<i>CLOCK</i>	0.53	2.39E-07	3.10E-05	-0.53	5.64E-06	5.05E-04
turquoise	<i>COPS2</i>	0.43	1.07E-04	3.12E-03	-0.42	3.44E-04	0.01
turquoise	<i>CRNKL1</i>	0.33	3.60E-03	0.04	-0.31	0.01	0.19
turquoise	<i>CSE1L</i>	0.36	2.87E-04	6.55E-03	-0.31	3.07E-03	0.08
turquoise	<i>CSNK1G3</i>	0.25	0.02	0.14	-0.33	3.48E-03	0.08
turquoise	<i>CSRNP3</i>	0.51	9.27E-04	0.02	-0.32	0.05	0.48
turquoise	<i>CTNNA1</i>	0.29	6.58E-03	0.06	-0.29	0.02	0.26
turquoise	<i>CUL2</i>	0.23	0.04	0.20	-0.34	8.69E-03	0.16
turquoise	<i>CULAB</i>	0.38	9.50E-05	2.88E-03	-0.36	3.33E-04	0.01
turquoise	<i>CUL5</i>	0.56	1.54E-08	3.42E-06	-0.63	5.68E-09	2.60E-06
turquoise	<i>DBF4</i>	0.42	6.08E-04	0.01	-0.58	2.73E-06	2.89E-04
turquoise	<i>DCLRE1A</i>	0.31	8.76E-03	0.08	-0.29	0.02	0.27
turquoise	<i>DCP2</i>	0.53	1.00E-07	1.57E-05	-0.40	3.54E-05	2.23E-03
turquoise	<i>DCUNID4</i>	0.34	1.13E-03	0.02	-0.36	7.32E-04	0.02
turquoise	<i>DDX10</i>	0.31	9.76E-04	0.02	-0.31	5.00E-03	0.11
turquoise	<i>DENND1B</i>	0.56	1.09E-05	5.62E-04	-0.52	3.25E-04	0.01
turquoise	<i>DENND4A</i>	0.27	0.02	0.11	-0.25	0.05	0.47
turquoise	<i>DIS3</i>	0.43	7.91E-05	2.55E-03	-0.41	5.46E-04	0.02
turquoise	<i>DLD</i>	0.33	1.07E-03	0.02	-0.21	0.04	0.43
turquoise	<i>DMXL1</i>	0.56	2.00E-08	4.30E-06	-0.62	9.46E-08	2.23E-05
turquoise	<i>DMXL2</i>	0.52	2.87E-05	1.20E-03	-0.60	1.88E-06	2.16E-04
turquoise	<i>DNAJB14</i>	0.61	3.69E-07	4.21E-05	-0.66	1.22E-07	2.55E-05
turquoise	<i>DNAJC13</i>	0.41	2.35E-05	1.02E-03	-0.50	2.27E-05	1.54E-03
turquoise	<i>DNTTIP2</i>	0.40	1.72E-03	0.02	-0.33	0.01	0.17
turquoise	<i>DOPEY1</i>	0.54	2.89E-06	2.15E-04	-0.32	0.02	0.26
turquoise	<i>DZIP3</i>	0.46	1.85E-04	4.67E-03	-0.58	6.78E-06	5.81E-04
turquoise	<i>ECT2</i>	0.58	2.64E-09	8.29E-07	-0.66	3.50E-10	4.02E-07
turquoise	<i>EDEM3</i>	0.37	1.70E-04	4.44E-03	-0.35	1.28E-03	0.04
turquoise	<i>EHBP1</i>	0.26	0.01	0.09	-0.25	0.03	0.37
turquoise	<i>EIF1AX</i>	0.31	0.01	0.09	-0.26	0.02	0.30
turquoise	<i>EIF2AK2</i>	0.21	0.04	0.20	-0.25	0.04	0.45
turquoise	<i>EPHA3</i>	0.48	1.51E-05	7.21E-04	-0.31	7.04E-03	0.14
turquoise	<i>EPM2AIP1</i>	0.39	3.62E-04	7.82E-03	-0.31	0.01	0.17
turquoise	<i>ERGIC2</i>	0.27	0.02	0.11	-0.26	0.02	0.32
turquoise	<i>ETNK1</i>	0.35	2.98E-04	6.72E-03	-0.32	2.26E-03	0.06

turquoise	<i>ETV1</i>	0.34	1.19E-03	0.02	-0.29	0.03	0.37
turquoise	<i>FANCI</i>	0.40	6.05E-05	2.10E-03	-0.25	0.02	0.25
turquoise	<i>FASTKD2</i>	0.27	0.01	0.09	-0.27	0.03	0.36
turquoise	<i>FILIP1L</i>	0.27	0.05	0.21	-0.32	0.02	0.34
turquoise	<i>FMRI</i>	0.23	0.04	0.18	-0.23	0.04	0.44
turquoise	<i>FZD3</i>	0.30	0.02	0.12	-0.55	1.35E-04	6.58E-03
turquoise	<i>GCC2</i>	0.57	6.00E-05	2.09E-03	-0.30	0.03	0.36
turquoise	<i>GMFB</i>	0.41	1.51E-04	4.09E-03	-0.41	1.90E-04	8.66E-03
turquoise	<i>GOLGB1</i>	0.39	0.03	0.15	-0.39	4.72E-03	0.10
turquoise	<i>GULP1</i>	0.41	1.15E-05	5.86E-04	-0.42	8.56E-05	4.50E-03
turquoise	<i>HDAC9</i>	0.28	2.05E-03	0.03	-0.23	0.02	0.29
turquoise	<i>HELLS</i>	0.51	1.43E-06	1.25E-04	-0.27	0.03	0.37
turquoise	<i>HIF1A</i>	0.39	1.14E-05	5.85E-04	-0.43	3.40E-05	2.16E-03
turquoise	<i>HSPA13</i>	0.25	0.02	0.11	-0.32	3.55E-03	0.08
turquoise	<i>HSPA4L</i>	0.37	1.56E-03	0.02	-0.36	4.28E-03	0.10
turquoise	<i>HSPH1</i>	0.38	2.84E-04	6.52E-03	-0.37	5.86E-04	0.02
turquoise	<i>HTATSF1</i>	0.27	7.34E-03	0.07	-0.21	0.04	0.46
turquoise	<i>ID2</i>	0.33	2.02E-03	0.03	-0.39	5.07E-04	0.02
turquoise	<i>IPO7</i>	0.25	0.01	0.11	-0.30	7.20E-03	0.15
turquoise	<i>IQCB1</i>	0.25	0.05	0.21	-0.28	0.03	0.37
turquoise	<i>JADE1</i>	0.29	5.19E-03	0.05	-0.31	8.22E-03	0.16
turquoise	<i>KIF11</i>	0.54	6.23E-08	1.08E-05	-0.60	2.21E-07	3.83E-05
turquoise	<i>KIF3A</i>	0.25	0.02	0.14	-0.36	2.40E-03	0.06
turquoise	<i>KITLG</i>	0.39	0.01	0.08	-0.85	7.44E-08	1.94E-05
turquoise	<i>KLHL28</i>	0.62	1.89E-05	8.47E-04	-0.40	7.26E-03	0.15
turquoise	<i>KNTC1</i>	0.53	3.26E-06	2.33E-04	-0.49	2.19E-05	1.49E-03
turquoise	<i>KPNA3</i>	0.28	3.72E-03	0.04	-0.22	0.04	0.45
turquoise	<i>KPNA5</i>	0.55	6.24E-05	2.16E-03	-0.46	1.05E-03	0.03
turquoise	<i>KRR1</i>	0.36	3.84E-03	0.04	-0.58	1.01E-05	8.08E-04
turquoise	<i>LIG4</i>	0.56	2.71E-05	1.15E-03	-0.70	1.35E-07	2.78E-05
turquoise	<i>LIN7C</i>	0.30	2.90E-03	0.04	-0.33	1.78E-03	0.05
turquoise	<i>LRPPRC</i>	0.27	5.24E-03	0.05	-0.33	2.26E-03	0.06
turquoise	<i>LRRC40</i>	0.52	7.05E-06	4.03E-04	-0.41	5.24E-04	0.02
turquoise	<i>LTN1</i>	0.48	1.64E-04	4.33E-03	-0.72	1.54E-09	1.01E-06
turquoise	<i>LYST</i>	0.54	5.94E-07	6.37E-05	-0.57	1.16E-05	8.89E-04
turquoise	<i>MANIA2</i>	0.31	1.95E-03	0.03	-0.29	0.01	0.18
turquoise	<i>MAPK6</i>	0.30	2.11E-03	0.03	-0.28	0.01	0.24
turquoise	<i>MARCH1</i>	0.60	9.08E-05	2.79E-03	-0.51	6.64E-04	0.02
turquoise	<i>MCM4</i>	0.32	7.54E-04	0.01	-0.21	0.04	0.42
turquoise	<i>MFAP1</i>	0.29	0.01	0.08	-0.28	0.01	0.22
turquoise	<i>MMP16</i>	0.65	9.37E-07	9.01E-05	-0.52	9.59E-04	0.03
turquoise	<i>MPHOSPH10</i>	0.33	6.67E-03	0.06	-0.43	9.53E-04	0.03
turquoise	<i>MPHOSPH8</i>	0.45	1.19E-04	3.41E-03	-0.45	1.33E-04	6.53E-03
turquoise	<i>MSH2</i>	0.44	2.88E-05	1.20E-03	-0.30	3.98E-03	0.09

turquoise	<i>MTIF2</i>	0.39	3.14E-04	7.04E-03	-0.25	0.05	0.48
turquoise	<i>MYCBP2</i>	0.49	3.04E-07	3.69E-05	-0.28	0.04	0.46
turquoise	<i>MYEF2</i>	0.46	1.86E-05	8.44E-04	-0.36	4.11E-03	0.09
turquoise	<i>MYO9A</i>	0.39	3.25E-04	7.21E-03	-0.43	6.73E-04	0.02
turquoise	<i>NAE1</i>	0.22	0.02	0.13	-0.24	0.01	0.24
turquoise	<i>NCKAP1</i>	0.29	9.88E-04	0.02	-0.22	0.04	0.41
turquoise	<i>NPAT</i>	0.55	1.52E-05	7.23E-04	-0.79	1.45E-08	5.42E-06
turquoise	<i>NRID2</i>	0.25	0.02	0.11	-0.28	0.01	0.18
turquoise	<i>NRCAM</i>	0.27	2.68E-03	0.03	-0.30	7.95E-03	0.16
turquoise	<i>NRIP1</i>	0.49	1.38E-04	3.83E-03	-0.45	1.89E-03	0.05
turquoise	<i>OPA1</i>	0.44	1.02E-05	5.40E-04	-0.61	8.45E-08	2.08E-05
turquoise	<i>ORC3</i>	0.33	0.01	0.09	-0.33	5.45E-03	0.12
turquoise	<i>OSBPL8</i>	0.44	3.18E-05	1.29E-03	-0.64	2.09E-08	7.20E-06
turquoise	<i>OXR1</i>	0.27	0.02	0.12	-0.42	4.62E-04	0.02
turquoise	<i>PAK3</i>	0.34	0.02	0.14	-0.34	0.02	0.29
turquoise	<i>PANK3</i>	0.42	1.80E-05	8.26E-04	-0.46	7.10E-05	3.85E-03
turquoise	<i>PDS5B</i>	0.53	3.89E-06	2.61E-04	-0.47	1.07E-04	5.42E-03
turquoise	<i>PGAP1</i>	0.56	8.37E-08	1.38E-05	-0.28	0.02	0.28
turquoise	<i>PHACTR2</i>	0.28	8.48E-03	0.07	-0.34	0.01	0.21
turquoise	<i>PHF14</i>	0.35	1.50E-03	0.02	-0.39	4.40E-04	0.02
turquoise	<i>PHF20L1</i>	0.39	3.28E-04	7.26E-03	-0.41	1.10E-03	0.03
turquoise	<i>PHTF2</i>	0.41	1.45E-04	3.96E-03	-0.33	6.40E-03	0.13
turquoise	<i>PIGK</i>	0.26	0.02	0.12	-0.23	0.03	0.40
turquoise	<i>PIK3C3</i>	0.34	0.01	0.08	-0.28	0.05	0.47
turquoise	<i>PIK3CA</i>	0.43	1.76E-05	8.10E-04	-0.54	8.89E-07	1.20E-04
turquoise	<i>PJA2</i>	0.36	3.69E-04	7.94E-03	-0.24	0.01	0.24
turquoise	<i>PLCB1</i>	0.31	0.04	0.18	-0.46	4.49E-03	0.10
turquoise	<i>PLEKHA1</i>	0.22	0.05	0.21	-0.22	0.05	0.49
turquoise	<i>PLK4</i>	0.35	3.54E-03	0.04	-0.42	1.34E-03	0.04
turquoise	<i>PMS1</i>	0.35	4.74E-03	0.05	-0.47	1.48E-04	7.03E-03
turquoise	<i>PPAT</i>	0.32	6.54E-04	0.01	-0.21	0.05	0.48
turquoise	<i>PPFIA2</i>	0.35	0.03	0.18	-0.56	4.97E-04	0.02
turquoise	<i>PPM1A</i>	0.27	0.02	0.12	-0.25	0.04	0.41
turquoise	<i>PPP1R12A</i>	0.43	3.48E-05	1.38E-03	-0.50	1.91E-05	1.35E-03
turquoise	<i>PPP2R5E</i>	0.25	6.45E-03	0.06	-0.23	0.05	0.48
turquoise	<i>PSIP1</i>	0.33	6.57E-04	0.01	-0.36	2.69E-04	0.01
turquoise	<i>PTPN4</i>	0.47	2.30E-05	1.00E-03	-0.41	1.01E-03	0.03
turquoise	<i>PUS7L</i>	0.46	8.05E-04	0.01	-0.68	1.07E-05	8.39E-04
turquoise	<i>RAB11FIP2</i>	0.35	4.98E-03	0.05	-0.45	8.49E-04	0.03
turquoise	<i>RAB27B</i>	0.28	0.03	0.16	-0.59	1.03E-04	5.25E-03
turquoise	<i>RABEP1</i>	0.49	1.19E-05	6.03E-04	-0.38	1.17E-03	0.04
turquoise	<i>RAD50</i>	0.63	7.61E-07	7.66E-05	-0.49	1.62E-04	7.58E-03
turquoise	<i>RAD51API</i>	0.39	2.24E-03	0.03	-0.31	0.02	0.27
turquoise	<i>RANBP2</i>	0.86	8.68E-13	2.79E-09	-0.89	1.09E-11	5.00E-08

turquoise	<i>RB1CC1</i>	0.54	1.02E-05	5.40E-04	-0.67	1.09E-07	2.43E-05
turquoise	<i>RBM26</i>	0.33	1.82E-03	0.03	-0.36	4.20E-03	0.10
turquoise	<i>RFC3</i>	0.32	6.07E-03	0.06	-0.26	0.02	0.33
turquoise	<i>RFX3</i>	0.59	3.02E-07	3.69E-05	-0.41	5.52E-04	0.02
turquoise	<i>RIOK2</i>	0.33	4.85E-03	0.05	-0.31	0.02	0.28
turquoise	<i>RLF</i>	0.48	1.18E-05	5.96E-04	-0.58	1.20E-06	1.52E-04
turquoise	<i>RM11</i>	0.52	1.04E-04	3.06E-03	-0.41	2.39E-03	0.06
turquoise	<i>RNF6</i>	0.29	3.63E-03	0.04	-0.42	4.39E-04	0.02
turquoise	<i>ROCK2</i>	0.57	2.37E-07	3.10E-05	-0.67	6.11E-07	8.68E-05
turquoise	<i>RPAP2</i>	0.44	6.19E-04	0.01	-0.49	6.47E-04	0.02
turquoise	<i>RPAP3</i>	0.43	1.88E-04	4.72E-03	-0.35	5.12E-03	0.11
turquoise	<i>RRP15</i>	0.28	5.93E-03	0.06	-0.41	5.65E-04	0.02
turquoise	<i>RSF1</i>	0.71	1.44E-09	5.97E-07	-0.70	5.84E-09	2.60E-06
turquoise	<i>RSRC2</i>	0.41	4.37E-04	0.01	-0.34	3.61E-03	0.09
turquoise	<i>SACS</i>	0.79	1.52E-08	3.42E-06	-0.68	1.18E-06	1.51E-04
turquoise	<i>SCAMP1</i>	0.28	0.01	0.09	-0.29	3.93E-03	0.09
turquoise	<i>SCAPER</i>	0.38	4.09E-03	0.05	-0.34	0.01	0.21
turquoise	<i>SCRN3</i>	0.30	7.55E-03	0.07	-0.27	0.03	0.34
turquoise	<i>SCYL2</i>	0.35	1.30E-03	0.02	-0.40	4.70E-04	0.02
turquoise	<i>SDADI</i>	0.36	1.22E-03	0.02	-0.33	5.14E-03	0.11
turquoise	<i>SEC62</i>	0.42	1.80E-04	4.59E-03	-0.52	2.31E-06	2.55E-04
turquoise	<i>SEC63</i>	0.21	0.01	0.10	-0.31	1.73E-03	0.05
turquoise	<i>SEMA3A</i>	0.49	3.62E-07	4.17E-05	-0.53	1.66E-06	1.97E-04
turquoise	<i>SEMA3C</i>	0.48	2.95E-06	2.17E-04	-0.32	1.08E-03	0.03
turquoise	<i>SHCBP1</i>	0.27	3.49E-03	0.04	-0.24	0.01	0.24
turquoise	<i>SKIV2L2</i>	0.48	7.31E-06	4.15E-04	-0.41	2.88E-04	0.01
turquoise	<i>SLC25A36</i>	0.38	5.29E-04	0.01	-0.41	1.33E-04	6.53E-03
turquoise	<i>SLC25A46</i>	0.32	3.30E-03	0.04	-0.26	0.01	0.22
turquoise	<i>SLC30A9</i>	0.26	0.01	0.10	-0.25	0.02	0.30
turquoise	<i>SLC4A7</i>	0.38	8.61E-05	2.68E-03	-0.34	1.82E-03	0.05
turquoise	<i>SMC2</i>	0.85	1.10E-12	2.83E-09	-0.89	7.47E-11	1.71E-07
turquoise	<i>SNX10</i>	0.26	0.01	0.10	-0.31	4.79E-03	0.11
turquoise	<i>SNX2</i>	0.22	0.02	0.12	-0.23	0.02	0.30
turquoise	<i>SPDL1</i>	0.44	5.49E-05	1.96E-03	-0.52	4.08E-06	3.97E-04
turquoise	<i>SSB</i>	0.31	0.01	0.08	-0.45	3.73E-05	2.29E-03
turquoise	<i>SSX2IP</i>	0.45	1.44E-05	6.93E-04	-0.36	6.22E-04	0.02
turquoise	<i>STIL</i>	0.32	2.26E-03	0.03	-0.33	7.05E-03	0.14
turquoise	<i>SUCLA2</i>	0.24	0.02	0.13	-0.27	0.02	0.29
turquoise	<i>SYNJI</i>	0.28	0.02	0.11	-0.24	0.04	0.45
turquoise	<i>TAF1B</i>	0.25	0.02	0.12	-0.33	6.11E-03	0.13
turquoise	<i>TAF9B</i>	0.37	7.81E-04	0.01	-0.28	0.02	0.24
turquoise	<i>TAX1BP1</i>	0.41	9.89E-05	2.92E-03	-0.53	3.86E-06	3.83E-04
turquoise	<i>TBK1</i>	0.37	8.55E-04	0.01	-0.27	0.04	0.42
turquoise	<i>TBL1XR1</i>	0.28	2.33E-03	0.03	-0.20	0.04	0.46

turquoise	<i>TCERG1</i>	0.30	8.56E-04	0.01	-0.22	0.03	0.37
turquoise	<i>TCF4</i>	0.52	4.32E-07	4.80E-05	-0.57	2.59E-06	2.79E-04
turquoise	<i>TFAM</i>	0.29	5.69E-03	0.06	-0.26	0.02	0.30
turquoise	<i>TLK1</i>	0.31	1.73E-03	0.02	-0.24	0.03	0.38
turquoise	<i>TMEM106B</i>	0.32	8.32E-04	0.01	-0.39	3.69E-05	2.27E-03
turquoise	<i>TMF1</i>	0.53	4.02E-06	2.65E-04	-0.61	1.17E-06	1.51E-04
turquoise	<i>TOP1</i>	0.26	0.01	0.09	-0.30	8.18E-03	0.16
turquoise	<i>TOPBP1</i>	0.46	8.08E-06	4.51E-04	-0.46	5.34E-05	3.02E-03
turquoise	<i>TPP2</i>	0.30	4.12E-03	0.05	-0.34	3.60E-03	0.09
turquoise	<i>TPX2</i>	0.22	0.02	0.15	-0.20	0.04	0.45
turquoise	<i>TRHDE</i>	0.46	5.33E-04	0.01	-0.34	0.03	0.37
turquoise	<i>TRIM23</i>	0.55	3.23E-06	2.33E-04	-0.37	1.85E-03	0.05
turquoise	<i>TRIM33</i>	0.35	2.10E-04	5.16E-03	-0.36	8.69E-04	0.03
turquoise	<i>TTC37</i>	0.53	1.21E-06	1.11E-04	-0.66	5.90E-08	1.63E-05
turquoise	<i>TWISTNB</i>	0.30	7.77E-03	0.07	-0.39	4.21E-04	0.02
turquoise	<i>UBE3A</i>	0.25	0.02	0.12	-0.22	0.04	0.45
turquoise	<i>UCHL5</i>	0.22	0.03	0.17	-0.33	1.89E-03	0.05
turquoise	<i>UHRF1BP1L</i>	0.46	2.17E-04	5.30E-03	-0.45	3.93E-04	0.02
turquoise	<i>UPF2</i>	0.50	3.45E-05	1.37E-03	-0.62	1.05E-06	1.39E-04
turquoise	<i>UPF3B</i>	0.35	2.70E-03	0.03	-0.56	1.87E-06	2.16E-04
turquoise	<i>USO1</i>	0.37	3.18E-04	7.09E-03	-0.40	1.48E-04	7.03E-03
turquoise	<i>USP25</i>	0.27	0.01	0.09	-0.35	2.73E-03	0.07
turquoise	<i>VEZT</i>	0.32	4.57E-03	0.05	-0.24	0.04	0.42
turquoise	<i>VPS13A</i>	0.72	6.89E-07	7.07E-05	-0.68	8.10E-07	1.11E-04
turquoise	<i>VPS26A</i>	0.22	0.03	0.15	-0.22	0.02	0.31
turquoise	<i>VPS50</i>	0.31	0.02	0.11	-0.59	8.87E-06	7.24E-04
turquoise	<i>WBP4</i>	0.54	6.99E-05	2.34E-03	-0.43	2.14E-03	0.06
turquoise	<i>WDHD1</i>	0.69	1.25E-08	3.05E-06	-0.46	4.70E-04	0.02
turquoise	<i>YTHDC2</i>	0.41	1.29E-04	3.65E-03	-0.34	1.77E-03	0.05
turquoise	<i>ZBED5</i>	0.35	1.83E-03	0.03	-0.35	2.66E-03	0.07
turquoise	<i>ZBTB11</i>	0.31	8.25E-03	0.07	-0.45	2.94E-04	0.01
turquoise	<i>ZC3H15</i>	0.36	6.48E-04	0.01	-0.26	0.02	0.31
turquoise	<i>ZDHHC17</i>	0.38	1.83E-03	0.03	-0.33	6.63E-03	0.14
turquoise	<i>ZFP30</i>	0.37	3.31E-03	0.04	-0.29	0.03	0.39
turquoise	<i>ZMYM2</i>	0.40	8.85E-04	0.01	-0.36	1.78E-03	0.05
turquoise	<i>ZMYM4</i>	0.35	1.59E-04	4.25E-03	-0.31	5.94E-03	0.13
turquoise	<i>ZNF12</i>	0.50	1.28E-05	6.37E-04	-0.50	4.55E-05	2.66E-03
turquoise	<i>ZNF136</i>	0.52	3.94E-04	8.30E-03	-0.32	0.03	0.35
turquoise	<i>ZNF148</i>	0.46	1.28E-04	3.63E-03	-0.55	7.30E-06	6.21E-04
turquoise	<i>ZNF189</i>	0.37	6.75E-03	0.06	-0.31	0.02	0.33
turquoise	<i>ZNF195</i>	0.51	5.22E-04	0.01	-0.29	0.05	0.49
turquoise	<i>ZNF510</i>	0.28	0.04	0.19	-0.33	0.02	0.31
turquoise	<i>ZNF675</i>	0.42	1.51E-03	0.02	-0.41	5.56E-03	0.12
turquoise	<i>ZNF770</i>	0.32	2.97E-03	0.04	-0.34	7.46E-03	0.15



turquoise	<i>ZNF804A</i>	0.68	3.19E-07	3.81E-05	-0.60	3.01E-05	1.96E-03
turquoise	<i>ZNF91</i>	0.54	1.79E-04	4.59E-03	-0.35	0.01	0.19
turquoise	<i>ZW10</i>	0.30	7.55E-03	0.07	-0.28	0.03	0.34
turquoise	<i>ZWILCH</i>	0.37	4.99E-04	0.01	-0.32	3.11E-03	0.08
turquoise	<i>ZWINT</i>	0.30	3.35E-03	0.04	-0.24	0.02	0.26
yellow	<i>AASS</i>	0.28	8.61E-03	0.07	-0.42	4.20E-04	0.02
yellow	<i>ACAP2</i>	0.40	1.51E-05	7.21E-04	-0.40	3.48E-04	0.01
yellow	<i>ADAM10</i>	0.32	3.69E-04	7.94E-03	-0.22	0.02	0.31
yellow	<i>ANKRD10</i>	0.36	3.49E-04	7.58E-03	-0.25	0.02	0.29
yellow	<i>ARHGAP5</i>	0.52	5.71E-06	3.50E-04	-0.75	1.29E-09	9.38E-07
yellow	<i>ATP6V0A2</i>	0.24	0.02	0.13	-0.31	0.01	0.17
yellow	<i>BAZIA</i>	0.44	2.36E-04	5.68E-03	-0.62	4.51E-07	6.83E-05
yellow	<i>BAZ2B</i>	0.64	2.07E-08	4.37E-06	-0.62	2.69E-06	2.87E-04
yellow	<i>BBX</i>	0.45	3.17E-05	1.29E-03	-0.54	1.21E-06	1.52E-04
yellow	<i>BCHE</i>	0.39	2.85E-04	6.52E-03	-0.27	8.94E-03	0.17
yellow	<i>BNIP2</i>	0.24	0.02	0.13	-0.24	0.02	0.33
yellow	<i>C1orf27</i>	0.34	2.73E-03	0.03	-0.53	3.61E-05	2.24E-03
yellow	<i>CALCRL</i>	0.47	1.11E-03	0.02	-0.44	1.68E-03	0.05
yellow	<i>CCNLI</i>	0.33	1.50E-03	0.02	-0.32	3.97E-03	0.09
yellow	<i>CDC42BPA</i>	0.33	4.18E-04	8.74E-03	-0.29	0.02	0.26
yellow	<i>CENPJ</i>	0.57	5.94E-06	3.53E-04	-0.57	3.97E-05	2.40E-03
yellow	<i>CEP350</i>	0.76	3.98E-10	2.05E-07	-0.74	1.52E-07	2.95E-05
yellow	<i>CNTLN</i>	0.25	0.02	0.14	-0.28	0.02	0.25
yellow	<i>CNTRL</i>	0.53	1.38E-04	3.83E-03	-0.50	6.20E-04	0.02
yellow	<i>CSPP1</i>	0.47	3.50E-04	7.58E-03	-0.29	0.05	0.48
yellow	<i>DAAMI</i>	0.25	0.03	0.18	-0.31	0.03	0.36
yellow	<i>DCUNID1</i>	0.41	1.03E-04	3.02E-03	-0.43	1.64E-04	7.63E-03
yellow	<i>DDX21</i>	0.22	0.02	0.13	-0.27	0.02	0.27
yellow	<i>DONSON</i>	0.27	0.02	0.14	-0.30	0.01	0.21
yellow	<i>EIF5B</i>	0.59	2.74E-07	3.42E-05	-0.65	7.92E-08	2.02E-05
yellow	<i>ELF1</i>	0.23	0.03	0.16	-0.23	0.05	0.48
yellow	<i>ERBIN</i>	0.42	4.20E-06	2.72E-04	-0.56	2.26E-07	3.84E-05
yellow	<i>ETAA1</i>	0.53	5.08E-05	1.85E-03	-0.37	6.53E-03	0.14
yellow	<i>FAM135A</i>	0.48	2.14E-04	5.24E-03	-0.37	4.95E-03	0.11
yellow	<i>FER</i>	0.72	1.21E-08	3.00E-06	-0.89	8.11E-10	7.47E-07
yellow	<i>FNBP1L</i>	0.35	8.69E-04	0.01	-0.23	0.04	0.46
yellow	<i>FRS2</i>	0.24	0.02	0.14	-0.25	0.04	0.41
yellow	<i>GABPA</i>	0.49	1.03E-05	5.44E-04	-0.43	4.73E-04	0.02
yellow	<i>HNRNPH1</i>	0.35	7.93E-05	2.55E-03	-0.21	0.03	0.40
yellow	<i>HNRNPM</i>	0.19	0.04	0.20	-0.19	0.04	0.46
yellow	<i>IFI44</i>	0.26	0.02	0.13	-0.33	8.46E-03	0.16
yellow	<i>IFT74</i>	0.36	0.01	0.08	-0.37	0.01	0.21
yellow	<i>ITSN2</i>	0.35	3.36E-04	7.41E-03	-0.35	3.68E-03	0.09
yellow	<i>KIAA1551</i>	0.58	2.56E-04	6.01E-03	-0.48	2.57E-03	0.07

yellow	<i>KIF5B</i>	0.53	6.98E-08	1.20E-05	-0.59	3.75E-07	5.88E-05
yellow	<i>LARP4</i>	0.45	5.83E-06	3.53E-04	-0.46	8.76E-05	4.59E-03
yellow	<i>LIFR</i>	0.47	1.40E-04	3.87E-03	-0.52	1.44E-04	6.92E-03
yellow	<i>MANEA</i>	0.44	9.70E-05	2.90E-03	-0.57	1.16E-05	8.89E-04
yellow	<i>MAP3K2</i>	0.39	3.62E-05	1.42E-03	-0.35	2.60E-03	0.07
yellow	<i>MARCH7</i>	0.36	1.77E-04	4.56E-03	-0.33	3.48E-03	0.08
yellow	<i>MBNL1</i>	0.37	2.94E-04	6.65E-03	-0.47	3.61E-05	2.24E-03
yellow	<i>MBNL3</i>	0.64	3.12E-08	6.19E-06	-0.54	4.70E-05	2.74E-03
yellow	<i>MDM2</i>	0.38	8.38E-05	2.64E-03	-0.25	0.03	0.37
yellow	<i>MED13</i>	0.48	2.63E-06	1.99E-04	-0.33	6.76E-03	0.14
yellow	<i>MRE11A</i>	0.50	3.55E-05	1.40E-03	-0.38	3.77E-03	0.09
yellow	<i>NEB</i>	0.63	1.70E-05	7.90E-04	-0.36	0.01	0.18
yellow	<i>NEK7</i>	0.21	0.05	0.21	-0.34	3.42E-03	0.08
yellow	<i>NHLRC2</i>	0.47	3.35E-06	2.37E-04	-0.37	5.47E-03	0.12
yellow	<i>NIPBL</i>	0.59	6.64E-07	6.90E-05	-0.57	1.05E-05	8.31E-04
yellow	<i>NKTR</i>	0.56	2.57E-06	1.96E-04	-0.58	1.68E-07	3.16E-05
yellow	<i>NUP54</i>	0.34	2.05E-03	0.03	-0.27	0.02	0.26
yellow	<i>OFD1</i>	0.49	3.17E-04	7.07E-03	-0.48	1.66E-03	0.05
yellow	<i>PAPOLA</i>	0.32	4.99E-04	0.01	-0.23	0.03	0.35
yellow	<i>PCF11</i>	0.49	2.76E-06	2.07E-04	-0.42	2.40E-04	0.01
yellow	<i>PHF3</i>	0.72	1.08E-10	8.68E-08	-0.78	8.59E-10	7.47E-07
yellow	<i>PKN2</i>	0.35	4.20E-04	8.77E-03	-0.46	1.69E-05	1.21E-03
yellow	<i>PNISR</i>	0.55	2.53E-07	3.20E-05	-0.58	3.62E-09	2.00E-06
yellow	<i>POLA1</i>	0.41	3.37E-04	7.41E-03	-0.34	3.41E-03	0.08
yellow	<i>PPIG</i>	0.45	9.80E-05	2.91E-03	-0.62	1.22E-07	2.55E-05
yellow	<i>PRPF38B</i>	0.31	3.08E-03	0.04	-0.31	6.30E-03	0.13
yellow	<i>PRR14L</i>	0.37	5.53E-04	0.01	-0.28	0.02	0.28
yellow	<i>PTPN13</i>	0.30	8.11E-03	0.07	-0.26	0.02	0.31
yellow	<i>PYGO1</i>	0.40	6.67E-04	0.01	-0.37	3.31E-03	0.08
yellow	<i>RBBP8</i>	0.48	7.96E-05	2.55E-03	-0.52	5.10E-05	2.92E-03
yellow	<i>RBM12B</i>	0.24	0.03	0.16	-0.25	0.04	0.45
yellow	<i>RBM41</i>	0.36	0.01	0.08	-0.31	0.03	0.37
yellow	<i>RECQL</i>	0.43	5.67E-05	2.01E-03	-0.43	1.82E-04	8.39E-03
yellow	<i>SKIL</i>	0.46	9.58E-06	5.16E-04	-0.39	2.24E-03	0.06
yellow	<i>SMAD5</i>	0.33	1.17E-03	0.02	-0.24	0.03	0.40
yellow	<i>SMC4</i>	0.61	8.49E-09	2.19E-06	-0.63	8.12E-08	2.04E-05
yellow	<i>SMC5</i>	0.63	1.91E-07	2.64E-05	-0.47	3.23E-04	0.01
yellow	<i>SP3</i>	0.34	6.15E-04	0.01	-0.23	0.02	0.33
yellow	<i>SP4</i>	0.27	0.04	0.20	-0.29	0.04	0.42
yellow	<i>SPG20</i>	0.24	0.02	0.14	-0.22	0.05	0.48
yellow	<i>STAG1</i>	0.43	8.60E-05	2.68E-03	-0.35	3.81E-03	0.09
yellow	<i>STAG2</i>	0.69	5.30E-09	1.52E-06	-0.73	3.47E-10	4.02E-07
yellow	<i>STAM2</i>	0.26	7.92E-03	0.07	-0.24	0.04	0.43
yellow	<i>SUZ12</i>	0.44	2.98E-05	1.24E-03	-0.44	7.70E-05	4.08E-03

yellow	<i>TAOK1</i>	0.34	9.16E-04	0.02	-0.28	0.02	0.29
yellow	<i>TMED5</i>	0.27	0.02	0.13	-0.42	1.39E-04	6.70E-03
yellow	<i>TMEM123</i>	0.21	0.02	0.14	-0.25	7.99E-03	0.16
yellow	<i>TNPO1</i>	0.37	4.49E-05	1.70E-03	-0.32	2.63E-03	0.07
yellow	<i>TROVE2</i>	0.45	1.64E-05	7.67E-04	-0.52	1.12E-05	8.74E-04
yellow	<i>UFL1</i>	0.33	5.33E-03	0.05	-0.52	4.82E-06	4.52E-04
yellow	<i>VPS13B</i>	0.46	3.69E-05	1.45E-03	-0.37	1.54E-03	0.04
yellow	<i>XPO1</i>	0.35	6.40E-04	0.01	-0.23	0.02	0.33
yellow	<i>ZBTB1</i>	0.33	2.45E-03	0.03	-0.28	0.02	0.28
yellow	<i>ZBTB33</i>	0.42	1.95E-04	4.86E-03	-0.32	4.18E-03	0.09
yellow	<i>ZCCHC11</i>	0.34	6.73E-04	0.01	-0.33	8.02E-03	0.16
yellow	<i>ZCCHC6</i>	0.32	0.01	0.08	-0.35	6.64E-03	0.14
yellow	<i>ZFX</i>	0.38	6.28E-04	0.01	-0.28	0.02	0.32
yellow	<i>ZMYM1</i>	0.44	1.08E-04	3.13E-03	-0.51	1.25E-04	6.17E-03
yellow	<i>ZNF107</i>	0.65	3.16E-05	1.29E-03	-0.47	2.91E-03	0.07
yellow	<i>ZNF197</i>	0.28	0.01	0.11	-0.32	0.01	0.24
yellow	<i>ZNF471</i>	0.30	0.04	0.20	-0.54	5.42E-04	0.02
yellow	<i>ZNF480</i>	0.36	2.58E-03	0.03	-0.35	7.67E-03	0.15
yellow	<i>ZNF83</i>	0.48	2.86E-05	1.20E-03	-0.39	6.28E-04	0.02

logFC, log2 fold change of gene expression in U251-APP cells with YAP1 knockdown or overexpression compared with scramble cells.

*P*: *P*-value of differential expression.

FDR: *P*-value of differential expression adjusted for multiply comparisons by the BH method.

Supplementary Figures

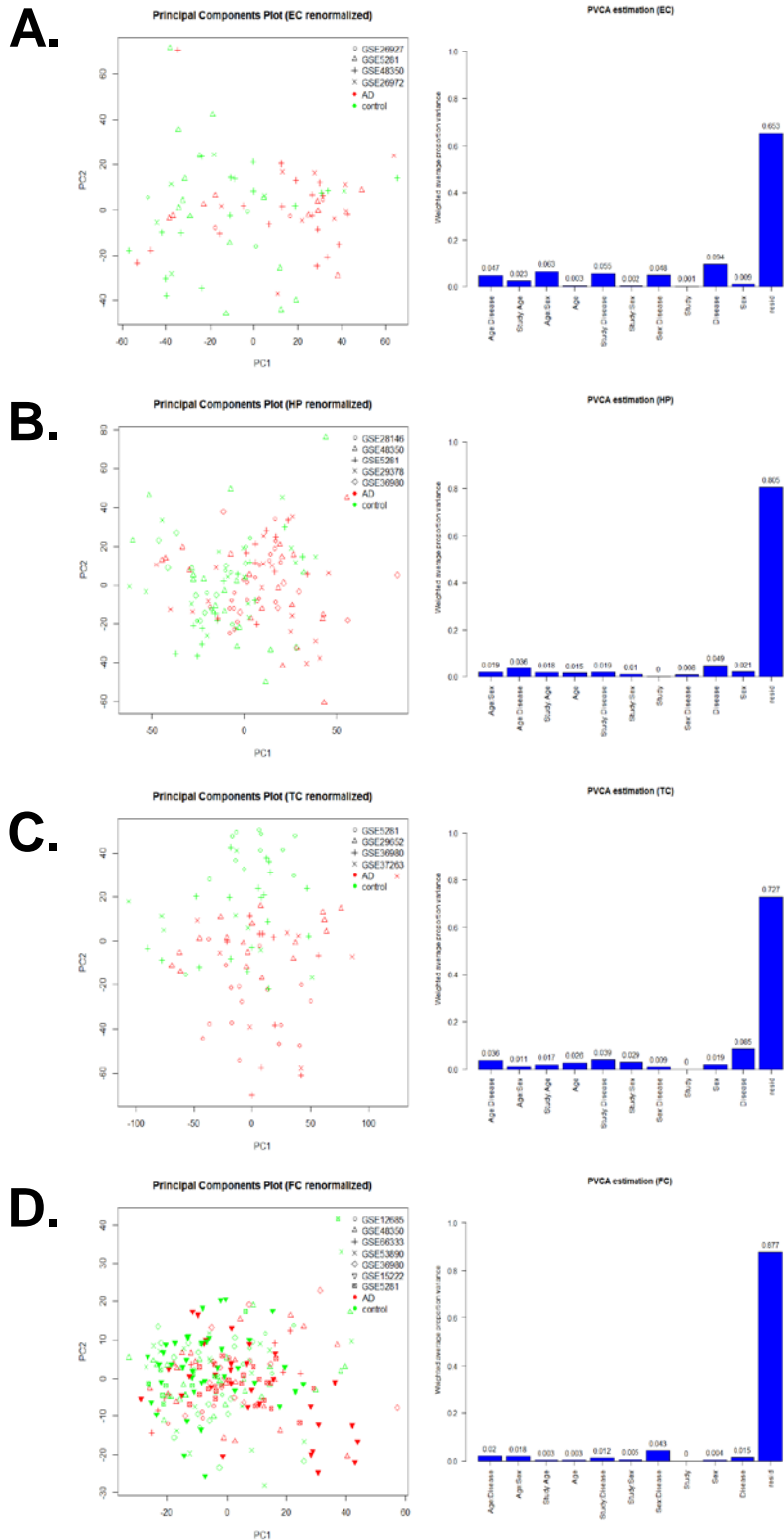


**Fig. S1. Principal component analysis (PCA) and principal variance component analysis (PVCA) of the merged datasets by using ComBat for (A) entorhinal cortex (EC), (B) hippocampus (HP), (C) temporal cortex (TC), and (D) frontal cortex (FC).**

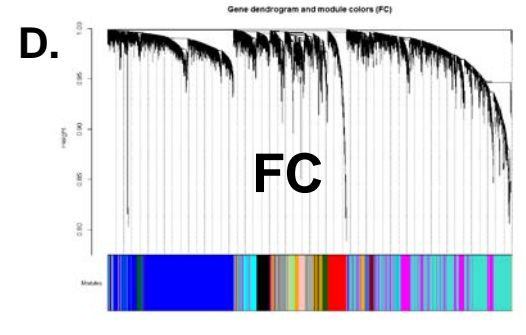
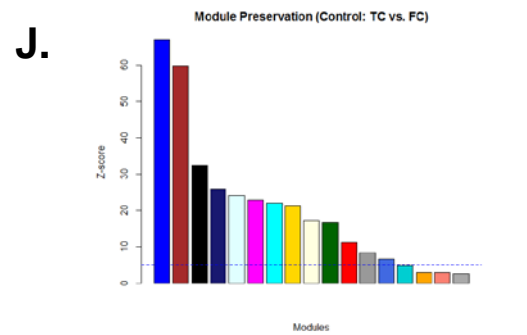
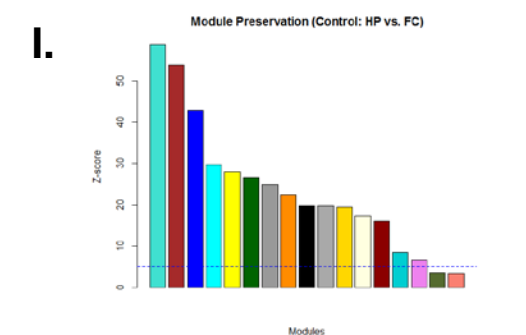
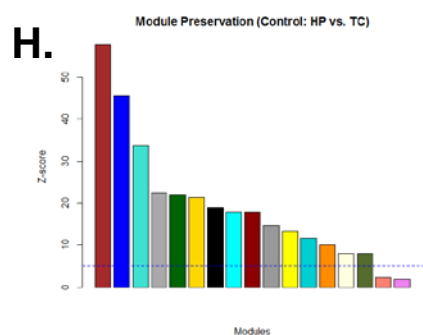
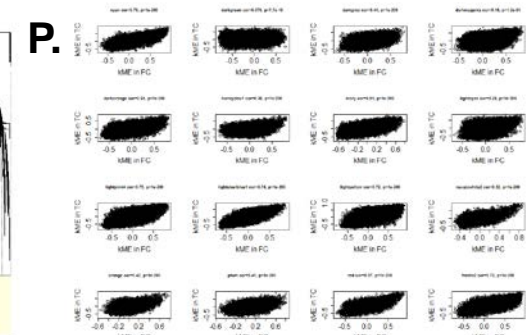
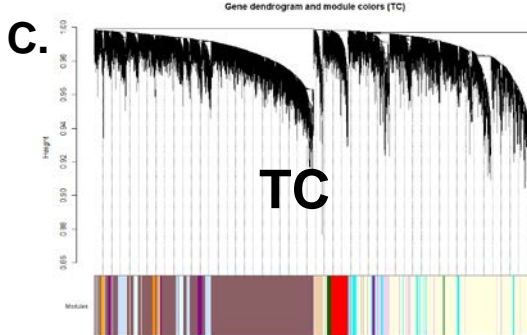
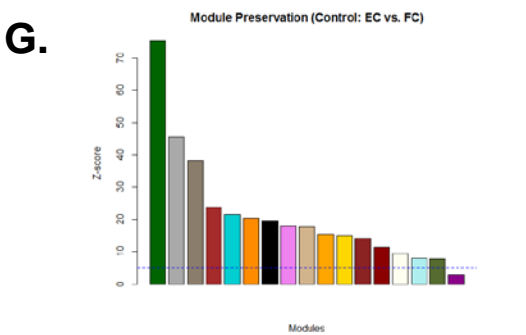
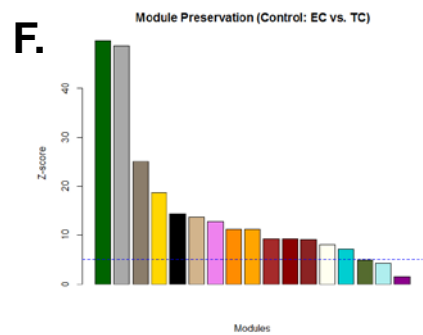
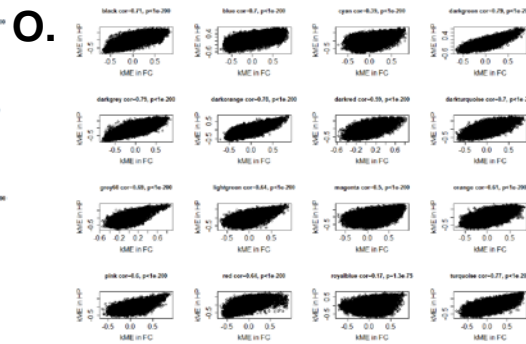
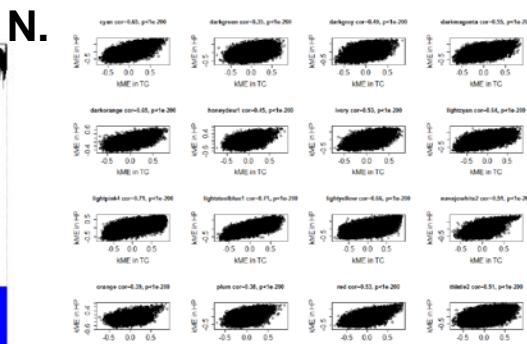
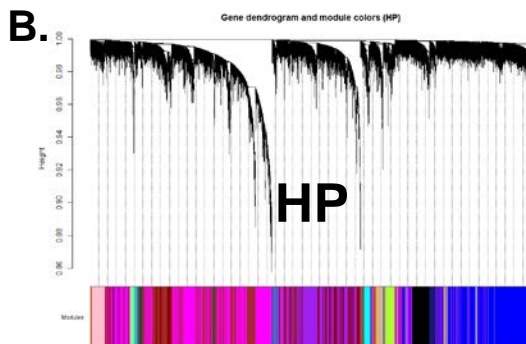
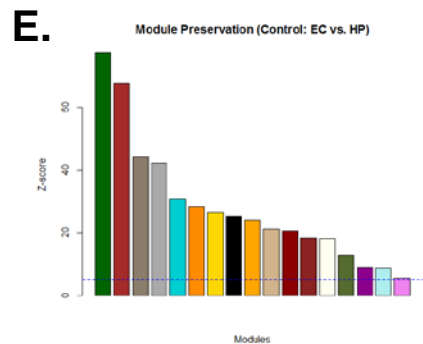
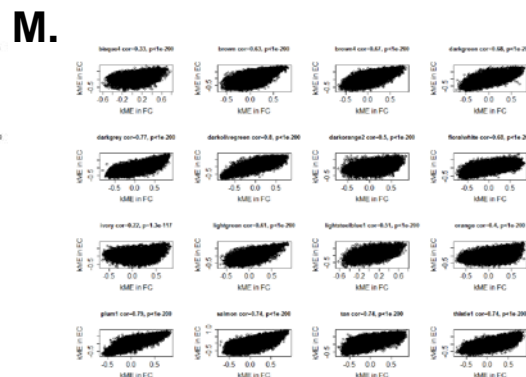
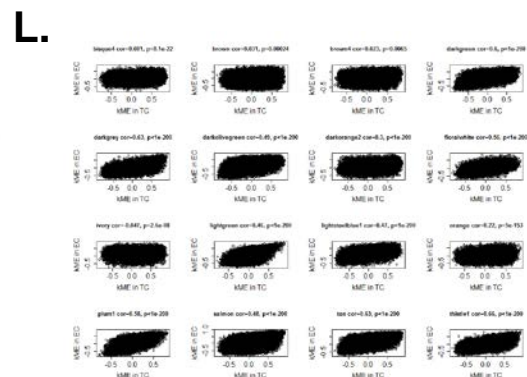
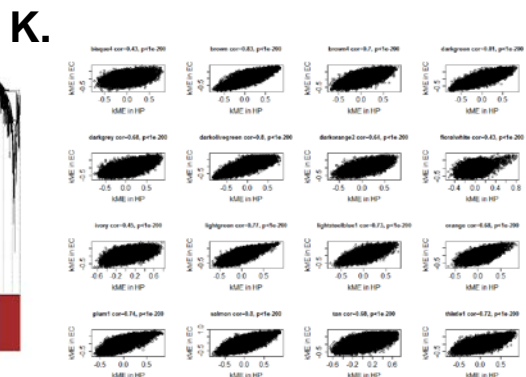
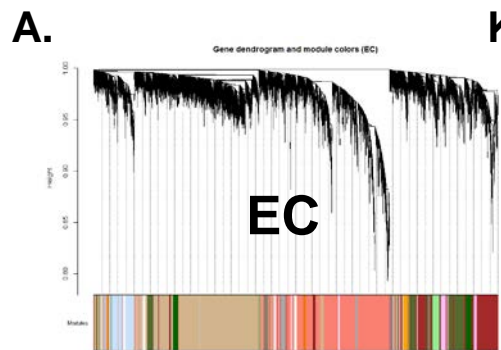


**Fig. S2. Module preservation of control co-expression networks among different brain regions.** WGCNA cluster dendrograms on control samples grouped genes into distinct modules for (A) entorhinal cortex (EC), (B) hippocampus (HP), (C) temporal cortex (TC), and (D) frontal cortex (FC). Pairwise comparisons of module preservation among EC, HP, TC and FC indicated that most of modules were highly preserved in different brain regions. Module conservation was represented by (E-J) Z-score and (K-P) module membership (kME) computed by WGCNA. Dash lines in blue in (E-J) define a Z-score = 5.

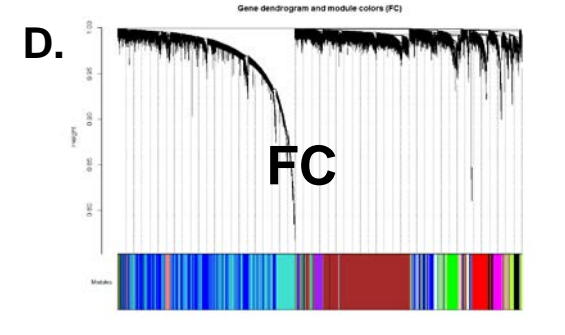
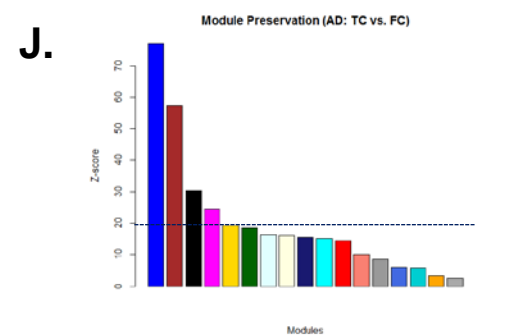
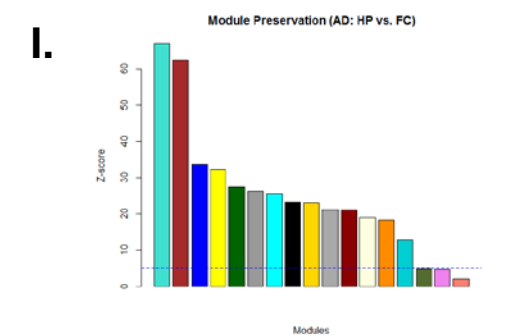
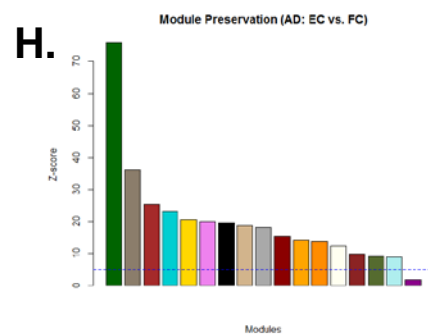
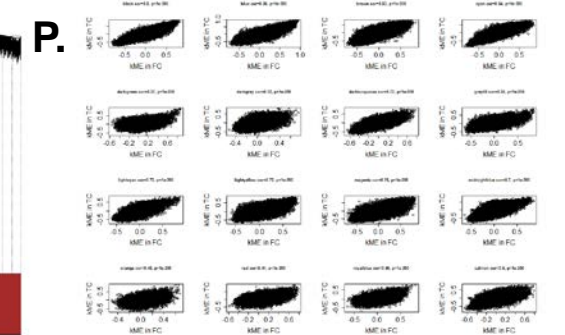
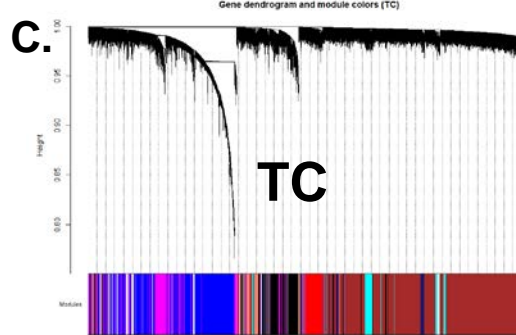
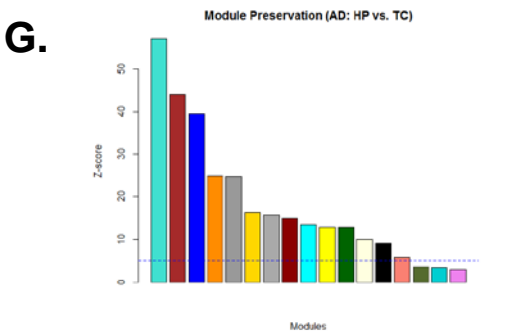
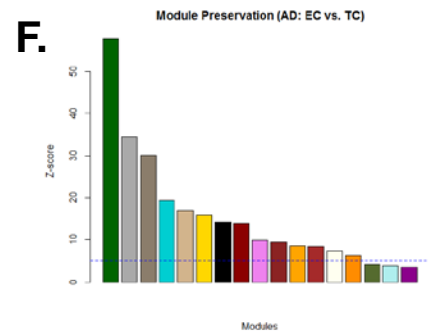
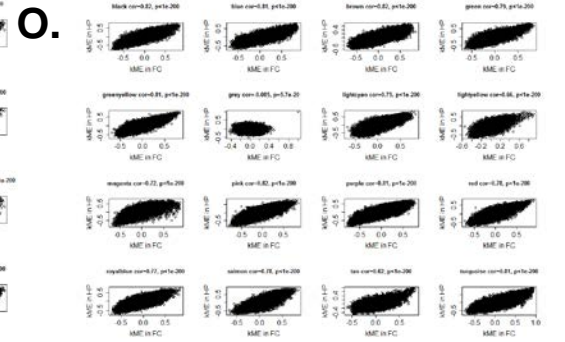
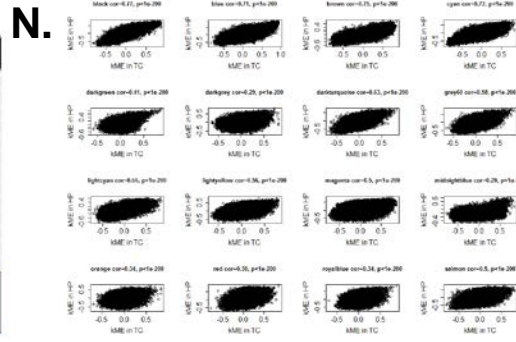
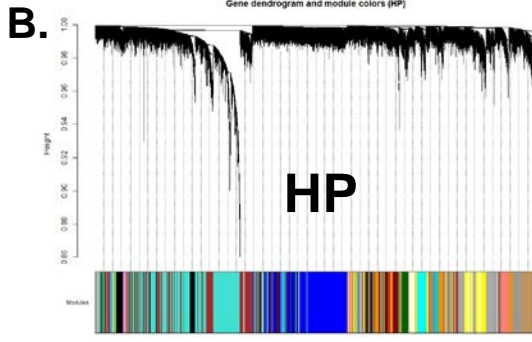
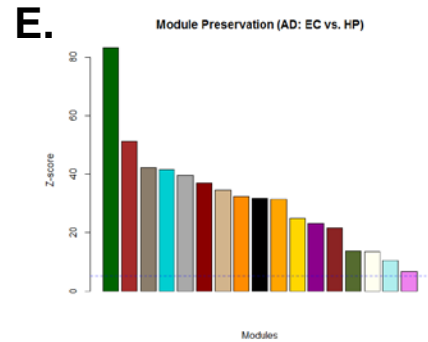
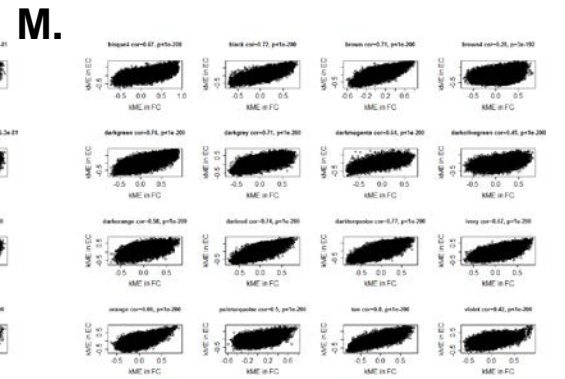
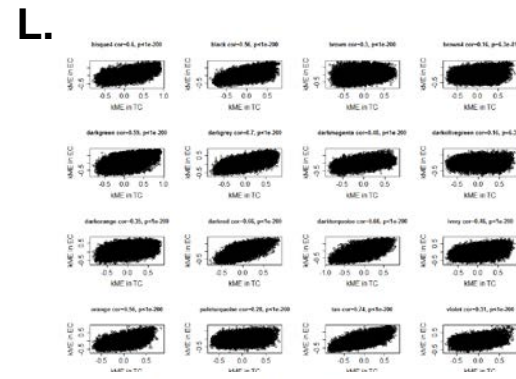
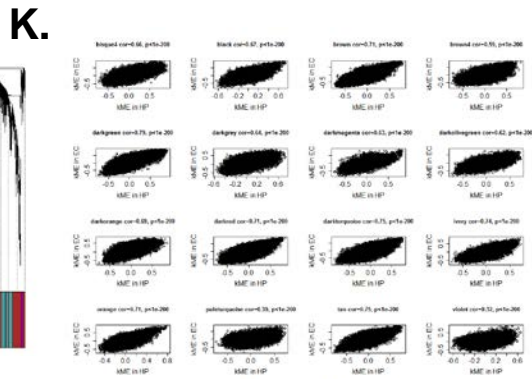
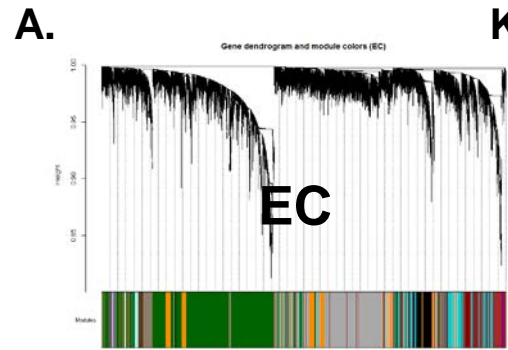


**Fig. S3. Module preservation of AD co-expression networks among different brain regions.** WGCNA cluster dendrogram on AD samples grouped genes into distinct modules for (A) entorhinal cortex (EC), (B) hippocampus (HP), (C) temporal cortex (TC), and (D) frontal cortex (FC). Pairwise comparisons of module preservation among EC, HP, TC and FC indicated that most modules were highly preserved in different brain regions. Module conservation was represented by (E-J) Z-score and (K-P) module membership (kME) computed by WGCNA. Dash lines in blue in (E-J) define a Z-score = 5.



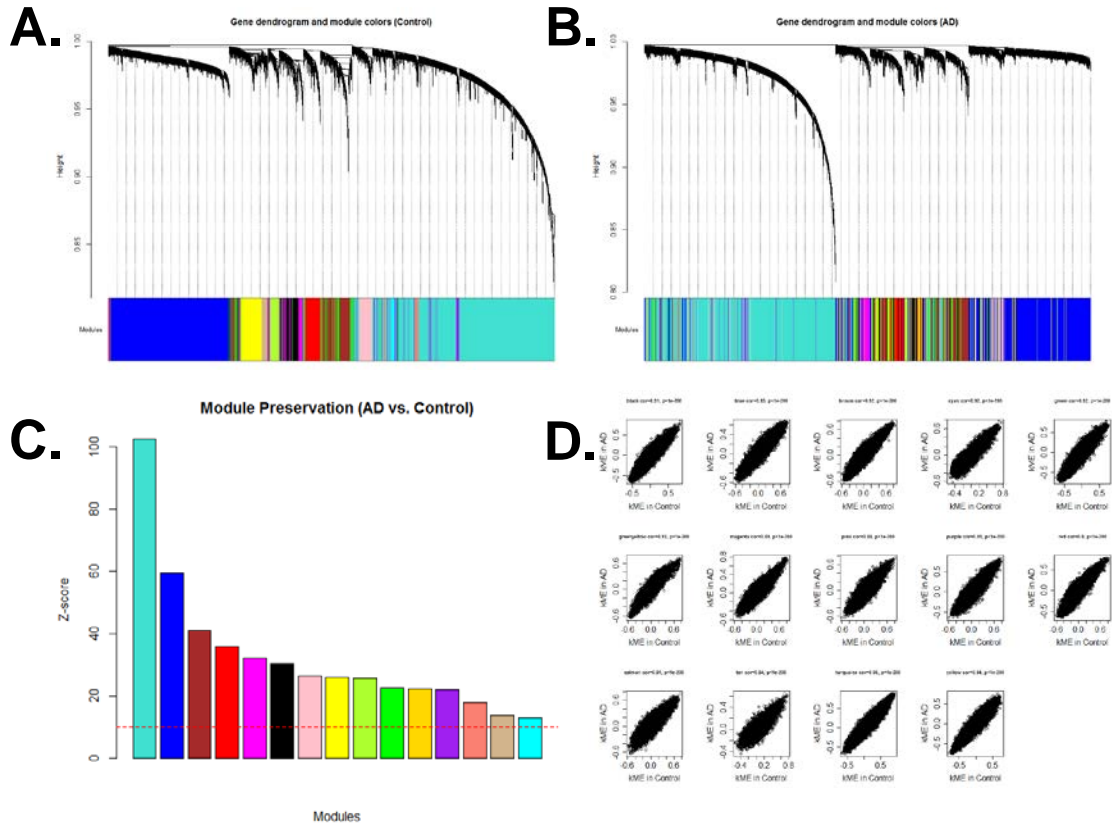


**Fig. S4. Module preservation of AD and control co-expression networks constructed using the merged datasets of four brain regions.** WGCNA cluster dendrogram on merged control / AD samples grouped genes into distinct modules for controls (A) and AD patients (B). Comparisons of module preservation between controls and AD patients indicated that all modules were highly preserved in control and AD co-expression networks. Module conservation was represented by (C) Z-score and (D) module membership (kME) computed by WGCNA. Dash line in red defines a Z-score = 10.

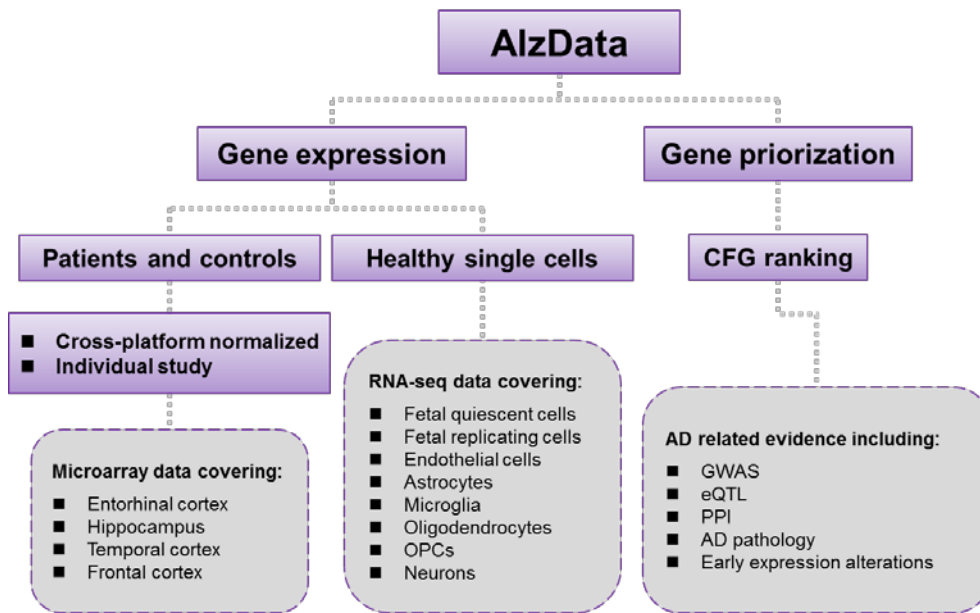


**Fig. S5. Structure of AlzData.org.** The AlzData contains two modules, i.e. gene expression module and gene prioritization module at present. Gene expression and differential expression states in AD patients compared to normal controls in cross-platform normalized dataset or in individual studies are available for search and download. Gene expression in various brain cell types at the single cell RNA-seq level is also included. CFG ranking module provides a feasible way to prioritize the AD-relevant genes by incorporating different aspects of AD-related evidence. The AlzData.org is available at [www.alzdata.org](http://www.alzdata.org).

# AlzData

## High throughput data collection of Alzheimer's disease

Home
Differential Expression
CFG Rank
Single Cell Expression
Download
About Us

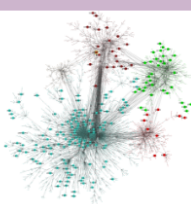
**Alzheimer's disease (AD)** is the most prevalent and rapidly increasing neurodegenerative disorder in the elderly, with no effective therapy. Complete understanding of the biological basis of Alzheimer's disease is the key for early diagnosis and intervention. Recent applications of high throughput technologies, e.g. genome-wide genetic analyses and expression profiling, have obtained some insights of the genetic and molecular mechanisms underlying the disease. With the technology develops, the data throughput grows. We are now in the "Big Data" time ---- omics for complex disease. However, it is elusive to translate the big data to reliable knowledge. Here, we developed a one-stop database called AlzData, to make a full collection of current high-throughput omics data. What's more, AlzData could serve as an in-depth integrating system to integrate data of different levels, to generate a prioritized gene list for further characterization.

**AlzData will cover:** 1) high-throughput omic data, e.g. Genomics (GWAS and Whole Exome Sequencing), Transcriptomes, Proteomics, and Functional genomics; 2) high-confident functional data, e.g. neuroimaging screening, population-based longitudinal studies, and transgenic mouse phenotyping.

Currently, we provide a searchable & downloadable web entrance for results of normalized brain gene expression profiling and whole exome sequencing. Other data is under continuously updating. Submission of any high-throughput data relevant to AD to our database is welcome. (updated at 2016/07/11)

**Top10 genes by CFG**


- APOE
- MAPT
- AP2A2
- RAPSN
- ARHGDB
- PAK4
- CAV1
- FLT1
- MAPK10
- CDH4





**Update history**


- 2016-06-20: first release
- 2016-12-15: single cell expression
- 2017-1-20: CFG rank
- 2017-3-15: YAP1 RNA-seq data


Useful links

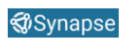
  
Gene Expression Omnibus

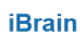















Copyright©2016 Kunming Institute of Zoology, Chinese Academy of Sciences. All Rights Reserved.

**Fig S6. Homepage of AlzData.org (www.alzdata.org).**



**Fig. S7. Search function of the “gene expression” module.** AlzData.org provides a convenient platform for exploring gene expression changes in AD patients compared with the controls in either (A) normalized datasets, or (B) datasets of individual datasets. (C) Gene expression pattern in different types of brain cells.



**Fig. S8. Prioritization of AD candidate genes based on the CFG score.**

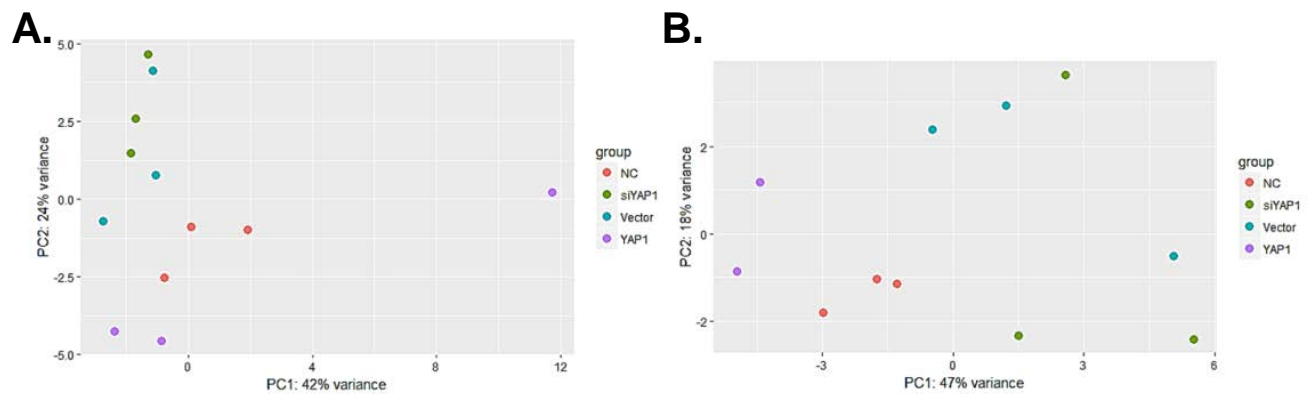


**Fig. S9. Principal component analysis (PCA) of U251-APP cells with overexpression or knockdown of *YAP1*.** PCA was performed on expression values of all genes, and each point represented a sample. (A) PCA of all samples. (B) PCA after removing one outlier (U251-APP overexpressed *YAP1*, replicate 2). The original data could be downloaded at [www.alzdata.org](http://www.alzdata.org) and GEO database ([GSE100891](https://www.ncbi.nlm.nih.gov/geo/query/acc.cgi?acc=GSE100891)).

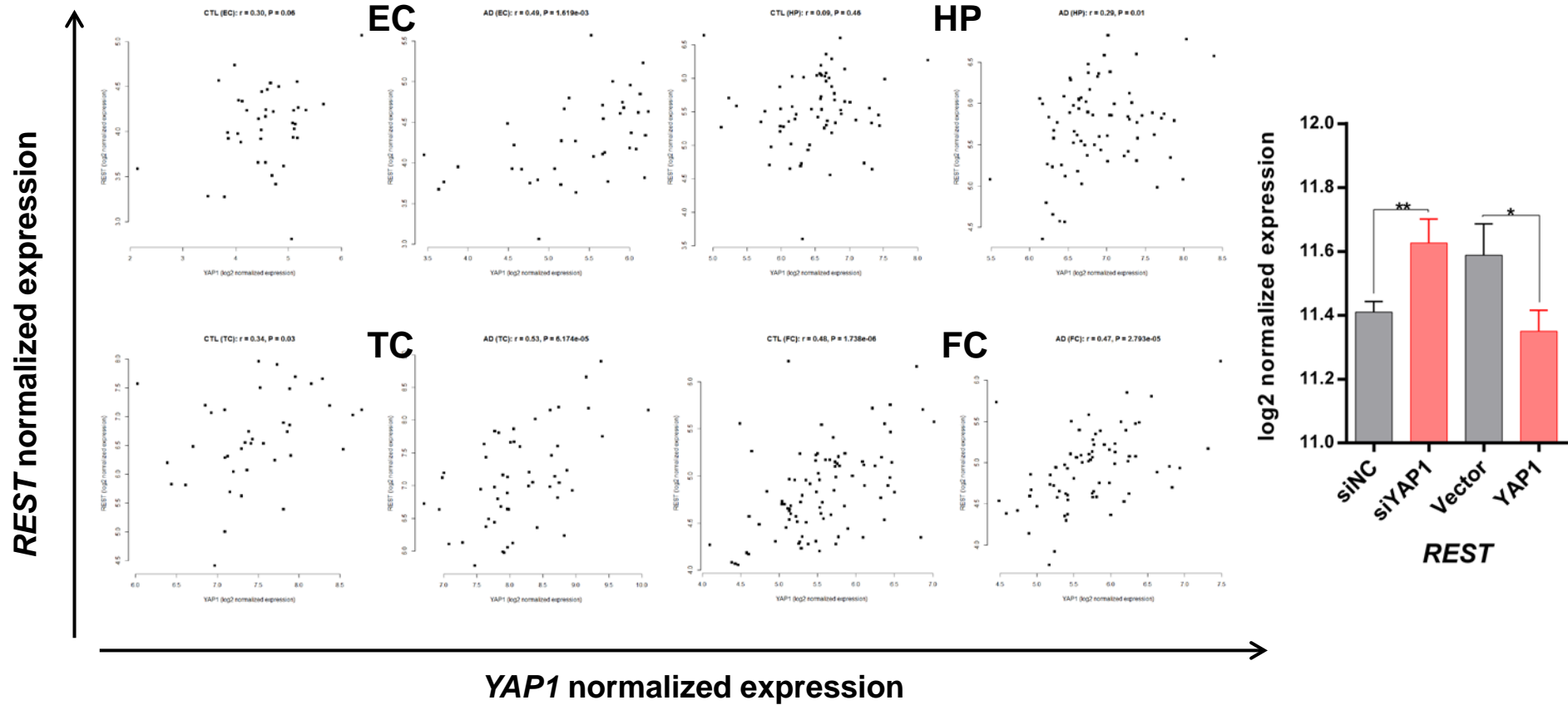


**Fig. S10. Correlation between mRNA expression levels of *YAP1* and *REST* and alteration of *REST* expression level in response to *YAP1* alteration.** Correlation between mRNA expression levels of *YAP1* and *REST* were measured in combined controls (left) and AD cases (right) of entorhinal cortex (EC, A), hippocampus (HP, B), frontal cortex (FC, C), and temporal cortex (TC, D) using the *Pearson's* correlation test. Alteration of *REST* mRNA expression level (retrieved from our RNA-seq data) in response to *YAP1* knockdown and overexpression was measured by the Student's *t* test (E). \*, *P*-value < 0.05, \*\*, *P*-value < 0.01.